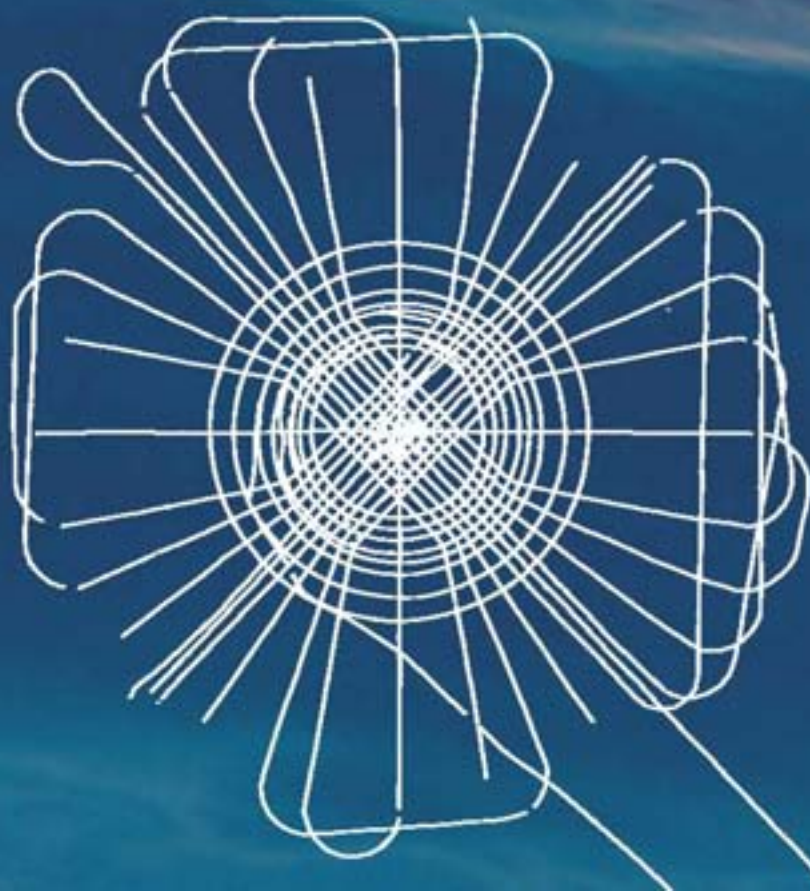




**Deep-water depositional systems and cold seeps of
the Western Mediterranean, Gulf of Cadiz and
Norwegian continental margins.**

Preliminary results of investigations
during the TTR-16 cruise of
RV Professor Logachev
May-July, 2006



**Deep-water depositional systems and cold
seeps of the Western Mediterranean, Gulf of
Cadiz and Norwegian continental margins**

Preliminary results of investigations during the TTR-16 cruise of
RV Professor Logachev
May-July, 2006

Editors: A.M. Akhmetzhanov
N.H. Kenyon
M.K. Ivanov
G. Westbrook
A. Mazzini

The designations employed and the presentation of the material in this publication do not imply the expression of any opinion whatever on the part of the Secretariats of UNESCO and IOC concerning the legal status of any country or territory, or its authorities, or concerning the delimitation of the frontiers of any country or territory.

For bibliographic purposes, this document should be cited as follows:

Deep-water depositional systems and cold seeps of the Western Mediterranean, Gulf of Cadiz and Norwegian continental margins.

IOC Technical Series No. 76, UNESCO, 2008

(English)

Cover design: A. Akhmetzhanov

Front cover image: Ship's track of an OBS seismic survey over G11 pockmark on the Voring Plateau (Norwegian margin).

Printed in 2008

by the United Nations Educational,
Scientific and Cultural Organisation

7, place de Fontenoy, 75352 Paris 07 SP

Printed in UNESCO's Workshops

©UNESCO 2008 *Printed in France*

TABLE OF CONTENTS

ABSTRACT	ii
ACKNOWLEDGEMENTS	iii
INTRODUCTION	1
LIST OF PARTICIPANTS	3
METHODS	4
I. GULF OF LIONS, WESTERN MEDITERRANEAN SEA (LEG 1): DEPOSITIONAL ENVIRONMENT OF THE DISTAL RHONE NEOFAN	12
I.1. Introduction	12
I.2. MAK-1M Data	13
I.3. Bottom Sampling	14
II. GULF OF CADIZ (LEG 2)	16
II.1. Introduction and Objectives	16
II.2. Geological Setting and Study Areas	17
II.3. MAK Deep-Towed Sidescan Sonar and Sub-bottom Profiler	18
II.4. Bottom Sampling Results	27
II.5. Biology - Macrofauna	30
II.5.1. Introduction	30
II.5.2. Methods	31
II.5.3. Results	31
II.6. Gas Biogeochemistry and Microbiology	35
III. VORING PLATEAU, NORWEGIAN MARGIN (LEG 3)	37
III.1. Introduction	37
III.1.1. Overview	37
III.1.2. Geological background	37
III.1.3. Objectives	38
III.2. Summary of Results	39
III.2.1. OBS	40
III.2.2. Reflection profiles	41
III.2.3. MAK-1M data	42
III.2.4. Sea floor observations and bottom sampling	44
REFERENCES	57
 ANNEX I. CORE LOGS	
 ANNEX II. LIST OF TTR RELATED REPORTS	

ABSTRACT

Interdisciplinary studies of deep-water environments including depositional systems and cold seeps were conducted by RV Professor Logachev in the Western Mediterranean, Gulf of Cadiz and Norwegian continental margins during the 16th Training-through-Research Cruise of UNESCO-IOC in the summer of 2006.

During the first leg TTR was working in the distal setting of the Rhone Neofan looking at the terminal depositional lobes that are developing there. The sampling showed that most of the depositional elements of the distal Rhone Neofan have been draped by hemipelagic sediments since its last active phase. The new data provides new insights into the hemipelagic processes in the area and emphasises the importance of cascading currents, originating in shallow water, for the modern deep-water depositional environment of the distal Rhone Neofan.

During the second leg in the Gulf of Cadiz a newly acquired high resolution sidescan sonar survey produced an excellent image of the two largest mud volcanoes in the Gulf - Yuma and Ginsburg. The new data were particularly useful for mapping the most active sites on the volcanoes which, in addition to being in the craters, were also found on their slopes.

Another high resolution sidescan sonar survey covered Pen Duick escarpment and imaged two extensive faults bounding the structure to the east and west. Video survey and sampling showed the western fault to be the more active seepage site and large carbonate crusts and chemosynthetic fauna were recovered here by a grab sampler.

The Darwin mud volcano, discovered a few months earlier by RRS Charles Darwin and which was found to host the largest population of chemosynthetic mussels *Bathymodiolus* Sp. observed so far in the Gulf of Cadiz, was mapped with high resolution sidescan sonar and sampled with TV-guided grab. The sidescan data show that the most active part of the volcano is on its top, being only about 100 m in diameter. Authigenic methane-derived carbonate crusts as well as living specimens of *Bathymodiolus* observed during video runs were successfully retrieved onboard.

Traces of gas hydrate presence were noticed on almost all deep-water mud volcanoes of the Portuguese margin. The long awaited acoustic image of the Bonjardim mud volcano allowed the selection of a sampling site from which large, up to 6 cm across, aggregates of gas hydrates were recovered.

Two gas chimneys were investigated in the Nyegga region on the Norwegian margin during the third leg with identical seismic experiments using an array of OBSs. The seismic experiment was designed to determine the structure of a chimney, which is typically 300-m in diameter, the presence of gas within it, the hydrate within and around it, and the presence and orientation of fractures through which gas and fluids migrate. The depth of investigation of the experiment was between 200 and 500 m beneath the seabed in a water depth of ~750 m, depending on the seismic source, and the experiment was to measure P-wave and S-wave velocities, and seismic anisotropy, through S-wave splitting.

For the first time, gas hydrates were sampled here from several sites, supporting the inference of several authors that hydrate was present, but which had never been verified by tangible evidence. As gas hydrate or strong bubbling were generally observed in the bottom part of several cores from different structures, it is inferred that the presence of gas hydrate prevented further penetration of the gravity corer at these sites. Although the presence of gas hydrates does not necessarily provide evidence of actual or very recent flow of free gas at the locations investigated, a near-constant flux of methane-rich fluid through the features containing hydrate is required to maintain the continued existence of hydrate, so close to the seabed.

ACKNOWLEDGEMENTS

The sixteenth Training-through-Research cruise received financial support from a variety of sources. Leg 1 was funded by the National Oceanography Centre, Southampton through its UK-TAPS (UK Turbidite Architecture and Processes Studies Group) initiative.

Leg 2 was funded by UNESCO-IOC (from its Regular Programme and two extra-budgetary projects, TTR-Flanders (513RAF2005) and EU-HERMES) and IFM-GEOMAR.

Leg 3 was funded by the HERMES EU Integrated Project (GOCE-CT-2005-511234) and STATOIL.

The cruise was also supported by the Russian Ministry of Science and Technological Policy, the Polar Marine Geological Research Expedition (PMGRE) of the Russian Ministry of Natural Resources and the Moscow State University (Russia). Logistic support was provided by the Netherlands Institute for Sea Research (NIOZ).

A number of people from different organizations supported the Training-through-Research Programme and were involved into the cruise preparation. The editors would like to express their gratitude for the contributions made by Prof. I. F. Glumov (Ministry of Natural Resources of the Russian Federation) and Dr. P. Bernal (Executive Secretary, IOC).

Credit also should be given to Dr. Maarten van Arkel of the NIOZ, Prof. Dr. D. Y. Puscharovsky (Faculty of Geology, Moscow State University) and Dr. A. Suzyumov (IOC Consultant) for their continuous support.

Thanks are due to the administration and staff of the PMGRE (St. Petersburg) for their co-operation and assistance with the cruise organization and execution. Captain V. Pidenko and the skilful crew of the RV Professor Logachev insured the smooth operations at sea.

Staff and students of the UNESCO-MSU Marine Geosciences Centre provided a valuable support in processing the acoustic data and preparation of illustrations.

INTRODUCTION

The TTR-16 cruise was carried out in the Western Mediterranean, Gulf of Cadiz and North Atlantic with the RV Professor Logachev, owned and operated by the Polar Marine Geosurvey Expedition (PMGE, St. Petersburg, Russia).

The cruise started in Barcelona (Spain) on the 16th of May 2006 and terminated in Bergen (Norway) on the 2nd of July 2006. Intermediate port calls were made in Almeria (Spain), Brest (France), and Alesund (Norway). The cruise programme was divided into 3 Legs with a total of 3 study areas.

Leg 1 (16 May – 26 May, from Barcelona to Almeria)

The Rhone Neofan and adjacent areas were investigated during the TTR cruises of 1992 and 1994 with the RV Gelendzhik and a comprehensive set of multidisciplinary data was obtained. The expedition of 2006 focussed on a detailed examination of the known structures as well as on new areas.

The first stage of Leg 1 involved a medium-resolution (30 kHz) deep-towed sidescan survey of the Neofan terminal lobe and adjacent areas. Then, specific sections of the lobe were selected and high-resolution (100 kHz) sidescan sonar survey was carried out, producing images at about a metre resolution. The images were processed onboard and then used to guide the coring phase of the leg, whereby a series of cores targeted key areas to calibrate the geophysical data from the specific environments of the terminal lobe, e.g. distributary channel, lobe, inter-channel areas etc.

Leg 2 (26 May – 8 June, from Almeria to Brest)

The area of the Gulf of Cadiz was intensively studied on several recent TTR expeditions, focussed mainly on mud volcanism, fluid venting and related phenomena. Many mud volcanoes have been discovered and confirmed by sampling. Gas

hydrates, carbonate crust and nodules, as well as benthic chemosynthetic communities were sampled from some of these structures. Large carbonate chimneys, possibly related to fluid escape were sampled and recorded by a deep-towed video system. During the TTR-16 Cruise, further detailed geological and geophysical investigations of known mud volcanoes, fluid escape features, gas hydrate accumulations and other related phenomena were conducted, together with a search for previously unknown structures of similar origin. The main areas of interest were the Moroccan Margin, including locations around the Pen Duick escarpment and Yuma and Ginsburg mud volcanoes and the deep water Portuguese margin where several mud volcanoes were surveyed.

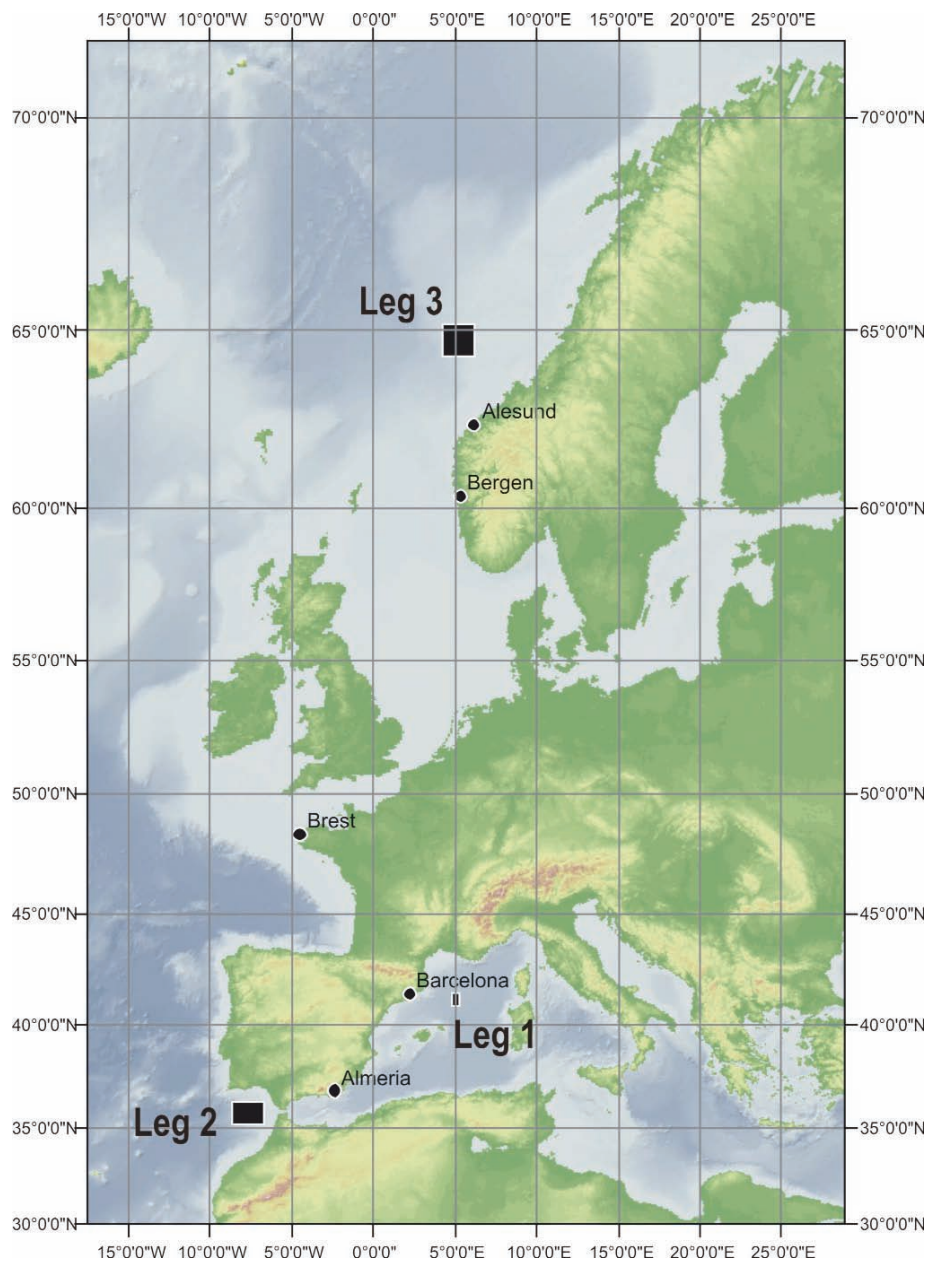
Leg 3 (8 June – 2 July, from Brest to Bergen)

The existence of hundreds of gas/fluid-escape chimneys on the continental margin of Norway in the region of the Voring plateau has been demonstrated by seismic reflection surveys and by multibeam sonar and sidescan sonar surveys of their seabed culminations as mounds and, more commonly, pockmarks. Some of these chimneys emit methane and other hydrocarbon gases and support communities of chemosynthetic biota.

The TTR cruises of 1998 and 2000 collected an essential set of geophysical and geological data on the gas seepage environment on the Voring Plateau, including a long-range side scan sonar survey of the area, bottom sampling and underwater TV runs across pockmarks, the discovery, mapping and sampling of mud volcanoes, gas composition analyses and study of chemosynthetic biota.

For the Leg 3 of the TTR-16 cruise two high-resolution seismic experiments employing OBSs have been designed to investigate the 3D structure of a gas/fluid escape chimney beneath an active seep/vent and to compare it with that of an inactive system. The exper-

iments employed deep-tow chirp seismic sources, in addition to near-surface mini GI guns, with deep-towed hydrophone streamers to provide near-3D seismic reflection images of the sub-seabed structure to complement the tomographic inversion of the OBS data. The experiments provided an order of magnitude better resolution than previous work on such features and should determine the distribution of free gas and hydrate in the gas/fluid escape chimneys. Selected locations were also studied with the deep-towed sidescan sonar and bottom sampling.



TTR-16 cruise location map

LIST OF PARTICIPANTS

TTR-16 Cruise
16 May to 2 July 2006.
RV Professor Logachev

FRANCE

Jacques Crozon
Yvon Peneaud
Mickael Roudaut
Herve Nouze

MOROCCO

Mustapha Chafic

NORWAY

Andreia Plaza Faverola
Adriano Mazzini

PORTUGAL

Luis Pinheiro
Marina Cunha
Vitor Magalhaes
Clara Rodrigues
Luisa Santos
Henrique Duarte
Ana Hilario
Joao Duarte
Ines Martins
Joao Castro

RUSSIA

Michael Ivanov
Elena Kozlova
Valentina Blinova
Dmitry Korost
Ruslan Khamidullin
Igor Kuvaev
Daria Titkova
Anna Zotova
Dmitry Nikonov
Ilya Fokin
Antonina Savelyeva
Dmitriy Nadezkin
Alexandra Sharapova
Nikita Kaskov
Dinara Garifullina
Julia Kolganova
Vladislav Malin

SPAIN

Renata Lucchi
Gemma Herrera Pujol

UK

Neil Kenyon
Russell Wynn
Peter Talling
Graham Westbrook
Andrey Akhmetzhanov
Michael Frenz
Esther Sumner
Pierre Cazenave
Marianne Nuzzo
Tim Minshull
Russell Exley
John William
Nicholas Schofield
James McIntosh
Paul Georgief
Tesmi Jose

METHODS

The RV *Professor Logachev* is a Russian marine geology research and survey vessel equipped with seismic and seabed sampling equipment. She is operated by the State Enterprise "Polar Marine Geosurvey Expedition" St. Petersburg. The vessel has a draught of 6.66 m, length of 104.5 m, width of 16 m, net tonnage of 1351 ton, displacement of 5700 ton and is powered by two 3500 hp diesel engines.

Navigation

Positioning during the TTR-16 cruise was acquired using an Ashtech GG24 GPS + GLONASS receiver. The use of both GPS and GLONASS satellite configurations allows for greater accuracy than is available from conventional GPS alone, with up to 60% greater satellite availability. Positions are calculated in real-time code differential mode with 5 measurements per second and an accuracy of ± 35 cm (75 cm at 95% confidence limits) with optimal satellite configuration. Realistic positioning accuracy under normal satellite configuration for European waters is assumed as c. 5 m. Positioning when the vessel is moving also utilizes Doppler velocity determinations from the differential code signal to generate a vessel speed accuracy of 0.04 knots (0.1 at 95% confidence limits) with

optimum satellite configuration. The GPS+GLONASS receiver is located centrally on the vessel with accurate ties to the coordinates of the sampling and equipment deployment positions on the vessel, allowing precise back navigation. The navigation of the ship along a course was computer-controlled, and in general, this gave very good accuracy in following the desired course, and near-constant spatial separation of shot points. The consequent variation in speed through the water, however, brought about by currents and tidal streams, did affect the depth of tow of the hydrophone streamer.

Underwater navigation

MAK1-M sidescan sonar and deep-towed video system are fitted with an acoustic transponder allowing precise navigation between the vessel and the underwater position. This is necessary as deep-towed equipment is subject to great spatial differences with respect to the vessel. Similarly, an acoustic transponder was attached to the coring cable to enable the OBS to be positioned accurately when being deployed on the seabed. The underwater navigation is based on the Sigma-1001 hydroacoustic system. Four hull-mounted transducers, spaced 14 m apart, send and receive acoustic signals from



RV Professor Logachev during port call to Barcelona.

transponders attached to deployed equipment in short-baseline mode operating between 7-15 kHz. The signal emitted by the sub-surface transponder is tracked on board and accurate x,y positioning of the device relative to the vessel is computed taking into account vessel roll, trim and ship's speed. Accurate level of the GPS+GLONASS antennae with the hull-mounted transducers allows precise positioning of deployed equipment. The error in positioning by the method usually does not exceed 1-2% of the water depth. Additional thrusters linked with the navigation system allow dynamic positioning of the ship. This is particularly useful during high-resolution surveys or precise bottom-sampling operations.

Ocean Bottom Seismometers

Deployment and Recovery Procedures

The high-resolution nature of the experiment during Leg 3 required that ocean bottom seismometers (OBSs) be precisely located on the seafloor. Therefore rather than being dropped from the sea surface, OBSs were dropped from an acoustically navigated coring wire about 50 m above the seabed, using a MORS acoustic release supplied by Ifremer. For this operation, all OBSs were fitted with c. 25 m long stray lines. Initially, the coring wire was attached to the stray line and the OBS lifted over the side by the ship's G-frame. The wire was let out until the end of the rope had gone through the G-frame block and was close to deck level, so that the OBS itself was well below the bottom of the hull. The rope was then brought close to the side of the ship and tied off. The Ifremer acoustic release was attached to the rope and the wire and a further short length of stray line with a ball of rope in a Turk's head knot at its end (Southampton OBSs) or a float (Ifremer OBSs) was also attached. Further wire was let out and the ship's acoustic beacon was attached. Once the ship's acoustic navigation indicated the right location and the appropriate amount of wire was out, a release command was sent to the Ifremer release. The OBSs were released, when at the correct

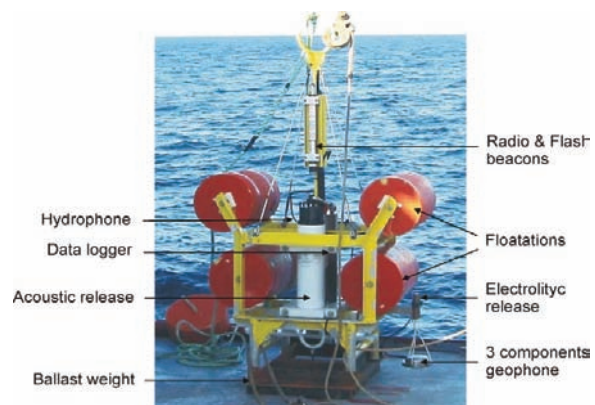
depth on the wire, if they were within 25 m of the desired position. The actual positions of the OBS on the seabed will be located from the arrival times of the direct waves from the shots.

OBS recovery was achieved by hooking the stray line with a grappling hook thrown from the afterdeck. This could be achieved only if the OBS was within a few metres of the ship. The large size of the ship made this operation difficult, and it was rare that an OBS was recovered on the first pass. OBSs were not visible from the Bridge when close to the bow, and on at least two occasions the stray line ended up passing under the bow.

Ifremer Ocean Bottom Seismometers

Ifremer's Ocean Bottom Seismometers (OBS, see figure below) are autonomous instruments deployed onto the seafloor. They are equipped with 4 sensors (1 hydrophone and 3 geophones), to record the pressure variations (hydrophone) and the seafloor vibrations in 3 directions (3 geophones). After shooting, the ballast weight is acoustically released, the instrument recovered, and the data downloaded from the memory cards in the data logger unit.

The Ifremer OBS were assembled in 1999, using a Send recording unit, an OAS 0-5000Hz hydrophone, and a Mors acoustic release. Initially, 3 geophones were included in the data logger unit. External geophones were added in 2002. The instruments are



Ifremer OBS

quite heavy (240 kg) and bulky, which implies the use of a crane for deployment and recovery, but have proved very reliable (99.9% success). For the Nyegga experiments, new 5000 Hz preamplifiers were installed, and sampling rate increased to a maximum sampling rate of 10 kHz. During the experiments the sampling rate was set to 2500 Hz.

All eight instruments were deployed on both CN03 and G11 study sites. All instruments were recovered and have recorded data on the four channels. There was a problem to convert MBS format data to Passcal format for the OBS deployed on CN03-09.

Southampton Ocean Bottom Seismometers

Ten OBSs from the UK Ocean Bottom Instrumentation Consortium (OBIC) were supplied by the University of Southampton. The OBIC consortium comprises the University of Southampton, the University of Durham and Imperial College London, and the instruments are operated by the Universities of Southampton and Durham. The OBSs comprise a logger tube, a release tube with Edgetech electronics and a burn-wire mechanism, a rectangular instrument frame, a floatation unit containing four glass spheres, radio beacon, flashing light and flag. The sensors comprise a broad-band hydrophone and a 2 Hz vertical geophone mounted on the instrument frame. A 40 kg mild steel anchor couples the OBSs to the seafloor. The data loggers installed in the OBIC instruments have a maximum logging frequency of 1000 Hz for 1 channel and 500 Hz for 2 channels. The loggers record on hard disk and require lithium rechargeable NiMH battery packs. The lithium packs provide power for longer periods and are lighter than the rechargeable packs.

For this experiment, seven high-frequency, four-channel data-loggers and seven three-component gimballed 4.5 Hz geophones were purchased from Scripps Institution of Oceanography. The loggers were designed to record four channels at up to 4 kHz per channel. These loggers record on scratch memory chips, which were pur-

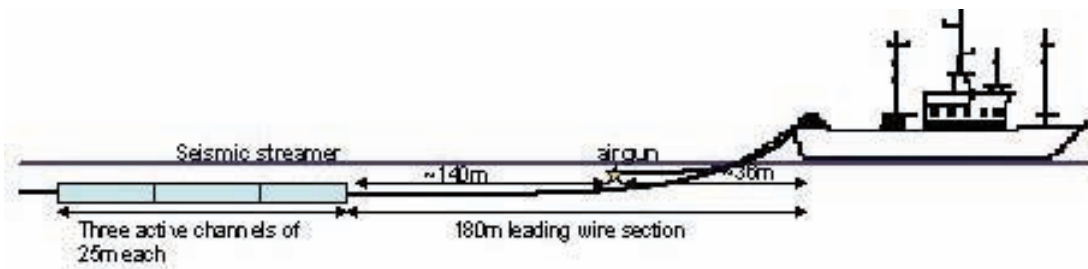
chased separately. Lithium batteries were purchased for these loggers since their power consumption, though expected to be lower than the lower-frequency loggers, was unknown.

The OBS transportation racks were installed in the Underwater Hangar. Data loggers were prepared and programmed in the adjacent Underwater Laboratory, and OBSs were then assembled in the Hangar on pallets, transported to the stern deck on a pallet truck, and lifted by the ship's crane to the Main Deck for deployment. This crane operation added a little to the time between deployments since typically only one winch driver was available, so the instruments could not be lifted until the coring wire had been fully recovered. Release acoustics were tested during OBS descent on the wire, rather than in a separate operation with a release rosette.

Clock offsets for the OBSs varied from less than 1 ms to a maximum of around 17 ms during a four-day deployment; a linear clock drift is assumed during SEG-Y conversion.

Air guns, hydrophone streamer and recording system

Seismic reflection data from two channels of the Logachev's hydrophone streamer were recorded using the CODA-DA200 (Data Acquisition) system, a 12-bit stand-alone module for acquiring and processing seismic (and sidescan) data. This system is designed for high-frequency sources, so cannot sample at low sample rates. It consists of a PC running on LINUX operating system functioning as the receiving, recording and quality control unit respectively. The DA system was operated in one of the two modes: data acquisition or data playback mode. In the acquisition mode, the two seismic channel inputs from the ship's streamer were connected to the system and each input digitally sampled. Normally the sampling frequency was 4 kHz. The system cannot record more than 32000 samples per shot; trace lengths were normally 3 s to give 24000 samples per shot. Navigation data were

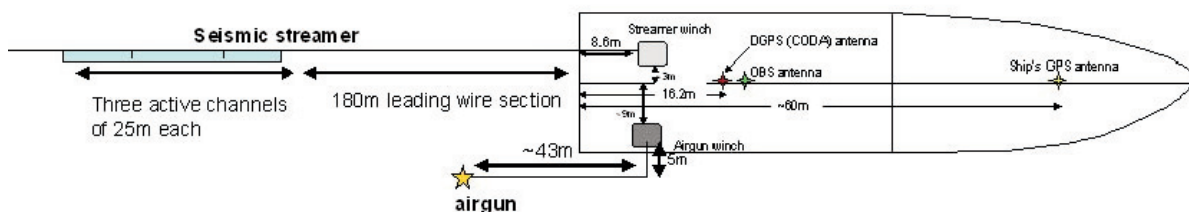


Schematic illustration of the disposition of the hydrophone streamer and airguns.

input into the DA system once per second via an NMEA string from a CSI Wireless-DGPS Max receiver, and stored in SEG-Y headers in units of 0.001". Because this process takes a finite time, both the time and position information stored in the headers correspond to a time one second before the trigger time. The display of the seismic data was manipulated by applying a band pass filter, time varying gain etc., for displaying on a scrolling screen where both the channels could be displayed at the same time. Unprocessed data were recorded on the PC hard disk in a 2-byte integer SEG-Y format and backed up onto DVD RAM disks at the end of each profile. It was necessary to stop recording for 2-3 minutes during such backup.

The acoustic source consisted of an airgun array with three S.S.I (Seismic Systems Incorporated) 70 cu in mini-GI guns towed about 36 m behind the ship at a depth of 1.5 m. The GI gun is made of two independent airguns, the generator, which produces the primary pulse, and the injector, which is used to control the oscillation of the bubble produced by the generator. The volume of both the generator and injector can be

changed from 13 cu in up to 35 cu in, thereby enabling control of the duration of the injection or its timing. This adaptability allowed the use of the guns in two different modes. In the true GI mode, the volume of the generator/injector was 13/35 cu in, whereby the injector was tuned to totally suppress the oscillation of the bubble and only one gun was used normally with a shot interval of 4 s, the minimum interval required for the injector chamber to recharge. In the harmonic mode (24/24 cu in), the timing of injection was adjusted to reduce the bubble oscillations to provide a better primary to bubble ratio. Two guns were used with a shot interval of 6 s in this mode; the shot interval was limited by the capacity of the compressors. The air pressure for both the modes was 2000 PSI. During the testing phase of the cruise, some shots were also fired at 3 s and 5 s intervals. The GI gun trigger box and the Coda recording system were both triggered on the exact second using a TTL pulse from a Zypher GPStarplus clock. Typically, the clock was operating with a TFOM (time factor of merit) of 4 throughout the cruise, giving an accuracy of less than 1 μ s. The GI guns



Plan of positions of deployment of hydrophone streamer and airguns relative to ship and navigational antennae

were tuned so that the firing pulse for the generator was 10 ms after the trigger time from the GPStarplus clock. The actual rising edge of the first pulse of air gun signal was 18 ms after the trigger time from the GPStarplus clock. The time of this pulse varied over a period of the order of 10 shots in a saw-tooth pattern, with a maximum shift of around 1 ms. The frequency range of the air-gun array was 30-300 Hz, with a variation of amplitude of less than 6 dB. The maximum energy of the source centred around 150 Hz. Above 300 Hz, its amplitude decreased by a further ~7 dB to 400 Hz before reaching a plateau between 400 and 800 Hz.

The seismic streamer contained three 25 m-long active sections, of which the front two were recorded, carrying 37 hydrophones per section at a spacing of 0.6 m. Coda channel 1 recorded the nearer of these two sections and channel 2 the farther. Because of the high intensity of acoustic noise generated by the ship, channel 2 generally provided better data. The streamer had no tow cable but instead was towed from a passive section that remained partly wound on the winch drum. There was no mechanism for depth control. The streamer was negatively buoyant, and had to be towed at 4 knots or above to keep it within 4 m of the surface. Observations of the sea-surface ghost in the recorded data suggested that the streamer depth was generally in the range 2-7 m, sinking during turns.

The streamer channels were connected via BNC leads to the recording system via transformers (to electrically decouple the streamer from the system), but no pre-amplifiers were available. The Coda channels were both set to maximum gain (1.25 V range), but nevertheless the recorded signals were relatively weak, with maximum peak-to-peak amplitudes of around 70 units for the single gun source and 200 units for the two-gun source, compared to a maximum peak-to-peak range of 4096 units for the recording system. Hence only a small proportion of the dynamic range of the recording system was used, and weaker signals will be poorly represented. The quality of reflection images does not appear to have been noticeably

degraded by this limitation. Significant 50 Hz electrical noise was observed on both channels. Later in the cruise, it was recognised that this noise could be reduced by more effective shielding of the signal cables: instead of using both the outer and inner wires of the BNC cables, inner wires only were used, with the sheath tied to the ship's earth. This required an additional two cable runs, but reduced the 50 Hz noise considerably.

Overall, the Coda system performed well during the cruise. It did crash occasionally, for reasons that were not always clear, but it was possible to restart recording very rapidly after a crash and therefore there was little loss of data. In these cases, the profile number was not changed, but there are two or more SEG-Y files corresponding to that profile number. Once during the cruise, the GPS clock trigger signal also stopped for an unknown reason, although it was quickly resolved. There were also a few isolated incidents of timing jumps; their origin can be established by careful examination of the corresponding OBS records.

Sparker and Mini-Streamer

A Geoacoustics sparker and mini-streamer with a 6 m active section were supplied for the cruise by the University of Southampton. The sparker had been used very successfully (with a longer, multichannel streamer) in similar water depths in the Gulf of Corinth. Neither system had been deployed from a large research vessel before. The sparker power supply was an Applied Acoustics CSP2200 system rented from Seatronics Ltd of Aberdeen, capable of delivering source energies of 900-2200 J. Both sparker and streamer had relatively short tow cables, 30-40 m long. This did not prove a significant limitation for the sparker, but did for the streamer.

During the testing phase of the cruise, initially both systems were towed directly from the stern deck. Even at maximum power, only the direct wave was distinguishable from noise on the mini-streamer record. In a second deployment, the mini-streamer

was towed from the starboard quarter, to distance it from propeller noise, and the sparker was towed from the port quarter to avoid any possible bubble streams astern of the ship. There was no significant improvement in the ministreamer record. Shots from the GI gun were successfully recorded on the ministreamer, but the data were significantly more noisy than those recorded with the Russian streamer.

The sparker shots were clearly visible on OBS records in cases where the sample rate was 1000 Hz or greater. However, the signal was relatively weak and signal levels even for the direct wave were only a factor of 2-3 greater than the noise of the ship. Therefore it was decided not to use the sparker for the main phases of the experiment.

Logachev's onboard single -channel seismic kit

The seismic source consisted of one 3.5 litre airgun, at a pressure of 140-170 atm. The airgun was towed at a depth of approximately 3.5 m and was shot every 9 seconds. The streamer consisted of one active section, 25 m long, with 50 hydrophones, towed at a depth of approximately 3.5 m. The offset between the seismic source and the centre of the live hydrophone array was 150 m. Throughout the seismic acquisition, the average ship's speed varied from 1.5 to 3 knots, so the shot spacing was 7-14 m.

The data were logged digitally using the MSU developed software and preliminarily processed with the RadExPro software, which was provided to the UNESCO MSU Centre for Marine Geosciences by GDS Productions, Moscow. The trace length is 8 s and the sampling rate is 1 ms. The signal was passed through an analogue filter of 50-250 Hz during the acquisition stage.

The preliminary onboard processing was carried out using the RadExPro software and also the SPW processing system (Seismic Processing Workshop). The basic processing sequence consisted of a static shifts correction and amplitude recovery by spherical divergence correction. F-K migration, spatial and F-K filters were also applied to some of

the seismic lines to attenuate the noise and remove diffraction effects.

Sidescan sonar systems

OKEAN

The OKEAN is a long-range sidescan sonar operating at a frequency of 9.5 kHz, which, with its up to 15 km swath range and 6 knots towing speed, is well suited for reconnaissance surveying of large deep-sea areas. The OKEAN vehicle is towed behind the ship at about 40-80 m below the sea surface. Depending on the water depth and resolution required the swath could be set to 7 or 15 km.

Deep-towed hydroacoustic system MAK-1M

The MAK-1M deep-towed hydroacoustic system contains a sidescan sonar operated at frequencies of 30 and 100 kHz, with a total swath range of up to 2 km (1 km per side and 350 m per side respectively) and a sub-bottom profiler, operated at a frequency of 5 kHz. Sidescan sonar provides an acoustic image of the sea bottom, and the profiler provides an acoustic section of the upper sediments.

The underwater vehicle was towed by the vessel with an electrical deep-tow cable. A depressor weight was used to stabilize the depth of the tow-fish. There should be a constant and predefined distance between the fish and the sea bottom depending on the mode of survey. During TTR-16, the tow-fish was towed at nearly constant altitude of about 100 m above the seafloor at a speed of 1.5-2 knots for 30 kHz surveys and about 50 m above seafloor for 100 kHz ones. Resolution of the sonar across track depends on the mode of survey (maximum range to centre). Resolution of the sonar along the track depends on the speed of the ship. The positioning of the tow-fish was achieved with a short-base line underwater navigation system.

The data from the tow-fish were transmitted on board through the cable, recorded digitally, and stored in SEG-Y for-

mat, with a trace length of 4096 2-byte integer samples per side.

The trace length of the profiler record is the same. Time-variant gain was applied to the data while recording, to compensate the recorded amplitudes for the irregularity of the directional pattern of the transducers as well as for the spherical divergence of the sonic pulse.

Onboard processing of the collected data included slant-range-to-ground-range (SLT) correction of the sonographs, geometrical correction of the profiles for recovery of the real seafloor topography, and smoothing average filtering of both types of records. Individual lines were geometrically corrected for the towing speed of the fish, converted into a standard bitmap image format. Some image processing routines, such as histogram equalization and curve adjustment, which are aimed at improving the dynamic range of the imagery, were also applied before printing out. Geographic registration of the acquired images was also done onboard.

Underwater photo and television system

The television system operating during cruise TTR-16 is a deep towed system designed for underwater video surveys of the seabed at depths of up to 6000 m. The TV system consists of the onboard and underwater units. The onboard part comprises the control units with video amplifier and VCR. The power for the underwater system is supplied through a conductive cable. The underwater equipment comprises the support frame with light unit, the high-pressure housing containing a "Canon M1" digital camera and the power supply unit.

The TV system is controlled from onboard by the winch operator, who visually controls the distance from the camera to the seafloor. This is assisted by a 1.5 m long rope with a weight at the end attached to the frame which is usually towed along the seafloor enabling estimation of the altitude of the instrument above the seafloor. Lights and video camera are switched on/off by the operator from onboard. The non-stop under-

water record on the digital camera lasts for 2 hours in the "LP" mode. Onboard VCR keeps a continuous record during the whole survey, which could be up to 6 hours.

Sampling Tools

Gravity corer

Coring was performed using a 6 m long 1500 kg gravity corer with an internal diameter of 14.7 cm and internal plastic liner for comfortable retrieval of sediment. One half of the opened core was described on deck, paying particular attention to changes in lithology, colour and sedimentary structures. All colours relate to Munsell Colour Charts. Targeted sampling was conducted for chemical investigations (total organic content, pore water and gas analyses).

Box corer

Box cores were taken using a Reineck box-corer with a 50 x 50 x 50 cm box capable of retrieving 185 kg of undisturbed seabed surface sample. Lowering and retrieving operations are conducted using a hydraulic A-shaped frame with a lifting capacity of 2 ton.

Kasten corer

The corer is a square crosssectioned sampling instrument with a weight of about 600 kg and dimensions of 40x40x180 cm. The recovery volume is up to 0.3 m³. The closure of the instrument is performed by two sliding plates and triggered during pull-up. The instrument is particularly useful for obtaining large samples of loosely packed coarse-grained sediment.

TV-guided grab

During the TTR-16 cruise the DG-1 grab system was used (first used during TTR-10, 2000). The 1500 kg system is able to sample dense clayey and sandy sediments as well as deep water crusts and boulders. Sampling with the DG-1 grab is carried out at

very low ship's speeds (typically 0.3-0.5 knots). The position of the grab is calculated using the short baseline SIGMA 1001 underwater navigation system. The relative position of the vessel is calculated by the automatic positioning system ASUD. DG-1 can be used at the depths up to 6000 m and closes by the difference in hydrostatic pressure. The triggering mechanism is set off when the seabed is touched. The grab is equipped with a build-in camcorder (model SONY TRV17E), which uses 90-minute cassettes and records in Hi-Fi Video8 format. Video signal is also transmitted on board enabling control for the grab operation and back-up recording. It is also equipped with a quartz-halogen bulb that is powered by a rechargeable battery, enabling 6 hours of continuous operation. A second battery kept on board, was set to perform further deployments.



TV-guided grab

I. GULF OF LIONS, WESTERN MEDITERRANEAN SEA (LEG 1): DEPOSITIONAL ENVIRONMENT OF THE DISTAL RHONE NEOFAN.

A. AKHMETZHANOV, R.B. WYNN, P. TALLING,
M. IVANOV AND SHIPBOARD SCIENTIFIC PARTY OF
THE LEG 1

I.1. Introduction

The short study during the 1st Leg of the TTR-16 cruise was focussed on high-resolution studies of the modern Rhone submarine fan in the Mediterranean Sea (Fig. 1). This is the second largest fan in the Mediterranean. A sinuous entrenched fan-channel with flanking construction levees continues from the base of the Petit Rhone Canyon across the fan (Droz and Bellaiche, 1985). A recent avulsion of this Rhone Fan-Channel, at a break in slope, has generated the most recent deposits (Torres et al., 1997). The Neofan is an elongate feature with an extent of some 50 x 25 km.

The growth of the Rhone fan started during the Pliocene (5 Ma) and was strongly controlled by the Quaternary glacio-eustatic

changes. The Rhone Neofan is formed as a result of the avulsion of the Rhone channel. The onset of the Neofan is extrapolated at a maximum of 80 ka BP. The onset of the channel-levee stage is extrapolated at a maximum of 40 ka. The end of the turbidite stage of the Neofan, corresponding to the end of sediment overspill from the neochannel, is dated at 15.1 ka BP (14C) (i.e. 18.0 ka BP (cal.) (Bonnell et al., 2005).

The depositional processes on the distal fringes of large deep-sea fans are poorly understood and geometry and facies architecture of the resulting sedimentary bodies are not well documented.

The early studies of the area (Kenyon et al., 1993) showed that a terminal lobe with characteristic finger-shaped features developed just beyond the mouth of a shallow channel on the Neofan. A single preliminary core from this area encountered ~ 2 m of medium to coarse sand a few centimeters below the sea floor (Mear, 1984) suggesting

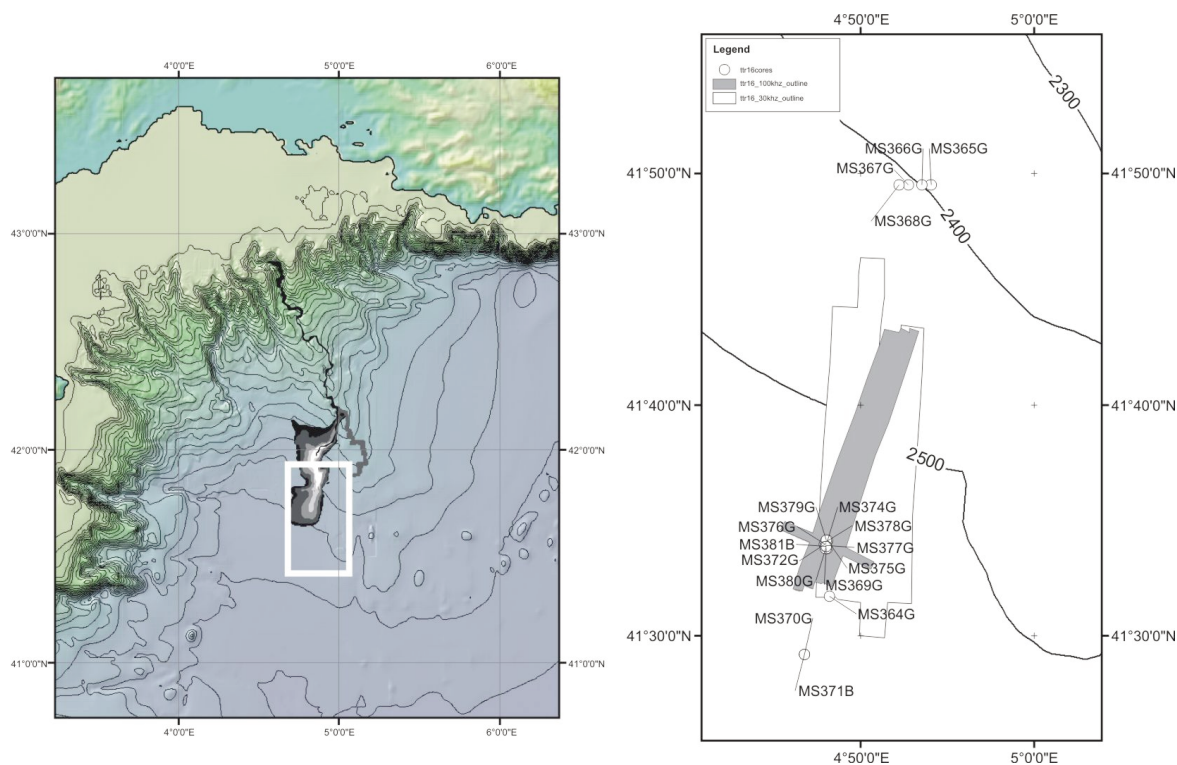


Figure 1. Location map of the Leg 1.

the presence of relatively thick sandy beds within the distal Neofan depositional sequence.

The terminal lobe was chosen as the main target for the Leg 1 studies which involved high resolution mapping with deep-towed 30 and 100 kHz MAK-1M sidescan sonar with built-in 5 kHz subbottom profiler. The acoustic data were processed onboard and the key features identified on the new data were sampled with a gravity corer.

I.2. MAK-1M Data

The survey area of about 190 km² was designed to cover the portion of the slope immediately to the south of the study area of the TTR-14 cruise (Kenyon et al., 2005). The aim was to trace the system of shallow channels emanating from the Rhone Neofan main channel and the lobe-shaped feature observed in the area on the TTR-2 sonographs (Kenyon et al., 1993). 30 kHz mode was chosen to obtain a reconnaissance coverage and then the area of interest was mapped with the working frequency of 100 kHz.

30 kHz data confirmed that the shallow channels imaged during the TTR-14

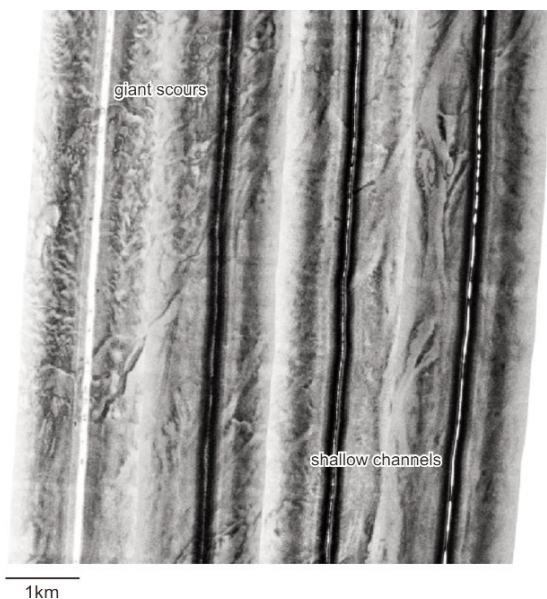


Figure 2. 30 kHz image from the distal part of the Rhone Neofan showing shallow channels and a zone of giant scours.

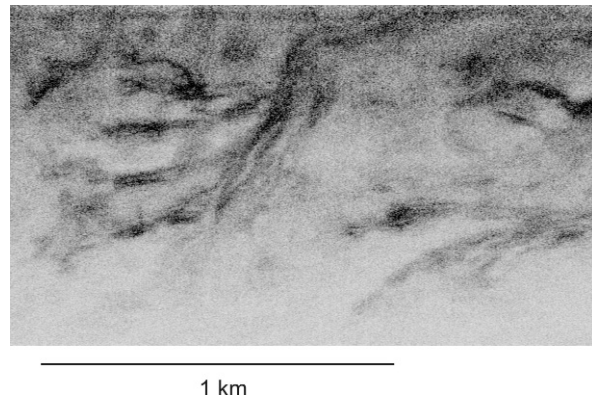


Figure 3. 30 kHz image from the distal part of the Rhone Neofan showing a network of channelised features within a terminal lobe.

cruise extend to the south. The channels are expressed on the seabed for 40 km from the main Neofan channel. The channels are observed in the eastern portion of the covered and are characterised by generally low backscatter (Fig. 2). They are up to 300 m wide with the majority measuring between 130 and 200 m. The sonographs show that the larger channels are, in fact, channel belts made by several coalescing smaller channels. Subbottom profiler records show the erosional character of the channels indicating that this is an area of sediment by-pass further to the basin. Some of the channels appear to have a low backscattering zone along their axis perhaps due to the presence of fine-grained in-fill.

A zone of giant scours, similar to those described previously (Kenyon et al., 1995), was observed on the sonographs in the west of the mapped area (Fig. 2). They are up to 900 m across and 10-20 m deep.

The terminal lobe is mapped at the south of the area. The sonographs showed a dendritic pattern of channel-like high

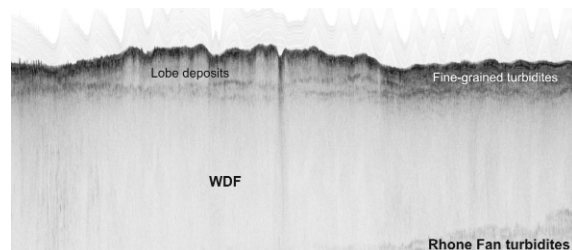


Figure 4. 5 kHz profile across the terminal lobe. Western Debris flow deposits (WDF, Bonnel et al., 2005) appear transparent.

backscattering features 15 to 50 m wide (Fig. 3) characterised by considerably reduced penetration on the associated 5 kHz profiler records (Fig. 4). The patchy distribution of low and high acoustic facies with the dominance of the former was interpreted as due to the presence of the fine-grained hemipelagic cover draping most of the terminal lobe deposits.

I.3. Bottom Sampling

20 sedimentary cores were collected in the study area (Table 1 and Annex I). The total recovery was nearly 16 m with individual core lengths of between 22 and 268 cm. The cores were taken from a variety of environments ranging from large by-pass channels to individual finger-shaped features within the terminal lobe.

Cores from the by-pass channels confirmed the presence of fine-grained hemipelagic in-fill in some of the channel. The cores (e.g. MS365G) recovered relatively thick sequence of hemipelagic clays with occasional fine-grained turbidites.

Most of the cores aimed at the finger shaped features had limited penetration of about 50 to 100 cm. A small amount of fine-grained sand found in the core-catchers suggest that the corer has been stopped by sand-rich deposits of the lobe. Further onshore analyses are planned to investigate the properties of these sands.

The cores from the interchannel area (e.g. MS-377G) usually have better recovery which is thought to be due to the ponding effect of the hemipelagic sediments in the lows within the lobe terrain.

Most of the cores contain intervals enriched in washed-out Pteropoda shells or thin layers of foraminifera sands. The cores taken from the areas where the ponding effect was anticipated, e.g. topographic lows, usually contain thicker Pteropoda-rich horizons (Fig. 5). The nature of these deposits is not clear. The absence of fine grained material in these horizons indicates the prolonged processing of the sediments by some sort of a current. The surge-like turbidity currents known to sweep the area (Bonnell et al., 2005) are unlikely to produce such deposits. The

Table 1. General information on the cores collected from the distal Rhone Neofan area during Leg 1.

Core №	Date	Time, UTC	Latitude	Longitude	Depth, m
TTR16-MS362G	19.05.06	03:29	41°33.763'N	04°48.005'E	2548
TTR16-MS363G	19.05.06	04:06	41°33.758'N	04°48.103'E	2552
TTR16-MS364G	19.05.06	07:25	41°31.705'N	04°48.200'E	2558
TTR16-MS365G	19.05.06	12:35	41°49.513'N	04°54.051'E	2444
TTR16-MS366G	19.05.06	16:53	41°49.517'N	04°53.532'E	2430
TTR16-MS367G	19.05.06	18:28	41°49.512'N	04°52.729'E	2445
TTR16-MS368G	19.05.06	20:02	41°49.514'N	04°52.237'E	2435
TTR16-MS369G	20.05.06	10:39	41°33.764'N	04°47.996'E	2552
TTR16-MS370G	20.05.06	13:35	41°29.182'N	04°46.747'E	2572
TTR16-MS371B	20.05.06	15:28	41°29.178'N	04°46.741'E	2572
TTR16-MS372G	23.05.06	02:31	41°34.006'N	04°48.028'E	2545
TTR16-MS373G	23.05.06	03:59	41°34.013'N	04°47.987'E	2544
TTR16-MS374G	23.05.06	05:29	41°34.109'N	04°48.058'E	2544
TTR16-MS375G	23.05.06	06:58	41°34.114'N	04°48.054'E	2548
TTR16-MS376G	23.05.06	08:36	41°33.963'N	04°47.936'E	2550
TTR16-MS377G	23.05.06	10:09	41°33.925'N	04°47.959'E	2551
TTR16-MS378G	23.05.06	11:39	41°34.020'N	04°47.987'E	2555
TTR16-MS379G	23.05.06	13:02	41°34.120'N	04°48.032'E	2550
TTR16-MS380G	23.05.06	14:50	41°33.847'N	04°47.995'E	2552
TTR16-MS381B	23.05.06	16:49	41°33.850'N	04°48.010'E	2552

recent finding of the cascading currents emanating from the shelf areas and spreading into deeper parts of the GOL margin (Canals et al., 2006) provides a better explanation for the formation of the Pteropoda-rich intervals. The sedimentary cores indicate the presence of multiple events when the large areas of the seabed have been swept by the cascading bottom current emanating from the shelf.

In summary, the sampling showed that most of the depositional elements of the distal Rhone Neofan has been draped by hemipelagic sediments since its last active phase. Our new data provide new insights on the hemipelagic processes in the area and emphasise the possible importance of shallow-born cascading currents for the modern deep-water depositional environment of the distal Rhone Neofan.



Figure 5. Pteropoda-rich intervals in the core AT377G.

II. GULF OF CADIZ (LEG 2)

II.1. Introduction and Objectives

During the TTR-9 (1999) a large mud volcano field was discovered in the Spanish and Moroccan sectors of the Gulf of Cadiz (Gardner, 1999; Kenyon et al., 2000; Gardner, 2001), based on the interpretation of a sidescan mosaic collected in the area in 1992 (courtesy of Joan Gardner, Naval Research Laboratory (NRL), Washington D.C.). Five mud volcanoes were then identified in this area: TTR, Kidd and Adamastor, in the Eastern Moroccan Field, and Yuma and Ginsburg, in the Middle Moroccan Field. Gas hydrates were recovered from the Ginsburg Mud Volcano. The following year, a deep mud volcano field was discovered in the South Portuguese Margin (Pinheiro et al., 2003). In the subsequent years the Gulf of Cadiz has been extensively investigated during 8 research cruises: TTR-10, Anastasya, TTR-11, TTR-11A, Tasyo, Cadipor, TTR-12,

GAP, TTR-14, Merian Cruise; Charles Darwin 178 and TTR-15. A large number of mud volcanoes (38 confirmed by coring), as well as several mud diapirs (e.g. Lolita, Ibérico) and elongated diapiric ridges (e.g. Guadalquivir, Cadiz, Formosa, Vernadsky and Renard) have been identified up to the present. Extensive areas of carbonate crusts and chimneys were found in the northern part of the Gulf of Cadiz, near the main channel of the Mediterranean Outflow (MOW), in several diapiric ridges, characterized by a strong-backscatter signature on sidescan sonar images (Diaz-del-Rio et al., 2003). Gas hydrates have been recovered from three mud volcanoes in this area: Bonjardim, Captain Arutjunov and Ginsburg, and there are indications that gas hydrates may also occur in the Carlos Ribeiro mud volcano.

The TTR-16 Leg 2 was focussed on two main areas (Fig. 6): (1) the Middle Moroccan Field, and (2) the Deep Portuguese

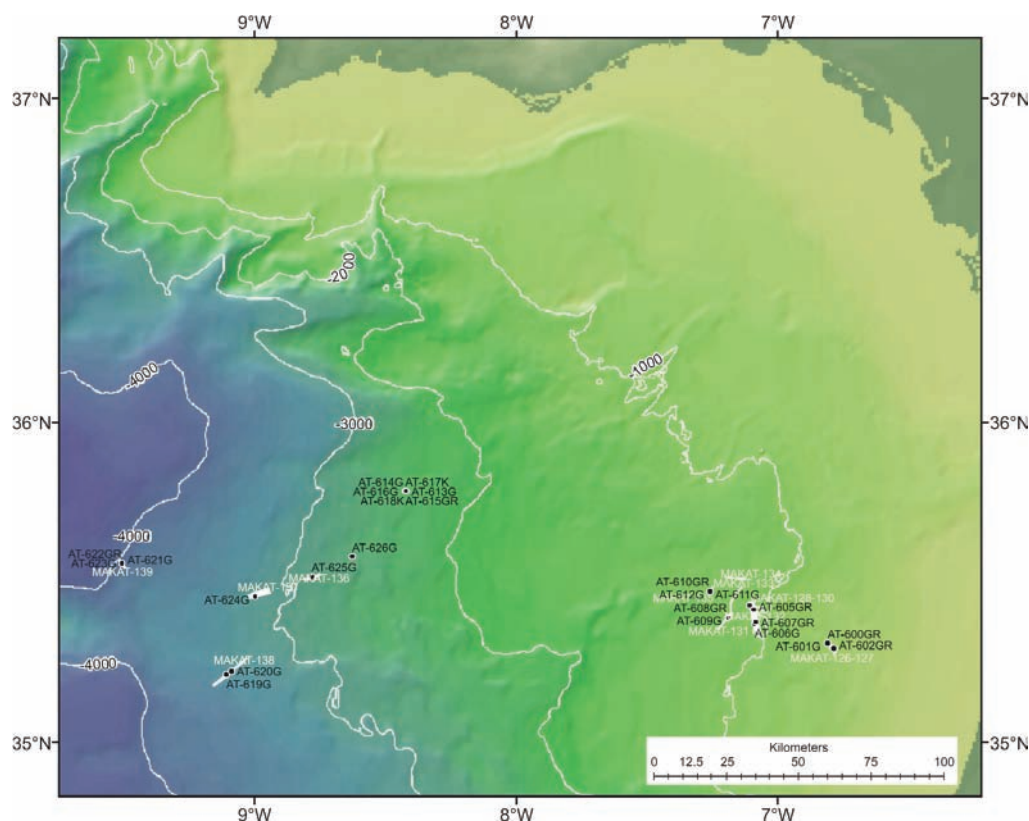


Figure 6. Summary of the research work carried out during the TTR-16 Leg 2.

Field. The Moroccan Fields are the area of the Gulf of Cadiz where the largest mud volcanoes are found (e.g. Al Idrisi, Mercator, Gemini, Yuma, Ginsburg). Several areas of carbonate mounds, often covered with cold water coral communities, as well as fault-controlled ridges (e.g. Pen Duick Escarpment, Vernadsky Ridge) are also found in this area. The Deep Portuguese field is the area where the deepest mud volcanoes were found in the Gulf of Cadiz.

The main objectives of this cruise were:

- (1) To investigate the Pen Duick Escarpment to better understand this complex feature and associated ecosystems, through TV-controlled grab profiles, high resolution deep towed sidescan sonar (MAK-100 kHz), single channel reflection seismic profiling, coring and sampling for geological, biological, microbiological and geochemical studies.
- (2) To re-visit the Yuma and Ginsburg mud volcanoes for detailed studies, in particular high-resolution 100 kHz MAK profiling, coring, TV-grab lines and to investigate several high-backscatter structures in their vicinity.
- (3) To carry out detailed studies in the Deep Portuguese Field. This includes re-visiting the Carlos Ribeiro mud volcano, to investigate one new high-backscatter structure between Olenin and Bonjardim, and to re-visit the deepest mud volcanoes discovered during the TTR-15 cruise: Semenovich, Soloviev, Carlos Teixeira and Porto.

I.2. Geological Setting and Study Areas

The Gulf of Cadiz is located at the westward front of the Betic-Rifian Arc, in the easternmost sector of the Azores-Gibraltar segment of the Africa/Eurasia collisional plate boundary. It has had a very complex geological history and has undergone several episodes of rifting, compression and strike-slip motion since the Triassic (Wilson et al., 1989; Dewey et al., 1989; Maldonado et al., 1999). The westward migration of the Alboran domain during the Miocene caused the Gulf of Cadiz to form as a forearc basin

associated with the formation of the Betic-Rifian Arc (Bonnin et al., 1975; Auzende et al., 1981; Maldonado and Comas, 1992; Lonergan and White, 1997; Maldonado et al., 1999). This phenomenon was related to the post-Oligocene extensional regime in the western Mediterranean and the formation of the Neogene backarc basins (Royden, 1993; Lonergan and White, 1997; Rosenbaum et al., 2002). In Tortonian times, a large body was emplaced in the Gulf of Cadiz.

During the final stages of the accretion of the Betic-Rifian Arc and the emplacement of the thrusting units, gravitational sliding of mobile shale and salt stocks formed a giant complex of mass-wasting deposits, generally known as the Gibraltar Olistostrome that reached as far west as the Horseshoe and Seine abyssal plains. This feature appears as a chaotic, highly diffractive body, with high-amplitude reflections on the seismic sections (Riaza and Martínez del Olmo, 1996) and it consists of a mixture of Triassic, Cretaceous, Paleogene and Neogene sedimentary units, overlying a Palaeozoic basement (Maldonado et al., 1999). It involves a huge volume of mud and salt diapirism of Triassic salt units and under-compacted Early-Middle Miocene plastic marls (Maldonado et al., 1999). The origin of this chaotic body is highly controversial. It has been interpreted as a complex of olistostromes and debris flows, originated by gravitational sliding, and tectonic thrust units - tectonic mélanges (Torelli et al., 1997; Maldonado et al., 1999; Medialdea et al. 2004). Alternatively, it is also interpreted as an accretionary complex related to the migration of the Alboran terrain as a consequence of an once active subduction zone (Royden, 1993; Lonergan and White, 1997; Rosenbaum et al., 2002). Recently, Gutscher et al. (2002) proposed that this subduction is still active beneath Gibraltar.

Throughout this area, extensive hydrocarbon-rich fluid venting and mud diapirism are observed, which includes numerous mud volcanoes, methane-related authigenic carbonates (crusts, chimneys and carbonate mounds) and pockmarks (Baraza and Ercilla, 1996; Gardner, 2001; Kenyon et

al., 2000; Pinheiro et al., 2003). These are related to both the high sedimentation rates during the Pliocene, associated with high subsidence (Maldonado et al., 1999), and to the lateral compression due to the Africa-Eurasia convergence, both of which promoted the fluid migration to the surface. Several NE-SW oriented mud diapiric ridges have been found in the NE sector of the Gulf of Cadiz, which are characterized by high backscatter on the available sidescan sonar imagery. There is a strong suggestion that these features are strongly structurally controlled. Sampling has shown that the high backscatter is related to a high abundance of carbonate chimneys and crusts on top of these ridges (Diaz del Rio et al., 2001; Somoza et al., 2003).

Focal mechanism solutions show that the stress regime along the Africa-Eurasian plate boundary in this area is a combination of dextral strike-slip and a NW-directed compression near Gorringer Bank and the Gulf of Cadiz (Fukao, 1973; Borges et al. 2001). Presently, the direction of maximum horizontal compressive stress along this segment of the plate boundary is estimated to be approximately WNW-ESE in the Gulf of Cadiz, leading to a general transpressive regime in this area (Cavazza et al., 2004).

Middle Moroccan Mud Volcano Field

TTR-16 Leg 2 concentrated on three main areas in the Middle Moroccan Field: (1) the Pen Duick Escarpment; (2) the Yuma and Ginsburg mud volcanoes; (3) three new structures west of Yuma and Ginsburg; (4) the Student mud volcano.

The Pen Duick escarpment was investigated with two 100 kHz sidescan sonar MAK lines, and three TV-controlled grab profiles and stations.

Yuma and Ginsburg mud volcanoes were covered with 100 kHz sidescan sonar imaging. One core (AT603G) and two TV-grab profiles and stations (AT604GR and AT605GR) were acquired on the Yuma mud volcano. One gravity core (AT606G) and one TV-controlled grab (AT607GR) were acquired on the Ginsburg mud volcano.

Deep Portuguese Mud Volcano Field

The Deep Portuguese mud volcano field is the area of the Gulf of Cadiz where the deepest mud volcanoes are found (e.g. Porto, Semenovich, Bonjardim, Olenin, Carlos Ribeiro). The main objective of the TTR-16 Leg 2 cruise in this area was to investigate one as yet unexplored high backscatter structure, between the Olenin and Bonjardim mud volcanoes and also to revisit several volcanoes (Porto, Semenovich and Carlos Ribeiro) for more detailed and complementary studies (seismic reflection profiles, high resolution 100 kHz sidescan sonar MAK lines and coring).

II.3. MAK Deep-Towed Sidescan Sonar and Sub-bottom Profiler

L.M. PINHEIRO, H. DUARTE, DUARTE, J., M. CHAFIC, A. AKHMETZHANOV, V. MAGALHÃES, J. CASTRO, AND I. MARTINS.

Lines MAKAT-126 and MAKAT-127 - Pen Duick Escarpment

The Penduick escarpment is a fault scarp about 4.5 km long, west of Gemini, with a general NNW-SSE to N-S trend. The escarpment is about 100 m high, and the water depth at its top is 525 m. The main escarpment is crossed by small parallel elongated E-W ridges with a sharp relief, with erosional scour channels, probably related to strong bottom currents. This area was previously investigated with sidescan sonar during the TTR-12, 14 and 15 cruises. During the TTR-16 cruise two MAK 100 kHz deep-towed sidescan sonar lines (MAKAT-126- MAKAT-127) were run to investigate in more detail this area (Fig 7).

An area of carbonate crust occurrence previously found during TTR-12 cruise (Kenyon et al., 2003) at the base of the escarpment was imaged with better detail to the northwest and southeast. The area of carbonate crusts corresponds to a high backscatter linear feature trending NNW-SSE parallel to the main escarpment and appear to extend towards the south, under a veneer of sedi-

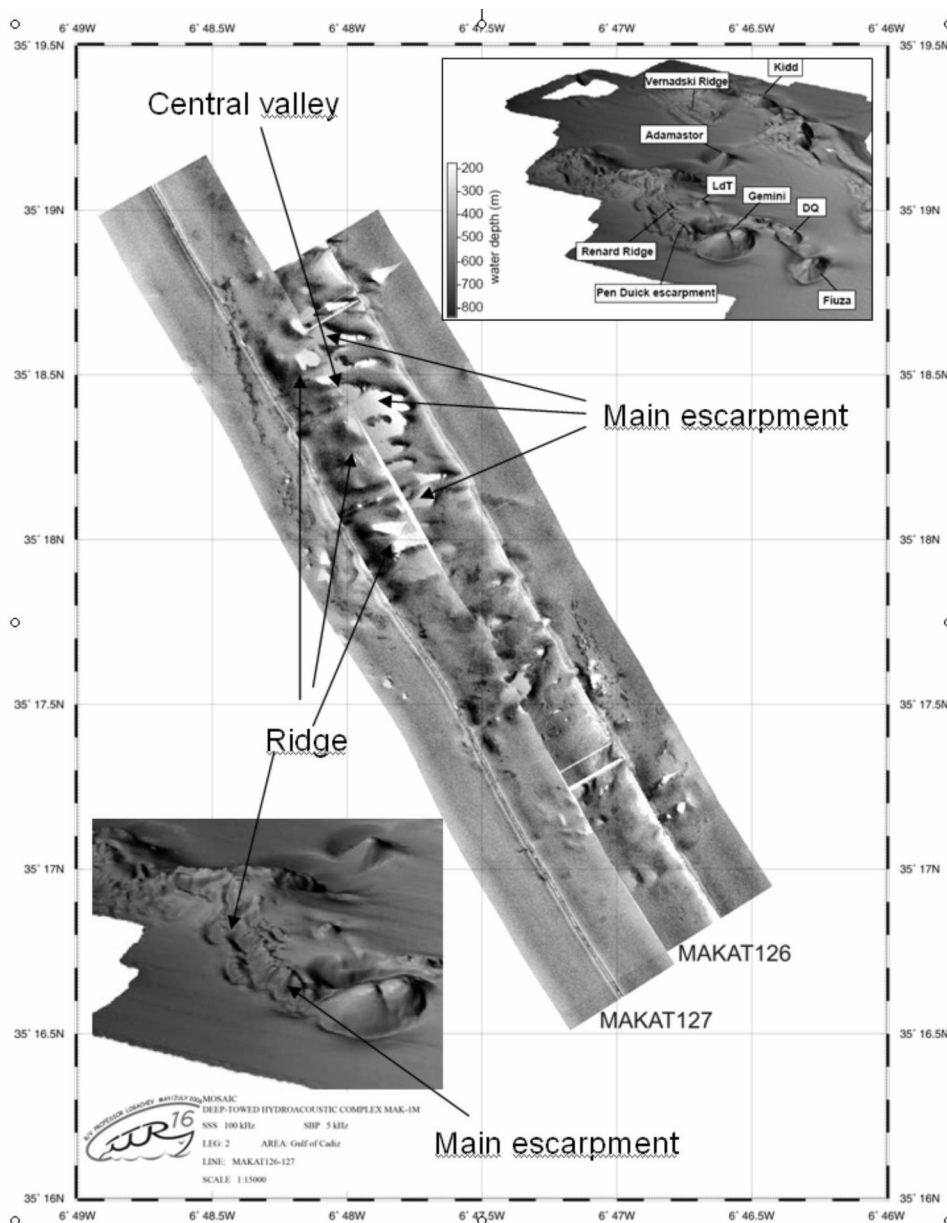


Figure 7. Pen Duick escarpment. 100 kHz sidescan sonar mosaic from lines MAKAT-126 and 127.

ments. The feature is interpreted as a major fault. The formation of the carbonate slabs is likely to be caused by the fluid escape along the fault. A series of elongate carbonate mounds growing perpendicularly to the escarpment along its edge is also imaged.

Lines MAKAT 128–130: Yuma and Ginsburg mud volcanoes

Three parallel NNW-SSE 100 kHz MAK lines (AT128, AT129 and AT130) were

acquired over the Ginsburg and Yuma mud volcanoes in order to obtain high resolution images of these features (Fig. 8). Ginsburg is a conical shaped mud volcano, 250 m high, with a diameter of about 3.8 km at the base and 0.4 km at the top. Yuma is also a conical shaped mud volcano, approximately 250 m high, about 4.5 km wide at the base and 2 km at the top.

The moats that surround both Yuma and Ginsburg mud volcanoes are clearly imaged on the three MAK 5kHz profiles (Fig. 9). The main sedimentary horizons are sub-

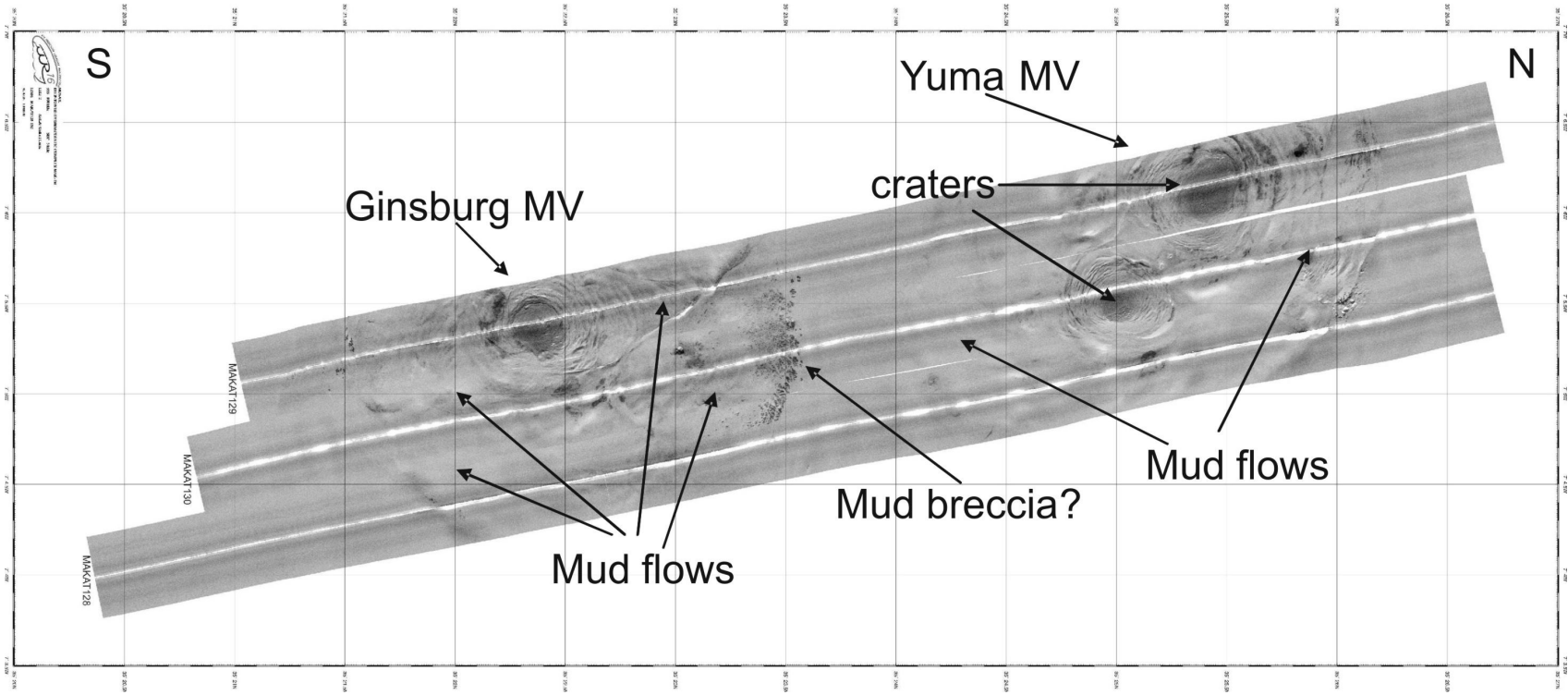


Figure 8. Yuma and Ginsburg mud volcanoes. 100 kHz sidescan sonar mosaic from lines MAKAT-128 to MAKAT-130.

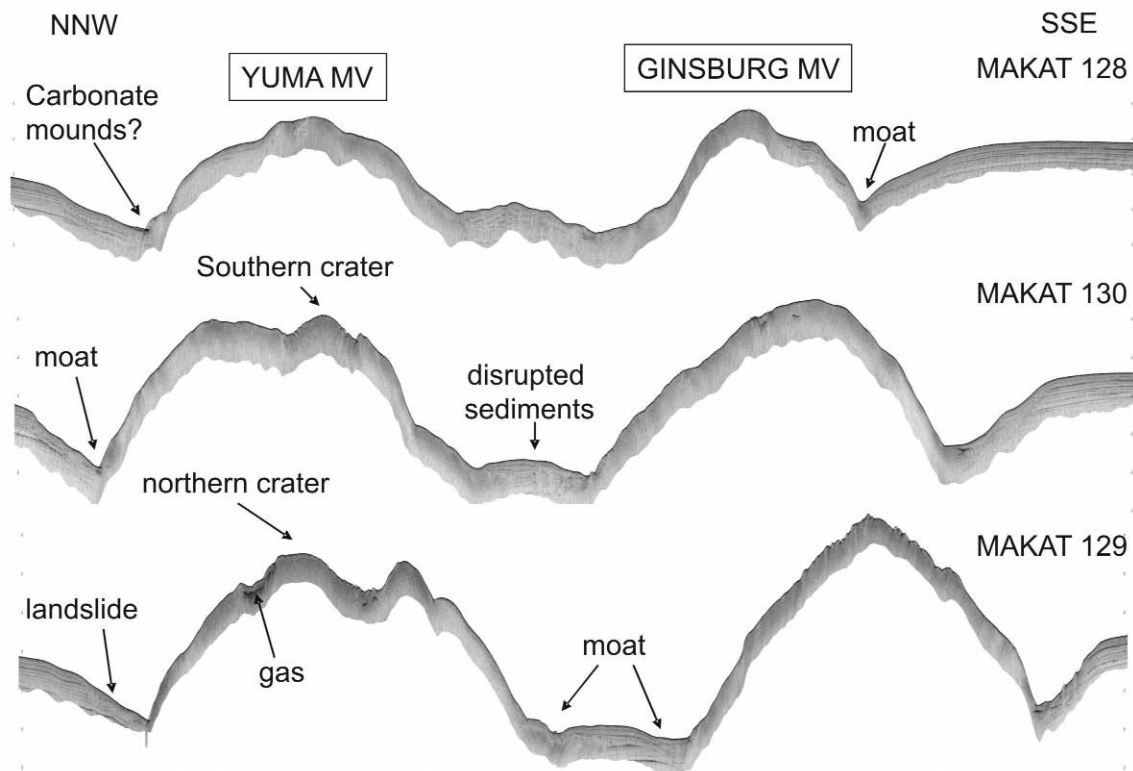


Figure 9. Yuma and Ginsburg mud volcanoes. 5 kHz sub-bottom profiles from Lines MAKAT-128 to MAKAT-13.

horizontal and undisturbed away from the mud volcanoes. However, the horizons progressively dip towards the mud volcanoes, are often faulted and small landslides are also observed in the vicinity of the mud volcanoes. The seismic horizons are clearly disrupted, folded and faulted in the segments close to and between the Yuma and Ginsburg mud volcanoes (Fig. 9).

MAKAT-128 5kHz profile crosses the eastern flank of the mud volcanoes. Folded seismic horizons characterize the southern flank of the Ginsburg mud volcano. The northern moat of the Yuma mud volcano corresponds to a very disturbed area, with evidence of extensive faulting, collapse structures and landslides. Two small elevations observed at the base of the mud volcano are associated with a high amplitude reflection and could be small carbonate mounds. MAKAT-129 profile crosses the centers of both mud volcanoes revealing the differences in their morphology. The Ginsburg mud volcano has a single crater while Yuma is wider due the presence of two.

MAKAT-130 5kHz profile crosses the second crater of the Yuma MV and the eastern flank of Ginsburg MV. The moats surrounding Ginsburg and Yuma MVs show an asymmetric V-shaped geometry.

Line MAKAT-131 – Pockmark and Darwin Mud Volcano

This line crosses two new structures which are imaged on the NRL Seamap mosaic (Gardner, 1999; 2001) as high-backscatter patches, and which were investigated with single-channel seismic profiling (Line PSAT-123) during the TTR-9 cruise (Kenyon et al., 2000). The southernmost structure looked like a collapse structure, whereas the northernmost one appeared to be a mud volcano. Line MAKAT-131 is approximately coincident with the TTR-9 PSAT-123 seismic line. Swath bathymetry recently acquired during the CD-178 (RRS Charles Darwin, 2006) confirmed that the southernmost feature is indeed a near circular collapse structure, probably a pockmark, that appears to be

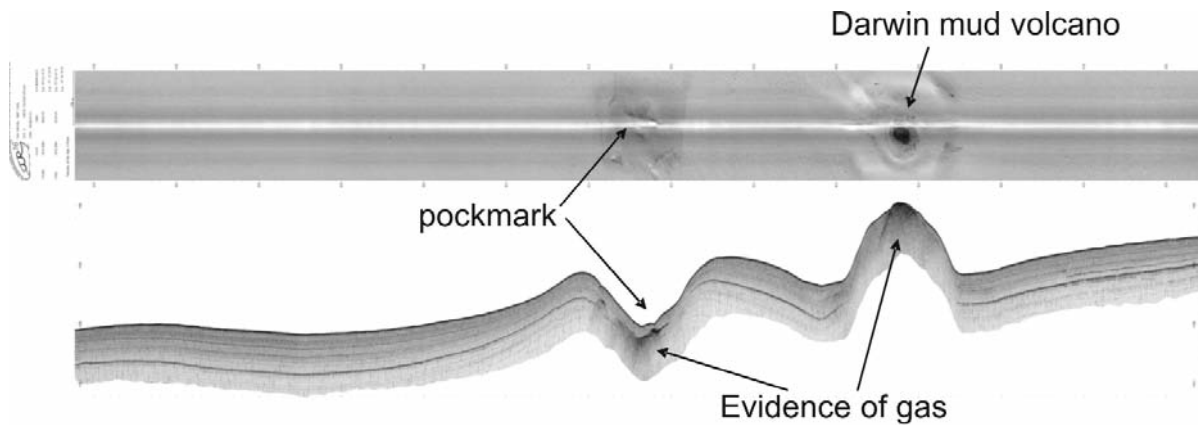


Figure 10. Line MAKAT-131: 100 kHz sidescan sonar image and sub-bottom profile across Darwin MV and associated pockmark.

located on an approximately WNW-ESE ridge. It is about 50 m deep and 700 m wide at the surface and its diameter at the bottom is about 130 m. There are clear indications of the presence of gas below the pockmark (Fig. 10). The surrounding strata are deformed under compression, forming an anticlinal ridge.

The northernmost structure is the Darwin mud volcano, with an approximate diameter of 750 m. The top of the volcano is characterized by the presence of very high backscattering patch about 100 m across, which was interpreted as its crater.

Line MAKAT-132 – possible inactive mud volcano

This N-S trending MAK line (Fig. 11) crosses a near circular structure, 70 m high,

surrounded by a moat, which can be observed on the NRL Seamap mosaic (Gardner, 1999; 2001), west of the Yuma mud volcano. The sedimentary layers to the south form an asymmetric fold, with minor extensional faulting, some of which reaches the seafloor, whereas the layers to the north are essentially undeformed. This structure, which is probably an inactive mud volcano covered with sediments, is located at the foot of the northern steepest flank of an asymmetric fold, possibly at the tip of a south-dipping thrust, which might have acted as the main fluid conduit (Fig. 11). The backscatter associated with this feature is low, but a few small dark spots with higher backscatter are observed at the top and also in the vicinity of the moat area; these could correspond to the presence of carbonates in localized seeps. One NE-SW fault and smaller WNW-ESE

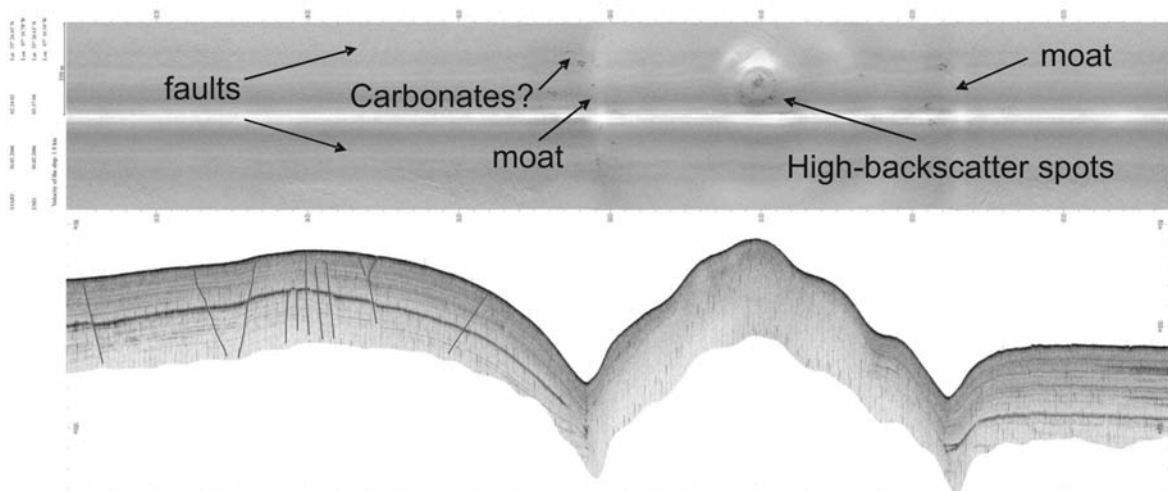


Figure 11. MAKAT-132: 100 kHz sidescan sonar image and sub-bottom profile.

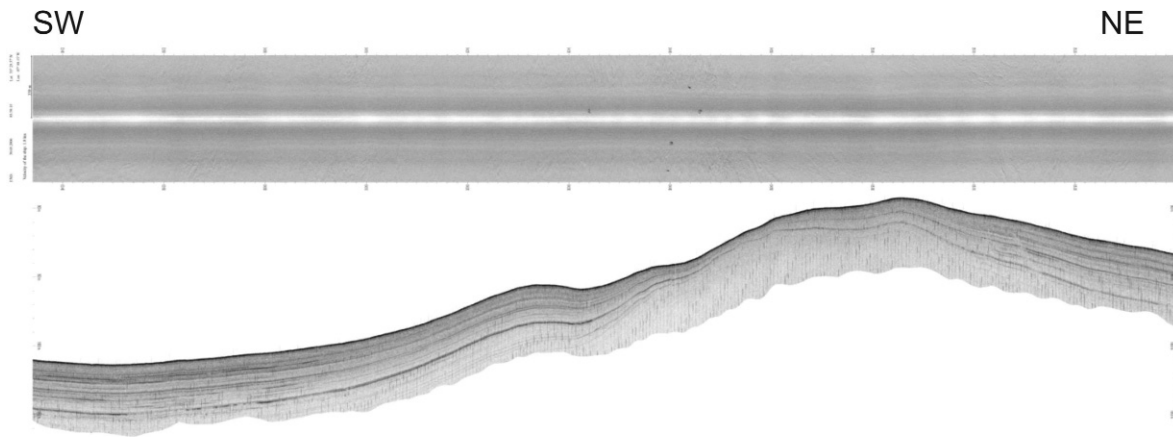


Figure 12. Line MAKAT-133: 100 kHz sidescan sonar image and sub-bottom profile.

faults are observed on the MAK record to the south of this structure (Fig. 11).

Line MAKAT-133

This SW-NE MAK line (Fig. 12) is a transit line to the line MAKAT-134. It crosses an area with a slightly high backscatter observed on the NRL sidescan sonar mosaic. The MAK line does not show any prominent features and the sub-bottom profiler record shows that the sedimentary layers thin towards the seafloor high in an asymmetric way, consistent with compressional deformation associated with thrusts dipping to the NE.

Line MAKAT-134

This E-W 100 kHz MAK line (Fig. 13) crosses the Student mud volcano, which was discovered during the TTR-10 cruise (Kenyon et al., 2001), based on the NRL sidescan sonar mosaic. This mud volcano is 200 m high and it has a very sharp morphology, with a diameter of about 1.7 km at its base and 0.2 km at the top. The new data clearly show that this mud volcano is delimited by a well-defined moat, particularly on the westernmost flank, where there are small features that are probably carbonate mounds. Several mud flows are also observed on the MAK line. The sub-bottom

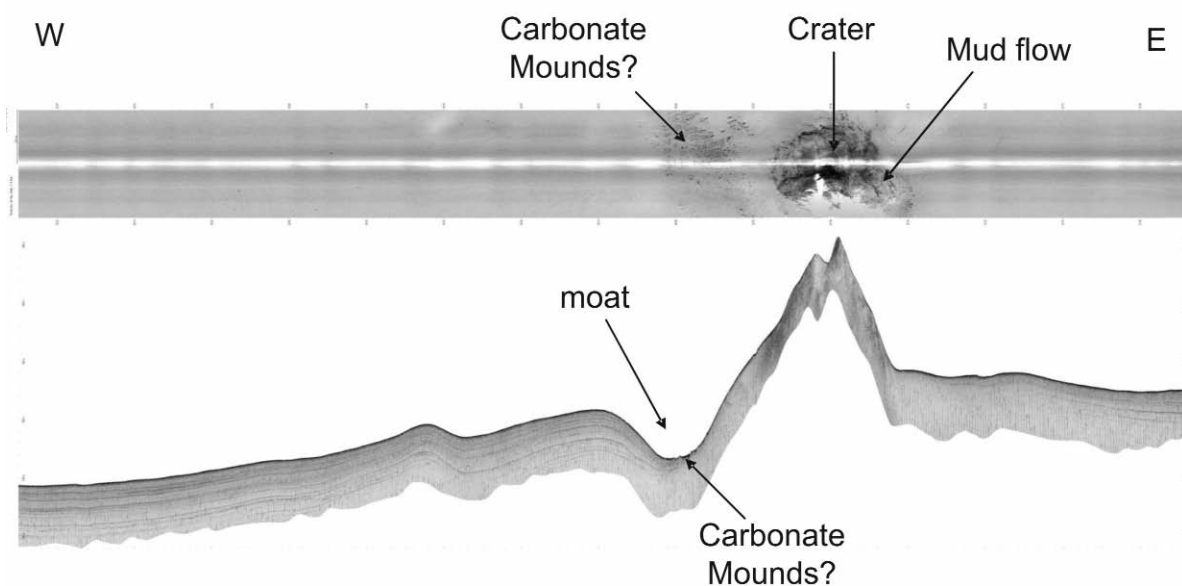


Figure 13. Line MAKAT-134: 100 kHz sidescan sonar image and sub-bottom profile across the Student mud volcano.

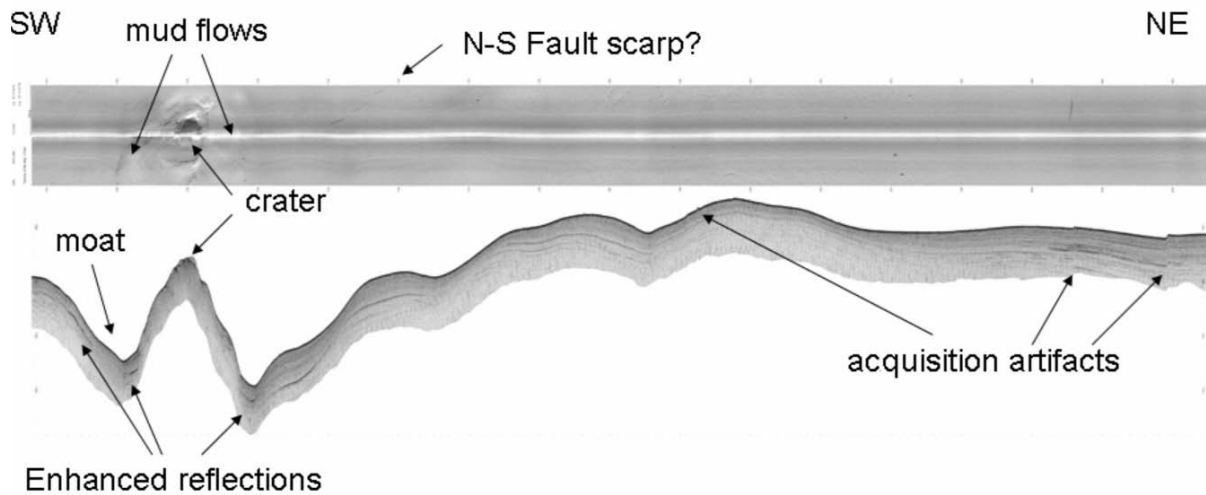


Figure 14. Line MAKAT-135: 100 kHz sidescan sonar image and sub-bottom profile across the Shouen volcano.

profiler shows that this structure is at the edge of an asymmetric long-wavelength east trending fold (Fig. 13).

Line MAKAT-135 – Shouen mud volcano

This NE-SW 100 kHz MAK line (Fig. 14) crosses a new mud volcano, named Shouen, that can be observed on the NRL mosaic as a high backscatter feature, approximately 16 km to the WNW of the Yuma mud volcano. It is conical-shaped, 150 m high, with a diameter of about 1.1 km at its base and 0.7 km at the top. During the TTR-16 Leg 2, one TV-controlled grab (AT610GR) and two gravity cores (AT611G and AT612G) were collected on this structure, revealing mud breccia covered by an hemipelagic marl layer, confirming it to be a mud volcano. The sidescan sonar line shows a clear moat surrounding this structure.

Line MAKAT-136 – Bomboca mud volcano

The line MAKAT-136 crosses a new mud volcano called Bomboca. It is a 130 m high, 1000 m in diameter, with very steep flanks (over 10° slopes), and a relatively shallow moat on its northeastern flank (Fig. 15).

It appears to have two high backscatter small craters, approximately 100 m wide. Mud flows observed on its southern flank are

marked by 100 metres long gullies that are parallel to the mud flow directions. A few, relatively high backscatter patches suggest the existence of carbonate slabs or corals at the foot of the southern flank. The surrounding sedimentary layers observed on the sub-bottom profile are parallel to the sea-floor and do not exhibit any lateral changes in thickness, nor any clear evidence of deformation. A few small negative relief features, probably pockmarks, less than 50 m wide, are also observed mainly on the southern flank of this structure.

Line MAKAT-137 – Bonjardim mud volcano

The line MAKAT-137 crosses the Bonjardim mud volcano, a structure which was discovered during TTR-10 (Kenyon et al., 2001) and revisited during TTR-15. This structure was previously investigated with seismic reflection profiles (lines PSAT-146 and 147), gravity cores (AT226G, AT227G, AT228G, AT246G and AT598G) and one TV controlled grab (AT597GR).

During the TTR-16 cruise, one 30kHz MAK line was acquired across the mud volcano (Fig. 16). The Bonjardim mud volcano is 150 m high and 2000 m in diameter. The crater rim is well developed, enclosing the 800 m wide, very high backscatter crater domain. On the southeastern end of the crater there is a small, elevated area about

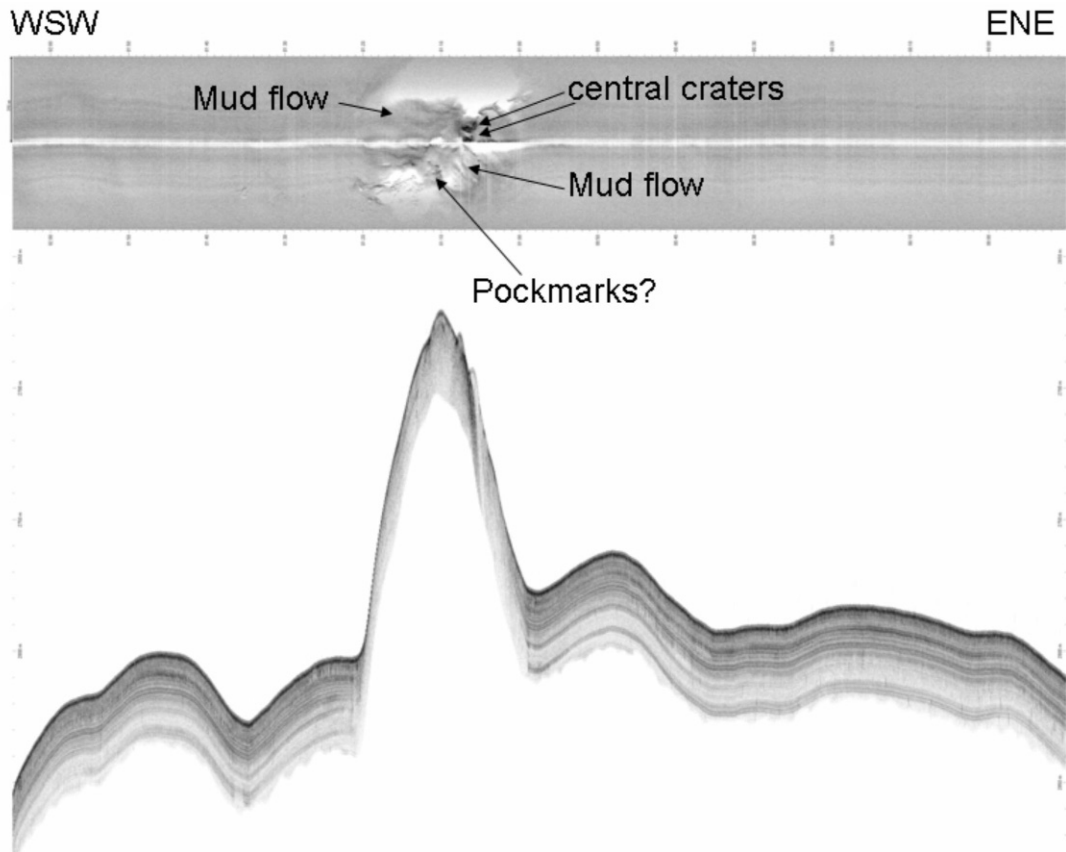


Figure 15. Line MAKAT-136: 100 kHz sidescan sonar image and sub-bottom profile across the Bomboca mud volcano.

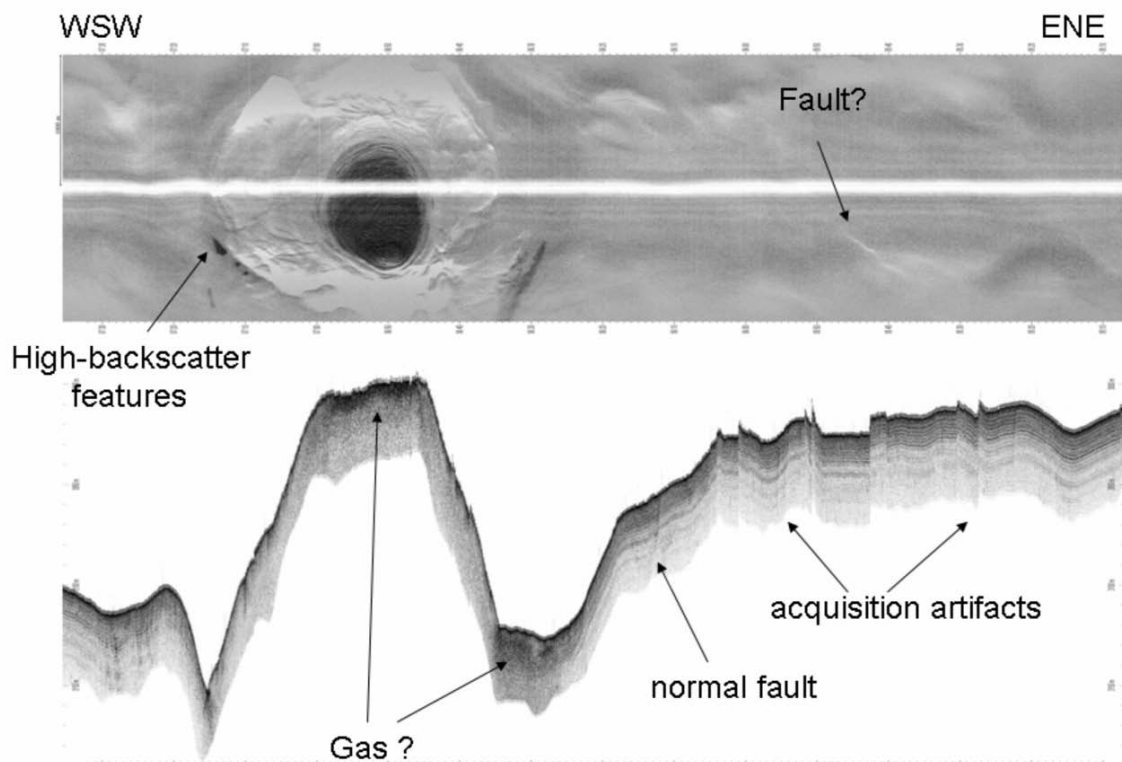


Figure 16. Line MAKAT-136: 30 kHz sidescan sonar image and sub-bottom profile across the Bonjardim mud volcano.

150 m in diameter. The western flank of the Bonjardim mud volcano is cut by a NE-SW slope failure, over 1000 m long that appears to be related to a particularly large mud flow. Various gullies with a general WSW-ENE trend (parallel to the nadir but that do not appear to be artifacts) cross the surface of this and other large mud flows that can be observed down to the moat edge. Several relatively high backscatter patches are observed in the moat (to the SW) that may be caused by carbonate slabs, mud breccia or corals. The sediment layering observed on the sub-bottom profile forms a continuous succession without significant lateral changes in thickness, and exhibits local interruptions of continuity close to the Northeastern edge of the moat, which suggests that the sediments are cut by normal faults. Local acoustic turbidity can be observed on the crater and moat segments of the sub-bottom profile.

Line MAKAT-138 – Semenovich, Soloviev and Carlos Teixeira Mud Volcanoes

These three NE-SW aligned structures – Semenovich, Soloviev and Carlos Teixeira were discovered during TTR-15, based on the interpretation of the NRL sidescan sonar mosaic and on high-resolution bathymetry from the Delila cruise

(Gutscher et al., 2004). During the TTR-15 cruise, they were then investigated with a seismic reflection profile (line PSAT 279), and three gravity cores, one on each of these three structures (AT593, AT594G and AT595G).

During the TTR-16 cruise, these structures were crossed with the 100 kHz MAK line MAKAT-138 (Fig. 17). This line shows that Semenovich, the northeasternmost mud volcano is located at approximately 3200 m water depth, it is 70 m high, with two craters with high backscatter and sharp rims, and well defined mud flows that are more developed to the Northwest. Strong acoustic turbidity, possibly caused by gas, is observed on the sub-bottom profile, not only on this mud volcano, but also on the Soloviev mud volcano. Soloviev mud volcano is located at approximately 3240 m water depth, it has a very high backscattering crater, 800 m wide and well defined mud flows.

The new 100 kHz MAK line shows that the Carlos Teixeira structure is very steep, 85 m high, located at 3350 m water depth, with a weak backscatter (which could also be caused by the steepness of the structure), without evidence of mud flows.

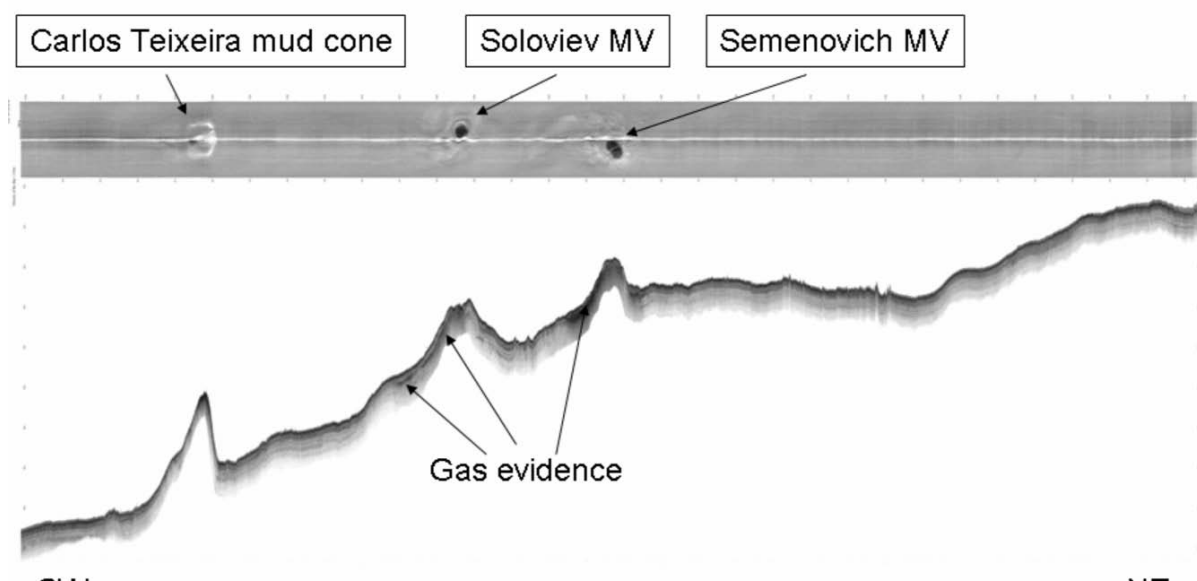


Figure 17. Line MAKAT-138: 100 kHz sidescan sonar image and sub-bottom profile across the Semenovich and Soloviev mud volcanoes and the Carlos Teixeira mud cone.

II.4. Bottom Sampling Results

A. AKHMETZHANOV AND THE SEDIMENTOLOGY TEAM OF LEG 2.

Bottom sampling during Leg 2 was focused on sites where fluid escape structures were detected on geophysical data. Sediments from 27 stations were retrieved using gravity and kasten corers and TV-guided grab (Tables 2 and 3, Annex I).

Sampling was conducted in two principal areas: Moroccan margin and deep water Portuguese margin.

Moroccan margin

Pen Duick escarpment

A newly obtained 100 kHz image of the escarpment served as a basemap for locating the sampling sites. A highly

backscattering fault running along the base of the escarpment was sampled by a TV-guided grab (AT600G) and a gravity corer (AT601G) (Fig. 18). The grab retrieved fragments of carbonate crusts together with coral and shell debris. The core recovered an almost 2.5 m long sequence of grey clay with strong H₂S smell topped by a layer of marl with abundant coral debris.

Area around Yuma and Ginsburg mud volcanoes

The new high resolution sidescan sonar data revealed several locations on the slopes of Yuma and Ginsburg mud volcanoes where the presence of cold seeps was anticipated (Fig. 19). The sites of interest were usually characterised by high backscatter and sampling by gravity corer and TV-guided grab confirmed that this is due to the

Table 2. General information on the cores from the Gulf of Cadiz, Leg 2.

Core №	Date	Time, UTC	Latitude	Longitude	Depth, m	Recovery
<i>Moroccan Margin</i>						
TTR16-AT600GR	28.05.06	07:40	35°18.779N	06°48.453W	610	0.5 t
TTR16-AT601G	28.05.06	09:03	35°18.764N	06°48.458W	642	236 cm
TTR16-AT602GR	28.05.06	12:31	35°17.693N	06°47.089W	556	0.1 t
TTR16-AT603G	29.05.06	08:06	35°25.823N	07°06.331W	1015	137 cm
TTR16-AT604GR	29.05.06	09:33	35°25.820N	07°06.330W	1030	0.5 t
TTR16-AT605GR	29.05.06	14:59	35°25.046N	07°05.450W	975	0.5 t
TTR16-AT606G	29.05.06	17:11	35°22.390N	07°05.320W	923	60 cm
TTR16-AT607GR	29.05.06	20:39	35°22.677N	07°04.979W	983	0.5 t
TTR16-AT608GR	30.05.06	16:49	35°23.531N	07°11.475W	1115	0.1 t
TTR16-AT609G	30.05.06	18:22	35°23.530N	07°11.477W	1125	CC
TTR16-AT610GR	30.05.06	22:21	35°28.468N	07°15.477W	1177	0.5 t
TTR16-AT611G	30.05.06	23:23	35°28.460N	07°15.473W	1180	169 cm
TTR16-AT612G	31.05.06	00:12	35°28.513N	07°15.533W	1173	147 cm
<i>Portuguese Margin</i>						
TTR16-AT613G	31.05.06	08:44	35°47.260N	08°25.241W	2204	251 cm
TTR16-AT614G	31.05.06	10:09	35°47.246N	08°25.298W	2210	85 cm
TTR16-AT615GR	31.05.06	12:22	35°47.238N	08°25.272W	2200	0.5 t
TTR16-AT616G	31.05.06	14:10	35°47.246N	08°25.300W	2200	167 cm
TTR16-AT617K	31.05.06	16:42	35°47.270N	08°25.360W	2230	50 cm
TTR16-AT618K	31.05.06	18:03	35°47.246N	08°25.303W	2220	40 cm
TTR16-AT619G	02.06.06	02:19	35°12.785N	09°06.450W	3295	117 cm
TTR16-AT620G	02.06.06	04:22	35°13.429N	09°05.198W	3243	143 cm
TTR16-AT621G	02.06.06	18:44	35°33.778N	09°30.396W	3921	135 cm
TTR16-AT622GR	03.06.06	02:12	35°33.773N	09°30.416W	3902	0.5 t
TTR16-AT623G	03.06.06	06:09	35°33.761N	09°30.459W	3875	162 cm
TTR16-AT624G	03.06.06	11:29	35°27.556N	08°59.840W	3065	195 cm
TTR16-AT625G	03.06.06	16:38	35°31.129N	08°46.870W	2750	266 cm
TTR16-AT626G	03.06.06	17:23	35°35.002N	08°37.544W	2628	480 cm

Table 3. Sedimentological, acoustic and geological characteristics of sampling stations from the Gulf of Cadiz.

Core №	Geographical setting	Sedimentary summary	Instrumentation	Acoustic characteristics
TTR16-AT600GR	Pen Duick escarpment	Mud breccia (?) covered by coral debris and carbonate crusts	MAKAT127, hull mounted profiler	High backscattering
TTR16-AT601G	Pen Duick escarpment	Coral debris, mud breccia	MAKAT127, hull mounted profiler	High backscattering
TTR16-AT602GR	Pen Duick escarpment	Hemipelagic sediments, shell debris cemented by carbonate crusts	MAKAT126, hull mounted profiler	High backscattering
TTR16-AT603G	Yuma mud volcano. Dark patch in the northern slope	Mud breccia covered by thin layer of marl	MAKAT129, hull mounted profiler, previous investigations	Very high backscattering
TTR16-AT604GR	Yuma mud volcano. Dark patch in the northern slope	Mud breccia covered by layers of carbonate crust and marl with living fauna (acaharax, worms, ophiuroidea etc)	MAKAT129, hull mounted profiler	Very high backscattering
TTR16-AT605GR	Yuma mud volcano, south-eastern crater	Mud breccia covered by thin layer of marl	MAKAT130, hull mounted profiler	High backscattering
TTR16-AT606G	Ginsburg mud volcano.	Mud breccia covered by thin layer of marl	MAKAT130, hull mounted profiler	High backscattering
TTR16-AT607GR	Ginsburg mud volcano	Empty bivalves and gastropods shells, carbonate slabs, crusts and coral branches	MAKAT130, hull mounted profiler	High backscattering
TTR16-AT608GR	Darwin mud volcano	Shell debris (empty bivalves, living acaharax). Slabs and crusts.	MAKAT131, hull mounted profiler	High backscattering
TTR16-AT609G	Darwin mud volcano	A few carbonate slabs and shell debris	MAKAT131, hull mounted profiler	High backscattering
TTR16-AT610GR	Shouen mud volcano	Mud breccia (clasts, carbonate crusts)	MAKAT135, hull mounted profiler	High backscattering
TTR16-AT611G	Shouen mud volcano	Mud breccia covered by strongly bioturbated marl	MAKAT, hull mounted profiler	High backscattering
TTR16-AT612G	Shouen mud volcano	Mud breccia covered by thin layer of marl	MAKAT, hull mounted profiler	High backscattering
TTR16-AT613G	Carlos Ribeiro mud volcano, northern part of the crater	Gas saturated mud breccia covered by marl	Previous investigation, MAKAT45 line (TTR11), hull mounted profiler, seismic line (TTR14)	High backscattering on the sonar image
TTR16-AT614G	Carlos Ribeiro mud volcano, Central part of the crater	Gas saturated mud breccia covered by thin layer of hemipelagic marl	Previous investigation	High backscattering on the sonar image
TTR16-AT615GR	Carlos Ribeiro mud volcano, Central part of the crater	Gas saturated mud breccia covered by thin layer of hemipelagic marl	Previous investigation	High backscattering on the sonar image
TTR16-AT616G	Carlos Ribeiro mud volcano, Central part of the crater	Gas saturated mud breccia covered by thin layer of hemipelagic marl	Previous investigation	High backscattering on the sonar image
TTR16-AT617K	Carlos Ribeiro mud volcano, Central part of the crater	Gas saturated mud breccia covered by thin layer of hemipelagic marl	Previous investigation	High backscattering on the sonar image
TTR16-AT618K	Carlos Ribeiro mud volcano, Central part of the crater	Gas saturated mud breccia covered by thin layer of hemipelagic marl	Previous investigation	High backscattering on the sonar image
TTR16-AT619G	Solovjev mud volcano, the crater	Gas saturated mud breccia covered by thin layer of hemipelagic marl (traces of gas hydrates)	MAKAT138, seismic line PSAT285, hull mounted profiler Previous investigation (TTR15)	High backscattering on the sonar image
TTR16-AT620G	Semenovich mud volcano, the crater	Gas saturated mud breccia covered by thin layer of marl	MAKAT138, hull mounted profiler, seismic line PSAT285	High backscattering on the sonar image
TTR16-AT621G	Porto mud volcano, the crater	Mud breccia with semilithified marlstone, covered by marl with Pogonophora tubes	MAKAT139, hull mounted profiler, seismic line PSAT286	High backscattering on the sonar image
TTR16-AT622GR	Porto mud volcano, the eastern part of the crater	Mud breccia with semilithified marlstone, covered by marl rich in Pogonophora tubes	MAKAT139, hull mounted profiler, seismic line PSAT286	High backscattering on the sonar image
TTR16-AT623G	Porto mud volcano, the central part of the crater	Gas saturated mud breccia (three flows), covered by marl rich in Pogonophora tubes. Traces of gas hydrates.	MAKAT139, hull mounted profiler, seismic line PSAT286	High backscattering on the sonar image
TTR16-AT624G	Bonjardim mud volcano, the upper part of the crater	Gas hydrates in the 3 and 4 sections. Gas saturated mud breccia covered by thin layer of marl with pogonophoras	MAKAT137, hull mounted profiler, seismic line PSAT283	High backscattering on the sonar image
TTR16-AT625G	Bomboca mud volcano, the crater	Sticky clay strongly bioturbated covered by marl. Strong smell of H ₂ S	MAKAT136, hull mounted profiler, seismic line PSAT283	High backscattering on the sonar image
TTR16-AT626G	Olenin mud volcano	Hemipelagic clay and marl strongly bioturbated. Smell of H ₂ S	Previous investigation	High backscattering on the sonar image

presence of outcrops of fresh mud breccia and fields of methane-derived carbonate crusts (AT604G). The sites were associated with the characteristic ecosystems including chemosynthetic species (see the biology section below). Large number of empty bivalve and gastropoda shells observed on the grab video record and in samples (e.g. AT607GR) suggests that these sites used to be very

active in the recent past but at the present time the level of seepage is not enough to support the chemosynthetic ecosystem. Darwin mud volcano was found to be the only location where abundant live colonies of chemosynthetic *Bathymodiolus* were observed and sampled (AT608GR). Video records from the survey with the TV-guided grab showed large fields covered by empty

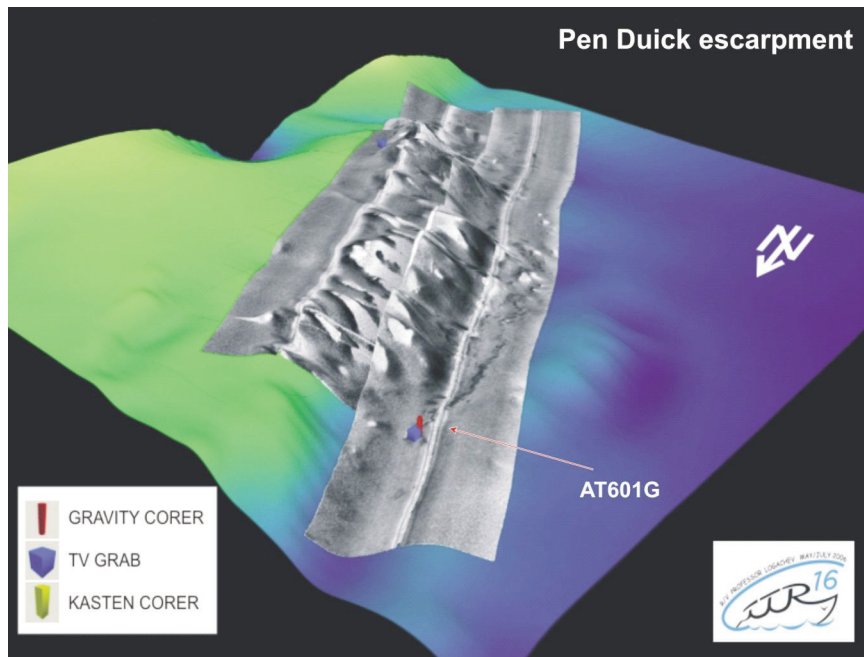


Figure 18. Sampling sites in the Pen Duick escarpment area.

Bathymodiolus shells, which suggest that the site has been the scene of active fluid discharge promoting thriving chemosynthetic life in the past. A modest number of living colonies observed today indicate that the level of activity is considerably reduced in at present time. The top of the mud volcano is covered by massive carbonate slabs which were also sampled by the grab. The slabs are covered by a dense network of fractures which is thought to result from upward movement of the material within the crater. Living colonies of the Bathymodiolus serve as good markers of the fractures along which the seepage still takes place.

Another conical feature, found about

11 km to the north of Darwin MV, was sampled during the campaign. The feature has a similar morphology to Darwin MV and was also hoped to be a site of active seepage. Although the cores and TV grab (AT610-612) did recover carbonate crusts and mud breccia, no chemosynthetic communities were encountered, suggesting the dormant status of the structure. It was named Shouen mud volcano.

Deep water Portuguese margin

Several known mud volcanoes including Olenin, Bonjardim, Porto, Carlos Ribeiro, Soloviev and Semenovich were

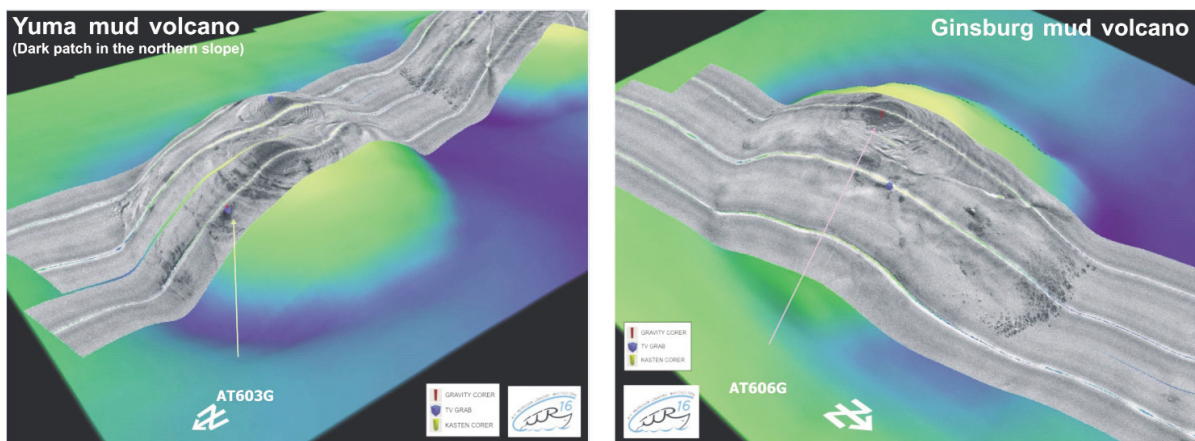


Figure 19. Sampling sites on the Yuma and Ginsburg mud volcanoes.

revisited on the deepwater Portuguese margin. A total of 6 cores (AT613-618) were collected from the Carlos Ribeiro mud volcano in an attempt to recover gas hydrates and specimens of chemosynthetic fauna. The sampling yielded only traces of gas hydrates in the lower sections of the cores suggesting the burial of a large hydrate accumulation.

The sampling site on the Bonjardim MV was selected after the analysis of new sidescan sonar data. The deep-towed sidescan survey obtained the first high resolution image of the mud volcano which had been studied by previous campaigns mainly by seismic and sampling. The image revealed the presence of the elevated patch at the southern edge of the volcano's crater (Fig. 20). A gravity core (AT624G) retrieved large aggregates of gas hydrates finally proving the gas-hydrate-bearing nature of deep Portuguese mud volcanoes. Traces of gas hydrates were also found in the cores from Soloviev and Porto mud volcano. One new conical structure about 1 km across, located about 20 km to the north-west of the Bonjardin mud volcano, was tested during the Leg. The core (AT625G) recovered gas-charged sediments confirming the presence of a mud volcano. It was named Bomboca

and the sampling and sidescan sonar image indicate a very low level activity at the present time.

II.5. Biology - Macrofauna

M. R. CUNHA, A. HILÁRIO AND C. F. RODRIGUES

II.5.1. Introduction

Seep sediments represent some of the most extreme marine conditions and offer unbounded opportunities for discovery in the realms of animal-microbe-geochemical interactions, physiology, trophic ecology, biogeography, systematics and evolution.

The benthic ecosystems associated with mud volcanoes in the Gulf of Cadiz have been studied on TTR cruises since 2000. The main goal of Leg 2 of TTR-16 cruise was to continue these studies with macrofaunal sampling from the Middle Moroccan and Deep Portuguese Margins fields. The biological material collected during the cruise will contribute to attain the following specific objectives:

- to gain more information on the biodiversity and distributional ecology of macroinvertebrates

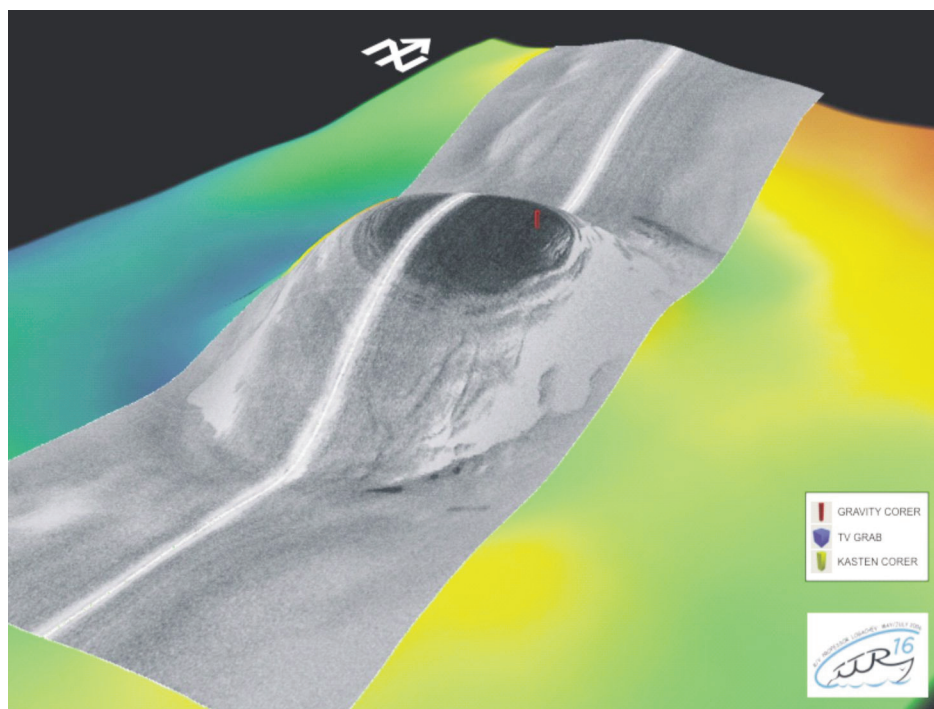


Figure 20. Sampling site on the Bonjardim mud volcano.

- to determine the trophic status of key species using stable isotope analyses ($\Delta^{13}\text{C}$, $\Delta^{15}\text{N}$, $\Delta^{34}\text{S}$)
- to identify chemosynthetic prokaryotic endosymbionts in macrofaunal hosts using molecular methods
- to initiate reproductive studies of Siboglinidae including anatomy, gametogenesis, larval development and dispersal, and population genetics.

II.5.2. Methods

Bottom sampling

The fauna observed during TV-assisted operations was recorded and listed.

Conspicuous animals were picked from the surface of the sediments and rocks collected with the grab. These specimens were photographed and then preserved in 95% ethanol (or deep-frozen) to enable future genetic analysis. A variable volume (~20 l) of surficial sediments and rock washings were sieved through 2, 1 and 0.5 mm mesh sizes. The fauna in the two coarser fractions was sorted and kept in 95% ethanol. The finer fraction (0.5 to 1 mm) of the sieved sediments was preserved in 4% buffered formaldehyde and stained with Rose Bengal to be sorted later under a stereoscopic microscope. Biological specimens will be curated and deposited in the Biological Research Collection of the University of Aveiro (Department of Biology) for further ecologic, taxonomic, morphologic and genetic studies.

Stable isotopes and molecular analyses

Analyses of the natural, stable isotopic composition of tissues ($\Delta^{13}\text{C}$, $\Delta^{15}\text{N}$, $\Delta^{34}\text{S}$) from bivalves and pogonophoran worms will be carried out in the specimens collected from several mud volcanoes. The same species will be used for phylogenetic 16S rRNA sequence analysis and DGGE community profiling of the chemosynthetic prokaryotic endosymbionts. Fluorescence in situ hybridization (FISH) will be used to confirm that the sequence obtained by PCR was originated from the host symbiont.

The bivalves were dissected and gill and muscle tissues were prepared for analysis. Tissues for stable isotope analysis and PCR-DGGE analysis of bacterial and archaeal 16S rRNA genes were frozen (-20°C). Tissues for FISH were fixed in a diluted solution of formaldehyde in sterile seawater (2%) and kept at 4°C overnight. After two washes in a phosphate-buffered saline solution (10 mM sodium phosphate, 130 mM NaCl), samples were stored at -20°C in a phosphate-buffered saline – ethanol solution (1:1).

Reproductive studies of Siboglinidae

Some specimens were removed from the tubes for a preliminary identification of the different species. The specimens were preserved in ethanol and in formaldehyde for further genetic and histological studies, respectively.

II.5.3. Results

Macrofaunal results consist of lists of macroinvertebrate organisms obtained from bottom sampling, and invertebrate megafauna, fish and life traces seen during TV-observations. These are compiled in Tables 4 and 5, respectively.

Specimens of *Acharax* sp. from Yuma (AT604Gr, AT605Gr) and Ginsburg (AT607Gr), of *Bathymodiolus* sp. from Darwin (AT608Gr), of *Thyasiridae* from Carlos Ribeiro (AT615Gr) and of *Siboglinum* sp. from Yuma (AT605Gr) were prepared for isotope and molecular analyses.

The Siboglonidae examined on board were provisionally ascribed to the genera *Siboglinum* (Yuma MV), *Spirobrachia* (Carlos Ribeiro MV) and *Siphonobrachia* (Porto MV). A preliminary description of the samples based on the material partially processed onboard is given below.

Pen Duick Escarpment (AT600Gr, AT602Gr)

The areas covered by the TV observations showed scattered small colonies of dead scleractinean corals, crusts and a

Table 4. Listing of the macrofauna and biological debris collected from bottom samples.

Phylum	Class	Order	AT600Gr	AT602Gr	AT604Gr	AT605Gr	AT607Gr	AT608Gr	AT610Gr	AT615Gr	AT617K	AT618K	AT622Gr
Porifera			+	+									+
Cnidaria	Hydrozoa		+			+			+				
	Scyphozoa					+							
	Anthozoa		+			+	+	+					+
Sipuncula						+					+		
Echiura						+							
Mollusca	Gastropoda		+			+	+	+					
	Bivalvia		+	+	+	+	+	+	+	+	+		
Annelida	Siboglinidae		+	+	+	+	+	+	+	+	+	+	+
	Other Polychaeta		+	+	+	+	+	+	+	+	+	+	+
Arthropoda	Cirripedia	Malacostraca				+	+	+					
		Decapoda	+			+	+						
		Euphausiacea		+									
		Amphipoda		+		+	+	+				+	
		Isopoda					+	+					
Tanaidacea			+		+	+					+		
Echinodermata	Asteroidea												
	Crinoidea		+										
	Ophiuroidea		+			+	+						
	Echinoidea						+						
Bryozoa		+											
Biological debris			AT600Gr	AT602Gr	AT604Gr	AT605Gr	AT607Gr	AT608Gr	AT610Gr	AT615Gr	AT617K	AT618K	AT622Gr
Coral		+	+							+			
Pteropods		+	+					+		+	+		
Gastropod shells		+	+	+	+	+	+						
Bivalve shells		+	+	+	+	+	+		+	+	+	+	
Brachyopod shells		+	+										

diverse community dominated by *Isidella elongata*, typically accompanied by stalked Hexactinellidae, whip corals and a diversity of other soft corals. Mobile fauna consisted mainly of abundant shrimps (*Pandalidae* and others) and several species of fish. Life traces such as clusters of burrows, large

decapod burrows and gastropod tracks were also abundant. Some of the crusts recovered in sample AT600Gr (Fig. 21) were colonized by several species of hydrozoans, anthozoans, sponges and crinoids. Ophiuroids, polychaetes and crustaceans (including one galatheid lobster) were retrieved from the

Table 5. Listing of the megafauna and life traces observed during TV-grab operations.

Phylum	Class		AT600Gr	AT602Gr	AT604Gr	AT605Gr	AT607Gr	AT608Gr	AT610Gr	AT615Gr	AT617K	AT618K	AT622Gr	
Porifera		Stalked hexactinellids	++	++		+							++	
		Other sponges	+			++				+				
Cnidaria	Hydrozoa Anthozoa	Cerianthids	+	+										
		Other Actinaria	+	+							+		+	
		Whip corals	++	++		+					+	+		
		Isidellidae	+++	+++										
		Pennatulids	++											
		Other soft corals	++	++			+	+	+	+	+			
		Scleratinid coral	+++				+			+				
Mollusca	Gastropoda	<i>Neptunea contraria</i>	++			+	+							
		Scaphopoda							+					
		Other gastropods											+	
		<i>Neptunea</i> shells			+++		++	+	+					
		<i>Bathymodiolus</i>						++	++					
		<i>Acharax</i> shells			+	+	+	+	+	+	+			
		<i>Bathymodiolus</i> shells				++	+++	++	+++					
Thyasirid shells								++						
Polychaeta		Siboglinidae				?					+	+++		
Arthropoda	Malacostraca	<i>Pandalidae</i> shrimps			+	+	+	+					+	
		Other shrimps	++	++							+			
		Galatheids												+
		Crabs	+											
		Cirripeds												+
Echinodermata	Crinoidea Asteroidea Ophiuroidea Holothuroidea		+				+						+	
							+						+	
												++	+	
			+										+	
Chordata	Osteichthyes	++	++	+	+			+			+			
			AT600Gr	AT602Gr	AT604Gr	AT605Gr	AT607Gr	AT608Gr	AT610Gr	AT615Gr	AT617K	AT618K	AT622Gr	
Burrows	Clustered Conical mounds Large (decapod) With feeding marks		+++	+++	++	++	+++	+	+++	+	+++			
			+	+	++	+	++	+	+	+	+			
														++
														+
Traces	<i>Neptunea</i> tracks Other tracks		++	+	+	+	++							
			+			+		+					+	

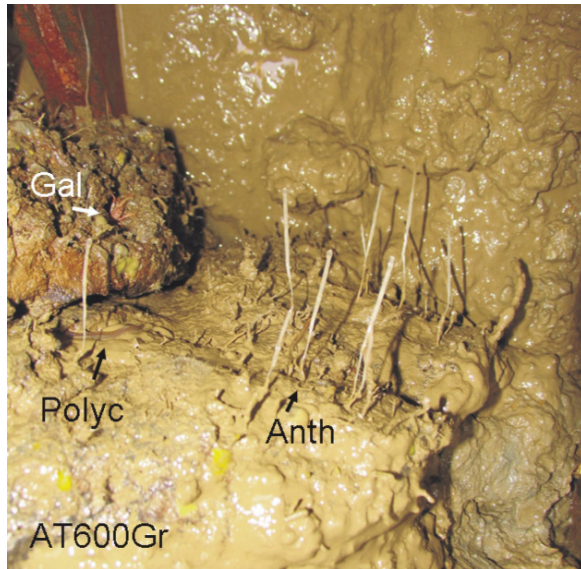


Figure 21. Carbonate crusts in sample AT600Gr colonized by several species of hydrozoans, anthozoans, sponges and crinoids.

sediments. Sample AT602Gr included several species of crustaceans, polychaetes and seep species such as *Acharax* sp. and *Siboglinum* sp.

Yuma MV

Observations were made in the northern slope (AT604Gr) and southeastern crater (AT605Gr) of the Yuma MV. The first area showed abundant biological debris (scattered *Neptunea* shells and *Bathymodiolus* graveyards, Fig. 22), some life traces (conical mounds) but except for some *Pandalidae* shrimps and a few fish no other animals were sighted. The sample yielded a few specimens of *Acharax* sp. infected by the polychaete *Natsushima bifurcata* and empty tubes of *Siboglinidae*. In the second area numerous life traces and biological debris. Soft corals and sponges attached to shells, scleractinean corals or rocks were rather frequent as well as mobile fauna (*Pandalidae* and other shrimps and a few fish). The sample was collected from a *Bathymodiolus* graveyard and included a variety of sessile (cnidarian and cirripeds) and mobile organisms (polychaete and echinuran worms, decapod and peracarid crustaceans, ophiuroids) and also some specimens of seep fauna (*Acharax* sp. infected by *N. bifurcata* and *Siboglinum* sp.).

Ginsburg MV (AT607Gr)

The area covered by TV observations at Ginsburg MV showed some similarities to the one described for Yuma crater (AT605Gr) but *Bathymodiolus* shells and graveyards were more frequent. The sample was taken from a *Neptunea* and *Bathymodiolus* graveyard and yielded several cnidarians, crustaceans (galatheid lobster, amphipods, tanaids), sipunculid and polychaete worms (including *Siboglinidae*), molluscs (gastropods and *Acharax* sp.) and echinoderms (echinoids and ophiuroids).

Darwin MV (AT608Gr)

The observations in Darwin MV were made in an area of large slabs and crusts. Scattered shells of *Bathymodiolus* and *Neptunea*, soft corals and other epifauna were occasionally sighted on the surface of rocks and sediment. The fissures among slabs and depressions with scattered crust were filled by abundant shells and occasionally small clumps of living *Bathymodiolus*. A successful attempt to sample one such clump was made and together with the *Bathymodiolus* specimens (Fig. 23), some polychaetes, gastropods, *Acharax* sp., cirripeds and anthozoans were also collected.



Figure 22. Abundant biological debris (scattered *Neptunea* shells and *Bathymodiolus* graveyards) observed during video survey of the site AT604Gr on the slope of the Yuma MV.

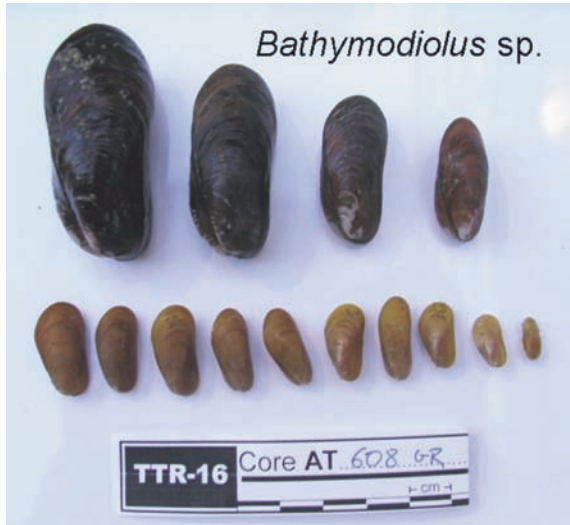


Figure 23. Specimens of *Bathymodiolus* collected from the Darwin MV during TV grab deployment at the site AT608Gr.

Shouen MV (AT610Gr)

Observations were made in the crater of the mud volcano that showed scattered crusts, clasts, small dead colonies of scleractinean coral and numerous life traces (mainly burrows of different kinds). Except for a few soft corals and pandalidae shrimps no other conspicuous living fauna was observed. The sample taken in this area yielded a few worms (Siboglinidae and other polychaetes), cnidarians (Hydrozoa and Scyphozoa) and one bivalve.

Carlos Ribeiro MV (AT615Gr, AT617K, AT618K)

A short observation of the crater showed numerous ophiuroids, several Thyasirid shells scattered at the surface of sediments and some black tubes (probably Siboglinidae). Thyasirids (Fig. 24a) and *Acharax* sp. were recovered from samples AT615Gr and At618K. The grab sample also yielded polychaetes including some Siboglinidae. The longest tube (Fig. 24b) measured 97 cm in length and ~2 mm in diameter.

Porto MV (AT622Gr)

The top of Porto MV was covered by a continuous field of Siboglinidae that in some areas formed clumps of 20-50 individuals (Fig. 25a). The tubeworms were accompanied mostly by stalked hexactinellid sponges and some crinoids. Many old tubes and sponge stalks are colonized by epifaunal organisms (hydrozoans, actinarians, cirripeds and other). Mobile fauna (galatheid lobsters, ophiuroids and holothurians), life traces (burrows with star-shaped feeding marks) and scattered *Acharax* shells were also observed among the tubes. The grab sample included one clump of Siboglinidae tubeworms (Fig. 25b).

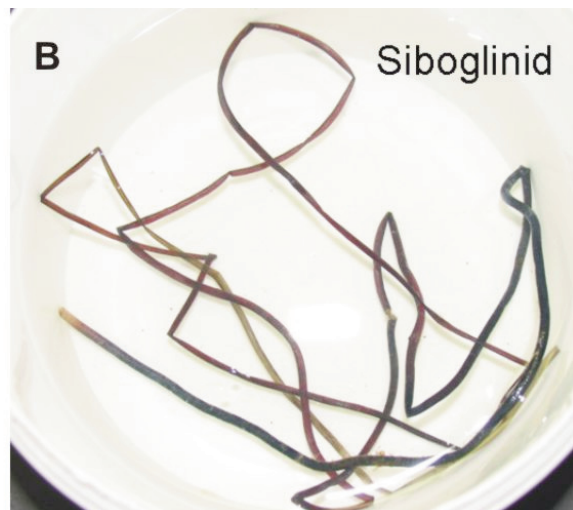


Figure 24. Macrofauna from the Carlos Ribeiro MV.

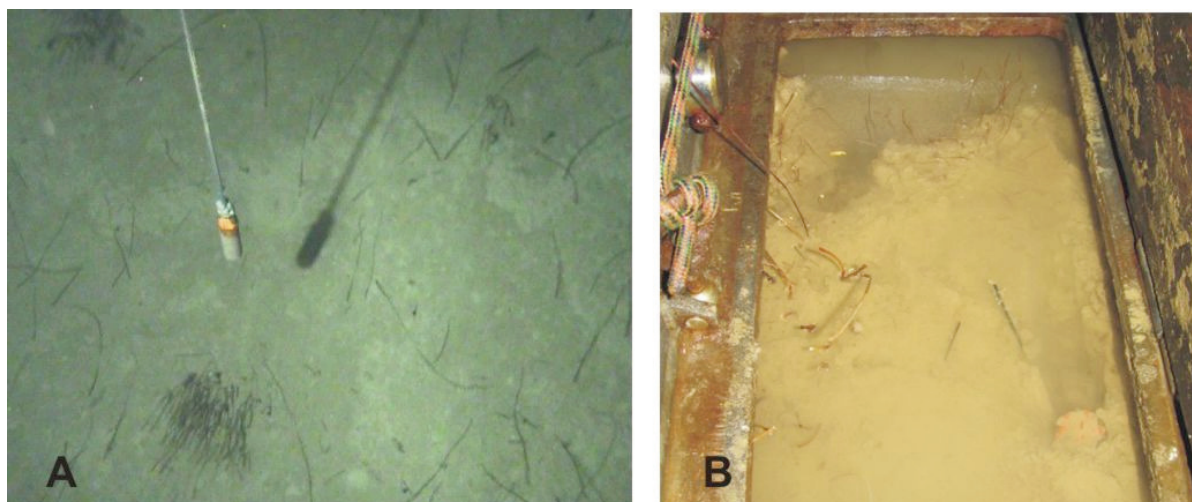


Figure 25. *Siboglinidae* tubeworms from the Porto MV (AT622Gr).

II.6. Gas Biogeochemistry and Microbiology

M. NUZZO, A. SHAPAROVA AND L. SANTOS

Sediments recovered from gravity cores were sampled for gas and pore water geochemical analyses, and for microbiological studies. All cores were collected from mud volcanoes, except for one core recovered on the Pen Duick escarpment (AT601G), which showed signs of methane venting (i.e. reduced grey mud breccia sediments) and one core (AT625G) recovered in a new structure which has not yet been confirmed as a mud volcano. Most cores were apparently retrieved from active mud volcanoes, the sediments being composed at all sites of reduced grey mud or mud breccia that were generally oxidized in the upper 40 cm or less. The sampling and analytical methods used for geochemical analysis are summarized in Table 6.

Additionally, gas hydrates were recovered from a gravity core at Bonjardim mud volcano. Four specimens ranging in diameter between 1 cm and 7 cm were preserved at -20°C for analysis at the Moscow State University and Aveiro University. Other specimens were thawed and the gas harvested for determination of the molecular and isotopic composition of the clathrate hydrocarbons at the Moscow State University and University of Bristol. Gas

hydrates were also present in gravity cores and TV-Grabs recovered at Carlos Ribeiro MV, but no specimen could be sampled as the crystals had dissociated during recovery in the water column, as indicated by the observation of seawater -bubbling due to gas hydrate dissociation during retrieval of a TV-Grab.

The aim of these studies is to characterize the microbial communities involved in anaerobic hydrocarbon oxidation of the venting fluids at different mud volcanoes. The sampling and processing methods employed for microbiology studies, performed at the University of Aveiro (Portugal) are presented in Table 7 below. The sites and cores sampled for this purpose include:

- Yuma MV (AT603)
- Ginsburg MV (AT613)
- Soloviev MV (AT619)
- Semenovitch MV (AT620)
- Porto MV (AT621)
- Bonjardim MV (AT624)
- Bomboca MV (AT625)

Additionally, sediment samples were stored at 4°C under anaerobic conditions for further determinations of microbial activity and biomass by ^3H -Leucine incorporation, ATP concentration and Extracellular Enzymatic Activity (EEA).

Table 6. Sediment sampling for geochemical studies

Analysis	Sample preservation	Analytical method	Sampling interval (cm)	Institution
Light hydrocarbons composition (methane to pentane)	Gas harvested by headspace equilibration in 10% KCl solution, sample preserved in 10% KCl pH1 or in supersaturated NaCl solution	Gas Chromatography-Flame Ionization Detector (GC-C-FID)	10	MSU, University of Bristol
Stable carbon isotope composition of hydrocarbons ($\delta^{13}C$, in per mil vs VPDB)	Gas harvested by headspace equilibration in 10% KCl solution, sample preserved in 10% KCl pH1 or in supersaturated NaCl solution	Gas Chromatography-Combustion-Isotope Ratio Mass Spectrometry	10	MSU, University of Bristol
Major anion and cation species in pore water	Sediment plugs stored at $-20^{\circ}C$ prior to thawing and centrifugation for pore water extraction	Ion Chromatography (IC)	10	MSU, University of Bristol
Organic carbon content in sediments and clasts	Sediment/clasts stored in plastic bags		20	MSU
Volatile organic acids (VFAs) in pore water	Sediment plugs stored at $-20^{\circ}C$ prior to thawing and centrifugation for pore water extraction	IC Exclusion	10	University of Bristol
Metal concentration in pore water	Sediment sample stored in acid-washed plastic bags at $-20^{\circ}C$ prior to extraction	Mass spectrometry	10	University of Bristol

Table 7. Sediment sampling for microbiological studies

Analysis	Sample preservation	Analytical method	Sampling interval (cm)
Bacterial abundance	Sediment samples were fixed with 2% formaldehyde solution and stored at $4^{\circ}C$	Enumeration by epifluorescence microscopy after Acridine Orange staining of sample	20
Viral abundance	Sediment samples were fixed with 2% glutaraldehyde solution and stored at $4^{\circ}C$	Enumeration by epifluorescence microscopy after SYBR Gold staining of sample	20
Fluorescence in situ hybridization (FISH)	Sediment samples were fixed with 2% formaldehyde solution, washed twice with PBS and stored at $-20^{\circ}C$ in a PBS:Etanol (1:1) solution	Hybridization with oligonucleotide probes for specific phylogenetic groups	20

III. VORING PLATEAU, NORWEGIAN MARGIN (LEG 3)

G. WESTBROOK AND SHIPBOARD SCIENTIFIC PARTY
OF THE LEG 3

III.1. Introduction

III.1.1. Overview

As part of the work packages WP3 and WP4 of the EU FP6 HERMES integrated project on Hotspot Ecosystem Research on the Margins of European Seas, to study gas-fluid seeps and the biological communities that are associated with them, two high-resolution seismic experiments employing OBS were designed to investigate the 3D structure of a gas/fluid escape chimney beneath an active seep/vent and compare it with that of an inactive system. The chimneys to be investigated, in the Nyegga region of the Norwegian continental margin (Fig. 26), may be representative of a class of feature of global importance for the escape of gas from beneath continental margins and for the provision of a habitat for the communities of chemosynthetic biota that are dependent, directly or indirectly, on the methane that flows through them. The experiments were to employ sparker and mini GI gun seismic sources to provide near-3D seismic reflection images of the sub-seabed structure over a

range of seismic resolution to complement the tomographic inversion of the OBS data. The experiments were anticipated to provide a much higher resolution 3D determination of seismic properties than previous work on such features and should determine the distribution of free gas and hydrate in the gas/fluid escape chimneys.

III.1.2. Geological background

The existence of hundreds of gas/fluid-escape chimneys in the continental margin of Norway in the region of the Voring plateau has been demonstrated by 2D and 3D seismic reflection surveys and by multibeam sonar and sidescan sonar surveys of their seabed culminations as mounds and, more commonly, pockmarks (e.g. Bouriak et al., 2000, although they interpreted as clay diapirs; Berndt et al, 2003; Bunz et al., 2003). Some of these chimneys emit methane and other hydrocarbon gases and support communities of chemosynthetic biota (Hovland et al., 2005; Hovland and Svensen, 2006). The existence of similar chimneys has been demonstrated off Vancouver Island and the Niger delta. All these chimneys pass through the methane hydrate stability field, and so some particular conditions or mechanisms are needed to allow methane to pass through water-saturated sediment without being converted to hydrate. Given the very large number of pockmarks that exist in continental margins, gas/fluid escape chimneys could be a (the?) major contributor of methane, from either deep sources or from dissociated hydrate, to the atmosphere, rather than submarine slides or mud volcanoes. They may also be a more important host to chemosynthetic communities of biota than mud volcanoes, which are individually much larger features but are far fewer in number.

High-resolution, chirp, seismic profiles across chimneys on the northern flank of the Storegga slide, obtained by Le Suroit in 2002 as part of the HYDRATECH project show that their interiors are seismically incoherent and that reflectors in the well-strati-

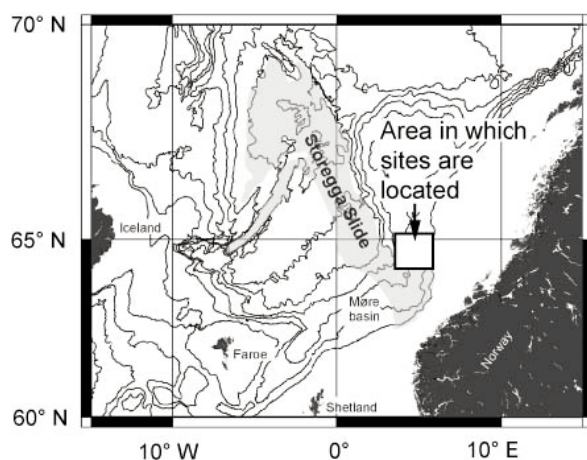


Figure 26. Location of the area in which the work of TTR Cruise 16, Leg 3, of the Professor Logachev was conducted.

fied sediments that the chimneys penetrate exhibit pull-up in the flanks of the chimneys, which is progressive with depth, and is indicative of the presence of a high-velocity material that could be hydrate or authigenic carbonate. These walls of hydrate or carbonate around the chimneys may isolate the centres of the chimneys from pore water in the surrounding sediments, enabling gas to migrate up to the seabed without being converted to hydrate.

An important condition for the success of the seismic experiments was to know how active was seepage of methane at possible target sites and also it was important to know the bathymetry of the target site very well to avoid deploying the OBS on rough carbonate rubble, where it is likely that they would be off-level and with very poor coupling of the geophones to the seabed. Some very useful information from ROV dives and a microbathymetric map had already been provided by Martin Hovland of Statoil for the G11 pockmark and neighbouring pockmarks, and the Vicking cruise of the *Pourquoi Pas* (20 May to 17 June 2006) was programmed to visit target sites in the Nyegga area with ROV Victor. During the Vicking cruise, the activity of the G11 pockmark was verified, two other pockmarks CN01 and CN03 were shown to have active seeps and they were mapped with the microbathymetric swath-mapping system on the ROV Victor. Following completion of the Vicking cruise and testing phase of the cruise of the *Professor Logachev*, the available information was reviewed to choose the two sites for the seismic experiments. CN03 and G11 were chosen, because they were quite different in character although both had evidence of active seepage. CN03 has a zone of intense scattering and attenuation at its centre and pull-up of the surrounding strata. G11 has neither. Both had good bathymetric maps on which to design the array of OBS, in contrast to the Tobic feature, initially explored during TTR-8 cruise in 1998, which although it is a much larger structure and probably more active than G11 or CN03, as subsequent investigation during the TTR-16 cruise confirmed, it exhibits large areas of

carbonate crust, the distribution of which and the precise shape of the feature were not known. CN03 was chosen in preference to CN01, because CN03 is an isolated feature, so the 'normal' structure is more clearly identifiable all around the feature than in the case of CN01, which is one of a linear group of enechelon features.

III.1.3. Objectives

Two chimneys were to be investigated with identical seismic experiments (Fig. 27). The seismic experiment was designed to determine the structure of a chimney, which is typically 300-m in diameter, the presence of gas within it and hydrate within and around it, and the presence and orientation of fractures through which gas and fluids migrate. The depth of investigation of the experiment was to be between 200 and 500 m beneath the seabed in a water depth of ~750 m, depending on the seismic source, and the experiment was to measure P-wave and S-wave velocities, and seismic anisotropy, through S-wave splitting. The principal S waves used in the experiment would come from P-S conversion on reflection. Seismic experiments with OBS conducted in the area in 2002 as part of the HYDRATECH project demonstrated that very clear P-S waves are generated from the sedimentary reflectors

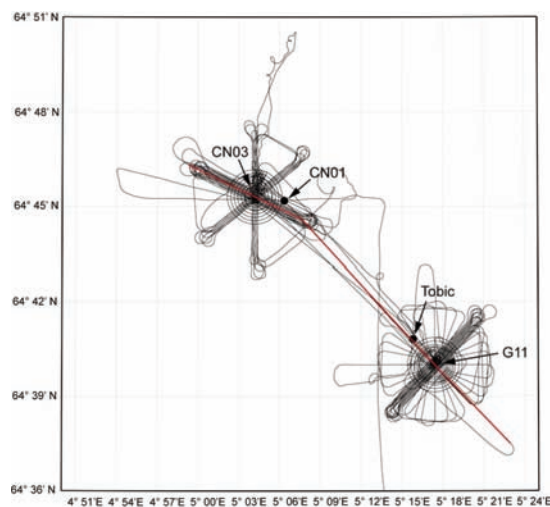


Figure 27. Locations of the principal gas/fluid-escape chimneys investigated and the ship's track.

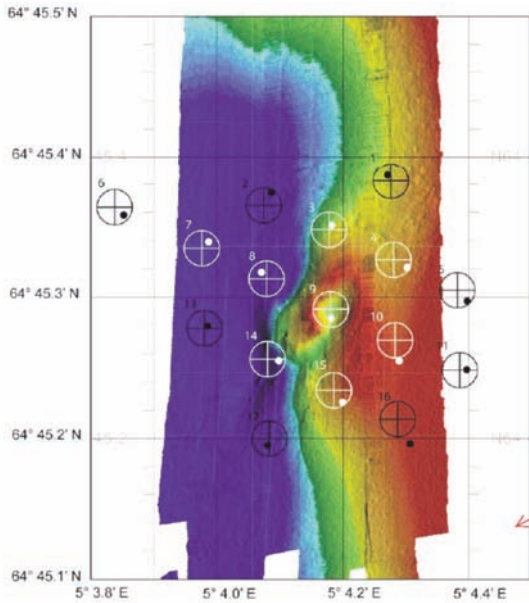


Figure 28. Positions of OBS deployed at the CN03 pockmark. The crosses, surrounded by a circle of 25-m radius, were the intended positions. The dots show the positions of the OBS when they were released, about 50 m above the seabed. White are Ifremer OBS. Black are Southampton OBS. The positions are superimposed on a bathymetric map made from a microbathymetric survey conducted from the ROV Victor during the Vicking cruise of the Porquoi Pas.

through which the chimneys penetrate. S waves are crucial to the evaluation of the presence of free gas.

An array of 18 4-component OBS with a spacing of ~100 m was to cover the top of each chimney and its immediate surrounding area (Figs. 28 and 29). Shots were to be fired into the array from a near-surface source (mini GI gun and sparker) on a grid of lines of minimum length 5000 m at 50m line spacing. The shots were also to be recorded on a short near-surface hydrophone streamer to provide near-3D seismic reflection images of the sub-seabed structure. To minimise the effect of drift through the water column on the spacing the OBS, deployment of the OBS were to use a core cable, navigated with an acoustic navigation beacon, and an acoustic release to drop the OBS from a height of about 50-100 m above their intended positions on the sea bed.

The data from the experiments should be suitable for:

a) 3D tomographic inversion of P-wave and

S-wave data using the JIVE package, which has been used successfully for similar investigations at lower resolution off Vancouver Island,

b) 2D inversion of both P and S waves along the principal axes of the chimneys,

c) detection and analysis of azimuthal anisotropy, from S-wave splitting caused by fractures,

d) 2D and 3D processing of the vertical incidence reflection data, utilising the velocity models derived from the OBS, and employing seismic attributes and 3D visualisation.

III.2. Summary of Results

In relation to the original design of the seismic experiments, the actual experiments were limited by the absence of a deep-towed seismic source with an operating frequency in the range 200-2000 Hz. The attempt to use a sparker for this frequency range proved unsuccessful, because of the

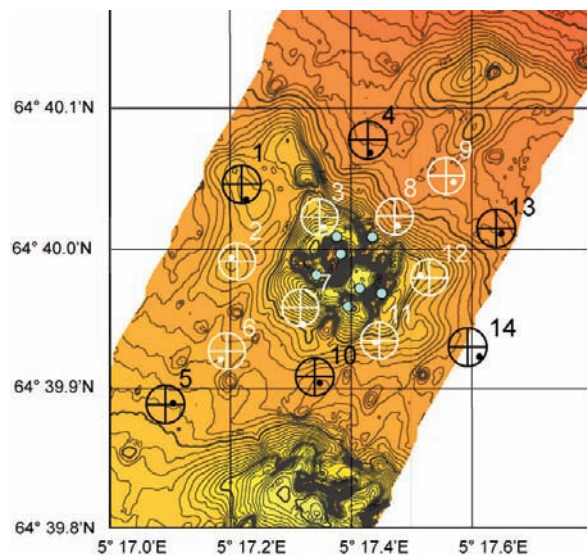


Figure 29. Positions of OBS deployed at the G11 pockmark. The crosses, surrounded by a circle of 25-m radius, were the intended positions. The dots show the positions of the OBS when they were released, about 50 m above the seabed. White are Ifremer OBS. Black are Southampton OBS. The positions are superimposed on a bathymetric map made from a microbathymetric survey conducted by Deep Ocean Surveys for Statoil in 2004 (courtesy of Martin Hovland). Contours are at 0.5 m intervals. Blue dots show the positions of hydrate pingoes described by Hovland and Svensen (2006).

very high level of acoustic noise emitted into the water by the ship. The sparker had been previously used in similar water depths with very good results using a surface-towed streamer. OBS usually have better signal-to-noise than a streamer, as shown, for example, by the HYDRATECH survey carried out in 2002 only a few miles to the NW of the work area for the TTR-16 cruise. The ship's noise is obvious on the records from the OBS, increasing to high levels when the ship is closest to an OBS. This high noise level is also a problem for the hydrophone streamer. The short, high frequency streamer was overwhelmed by the noise. The Logachev's streamer, towed 180 m astern of the ship and with 25-m long active sections, was better able to cope with the noise, but had a lower frequency response. Given that the high-frequency loggers for the Southampton OBS were not operational, it was decided that to ensure reasonable levels of signal-to-noise only the mini GI guns would be used as seismic sources. To give the highest frequency, a single gun with a 13 cu in generator and 35

cu in injector (true GI mode) was used. The trial results from the mid-water hydrophone on an Ifremer OBS indicated useful frequency content at 500 Hz. To ensure penetration of 500 m or more and P-S conversion, two 24/24 cu in. guns were used in harmonic mode, increasing the power of the source but reducing its resolution. The single-gun lines were shot with 50 m spacing and the two-gun lines were shot with 100 m spacing between lines. Not all the two-gun lines were repeated with single-gun lines. The single-gun lines were shot to provide near-3D seismic coverage of the uppermost 200 m. The two-gun lines gave the full range offsets and azimuths for the OBS array.

III.2.1. OBS

In terms of their performance, recording seismic data, all of the OBS operated well, with the exception of one of the Ifremer OBS, which recorded data but gave a problem in conversion from MBS format data to Passcal format. This is expected to be

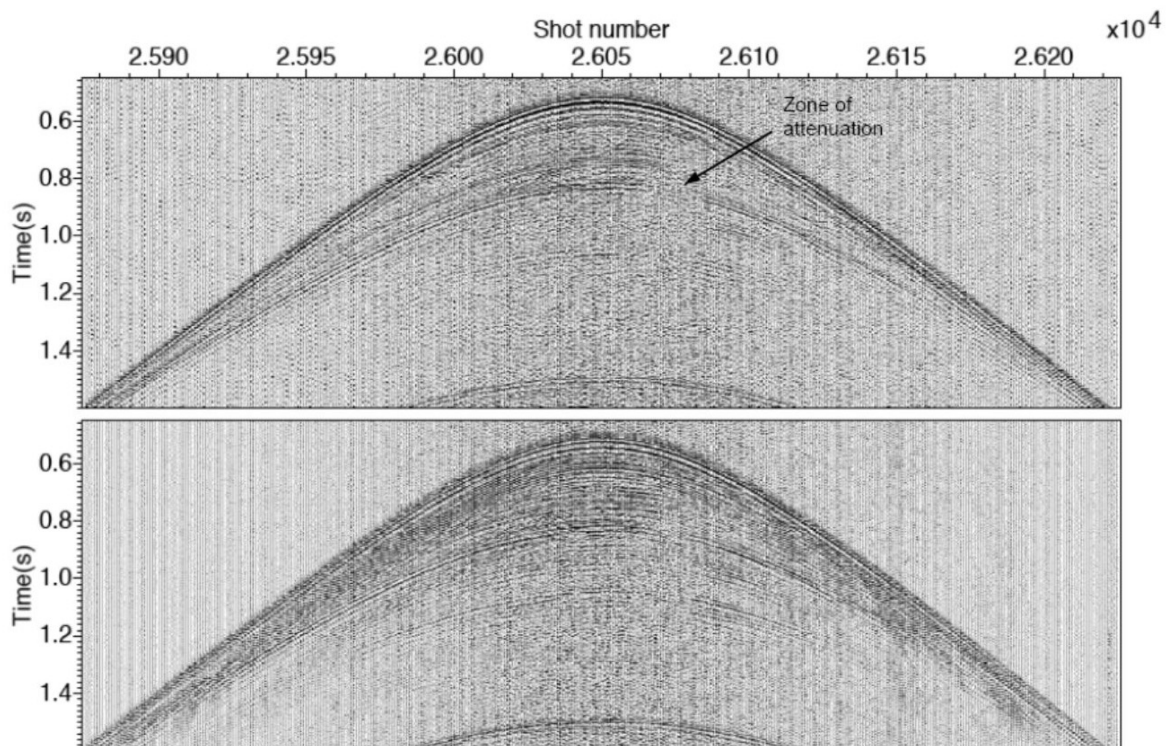


Figure 30. Representative data from the two-gun source during the first main deployment (site CN03_2, line CN25). Upper panel: hydrophone. Lower panel: vertical geophone. Data are from a line through the OBS location. A Butterworth high-pass filter rolling off between 30 Hz and 50 Hz has been applied to remove ship noise.

resolved. The OBS imaged reflectors down to depths giving an equivalent arrival time to the water-column multiple, which is greater than ~ 750 m. A zone of scattering and attenuation that corresponds to the position of the chimney at pockmark CN03 is evident in the OBS records, for example around shot points 206080 in Figure 30. Also, clear S-wave arrivals are shown in the records of the horizontal seismometers from the Ifremer OBS (Fig. 31). Taken together, these results promise well for the prospect that inversion and modelling of the data will be able to discriminate between the presence of free gas and other causes of scattering associated with the chimneys.

III.2.2. Reflection profiles

Although during TTR-16 Leg 2 in the Gulf of Cadiz, the Logachev's streamer had been set up to tow at a depth of about 3 m at speeds not greatly exceeding 2 knots, it was soon appreciated that it was negatively buoyant, and that to ensure that it towed at a reasonably shallow depth (4 m) it was necessary, taking into account the effect of currents and tidal streams on speed through the water for a particular speed over the ground, for the ship to make a speed over the ground of about 4 knots. At this speed the streamer kept to a fairly constant depth and the separation between the primary reflected arrivals and their sea-surface ghosts was not too great. Deconvolution to suppress the ghost will improve the resolution of the seismic sections (Fig. 32). The seismic reflection profiles, even at the relatively early stage of processing in which they currently exist, reveal several interesting features of the subsurface geology in the region of the chimneys.

1. Many chimneys, such as those associated with the CN03 pockmark and Tobic, show pull-up of the reflectors at the margins of the chimneys. Much of this has been produced by deformation related to the formation of the chimneys, but many show a differential pull-up, in which the amount of pull-up increases with depth. This is consistent with the presence of higher velocity

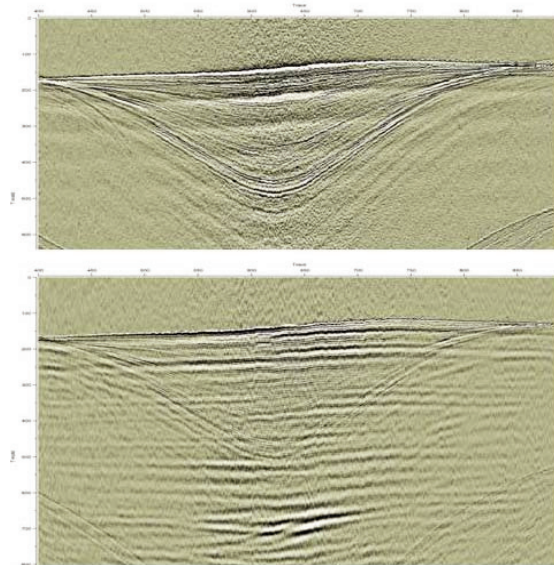


Figure 31. Hydrophone (top) and horizontal geophone data (bottom) from G11 line 10, after application of a hyperbolic reduction to flatten the direct wave through the water. The source consisted of two 24/24 in³ mini-GI guns. Note the P to S converted arrivals on the horizontal geophone section, clearly visible between 500 and 750 ms (reduced time).

material in the margins of the chimney than in the surrounding strata. If this is so, and we expect to be able to detect the presence of the high velocity material from the OBS data, then the material could be hydrate or authigenic carbonate. If there is no higher velocity material, then a more complex mechanism of formation for the chimneys will need to be considered.

2. Chimneys, such as those associated with the CN03 pockmark (Fig. 32) and Tobic (Fig. 33), show seismic scattering and attenuation.

3. The chimney at G11 does not show significant pull-up or scattering and attenuation (Fig. 33).

4. There are several reflectors, which from their high amplitude and negative polarity appear to be gas-charged (Fig. 33). One prominent group of these reflectors lies beneath the area of the G11 pockmark at a travel time of ~ 1.4 s. Where they pass beneath the slope at the edge of the Storegga slide, they are intersected by the base of the gas hydrate stability field, and lose their high amplitude where they pass through it, producing a form of BSR that is common in this

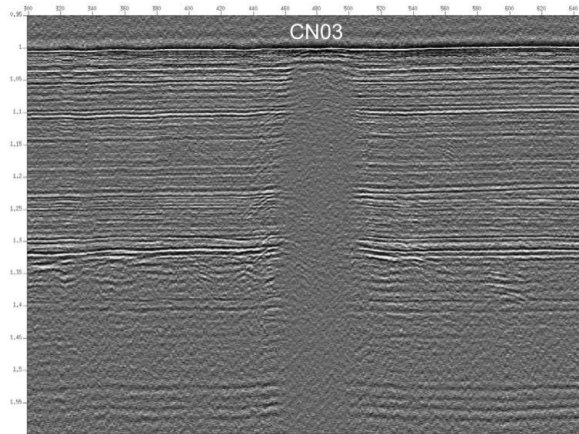


Figure 32. Part of seismic section from line PSAT312/CN19, which intersects line PSAT302/CN09 at the CN03 pockmark, shot with a single 13/35 mini-GI-gun. Display is of channel 2 following static correction, band-pass filtering and deconvolution. Vertical scale: seconds. Horizontal scale: shot points (~8-m separation).

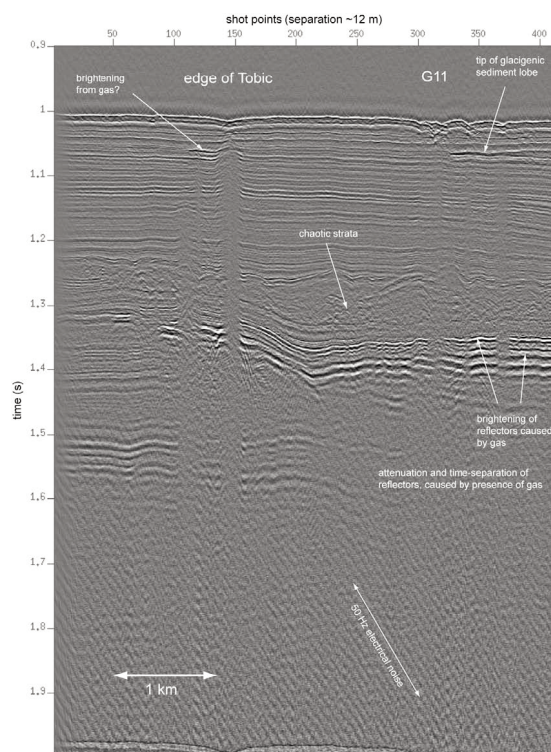


Figure 33. Section from part of seismic line PSAT362/G20, running NW-SE across pockmark G11. The source was two 24/24 mini-GI-guns. The section has undergone static correction, time-variant gain and band-pass filtering, and migration.

region. Beneath this group of bright reflectors, other reflectors show strong attenuation and increases in inter-reflector travel times, indicating a thick zone in which free gas exists.

5. The G11 pockmark lies at the western tip of a lobe of what appears to be glaciogenic sediment that thickens eastward, and the top of which lies about 40 m below the seabed (Fig. 33). The presence of several lobes is shown by the multibeam bathymetry to the east of G11.

6. A zone of chaotic, apparently mobilised, sediment lies above the bright reflectors in the G11 area. Its top surface is irregular and appears to have displaced and deformed the strata that immediately overlie it. Beneath the G11 chimney, the zone achieves a local culmination. Beneath Tobic, the bright reflectors ramp upward to the northwest, and the chaotic zone thins and pinches out, but is replaced by another poorly stratified zone beneath, which underlies the area of the CN03 pockmark (Fig. 34). This zone varies in thickness, but is typified by a broadly convex upper surface with local depressions. At the ramp some of the strata underlying the upper chaotic zone are truncated. For a distance of ~5 km NW of Tobic, the two zones overlap, separated by the interval containing the bright reflectors. It is interesting to speculate how much these zones owe their origin to an originally unstratified deposit, probably of glacial origin, and how much to sediment mobilisation in an overpressured state. The chimneys appear to cut straight through these zones.

III.2.3. MAK-1M data

Eight MAK lines (MAKAT-140-147) were run during the cruise. The sub-seabed penetration achieved with the 5 kHz sub-bottom profiler, of up to 70 m, was very good. The quality of the profiler records was improved by removing interference from the ship's hull-mounted sub-bottom profiler (~3.5 kHz) by not running it at the same time, although to do so is usually the practice with the Logachev. Seven of the lines were run with the 100 kHz sonar 50 m above the

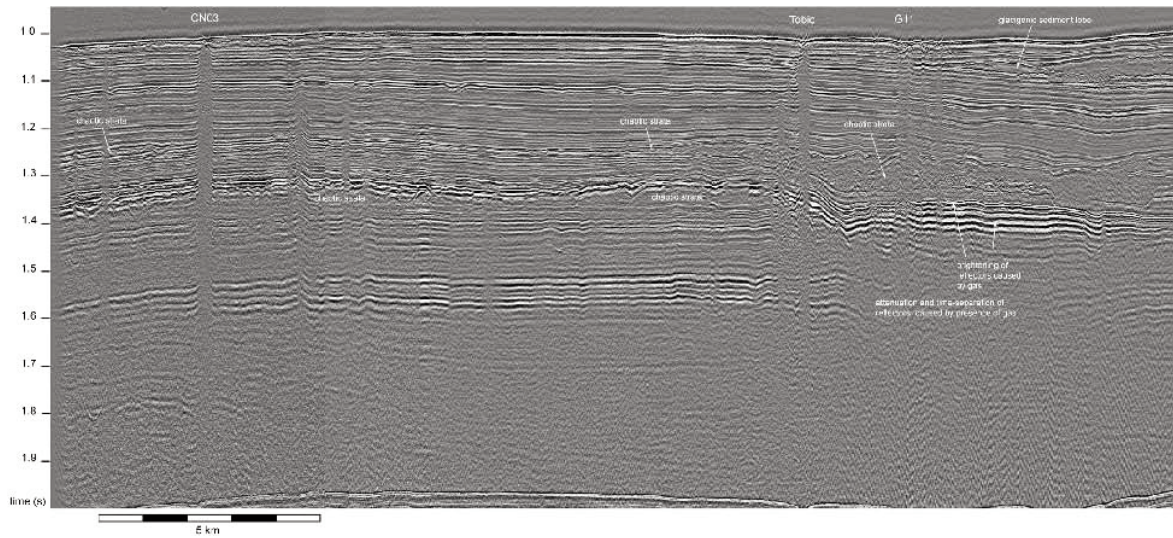


Figure 34. Composite seismic section between pockmarks CN03 and G11, formed from parts of sections from seismic lines PSAT-324, PSAT-387 and PSAT-362. Seismic source was two 24/24 mini-GI-guns. Static correction, time-variant band-pass filtering and migration have been applied to the data.

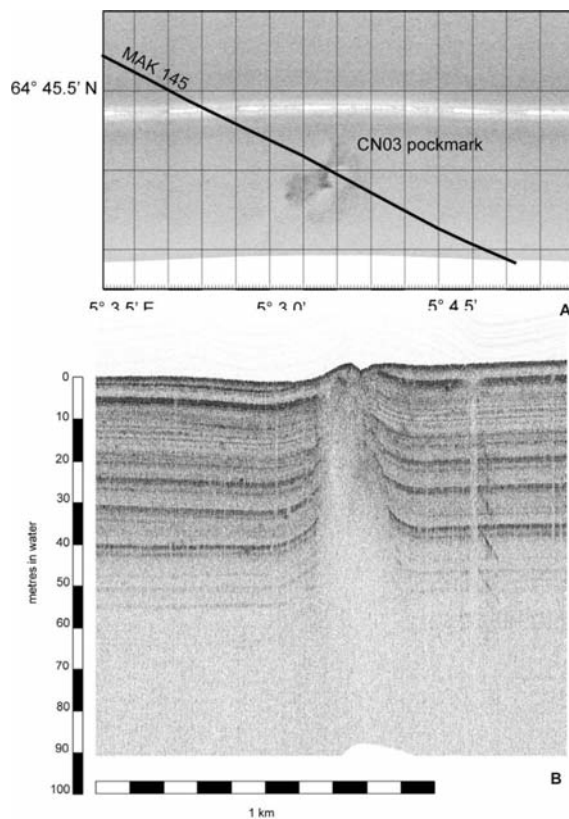


Figure 35. A: Sidescan sonar image of CN03 pockmark on MAK line 141, showing position of 5 kHz profile along MAK line 145. In this image, strong backscatter is shown dark. B: 5 kHz sub-bottom profile along MAK line 145 across the CN03 pockmark. Note the increase with depth in the amount of pull-up of strata at the margins of the chimney, the scattering and attenuation, which may be caused by free gas, and the fault-displacement of the shallow strata.

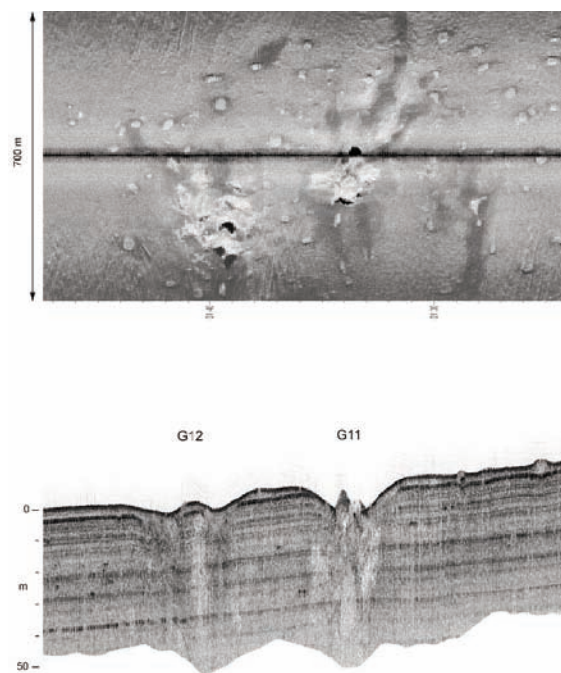


Figure 36. Line MAKAT-140. Upper: Portion of 100 kHz sidescan image across the G11 and G12 pockmarks. Bright is high intensity backscatter. Black is shadow. Carbonate mounds in the centres of the pockmarks show high backscatter. Smoother surface of sediment filling depressions shows lower backscatter (dark grey). Note numerous small mounds in the area in addition to the pockmarks; Lower: Portion of MAK 5 kHz profiler section across the G11 and G12 pockmarks. There is an absence of pull-up affecting the strata adjacent to the pockmark. Some scattering and attenuation of the 5 kHz signal is caused by the carbonate mounds. The small mounds depress the strata beneath them.

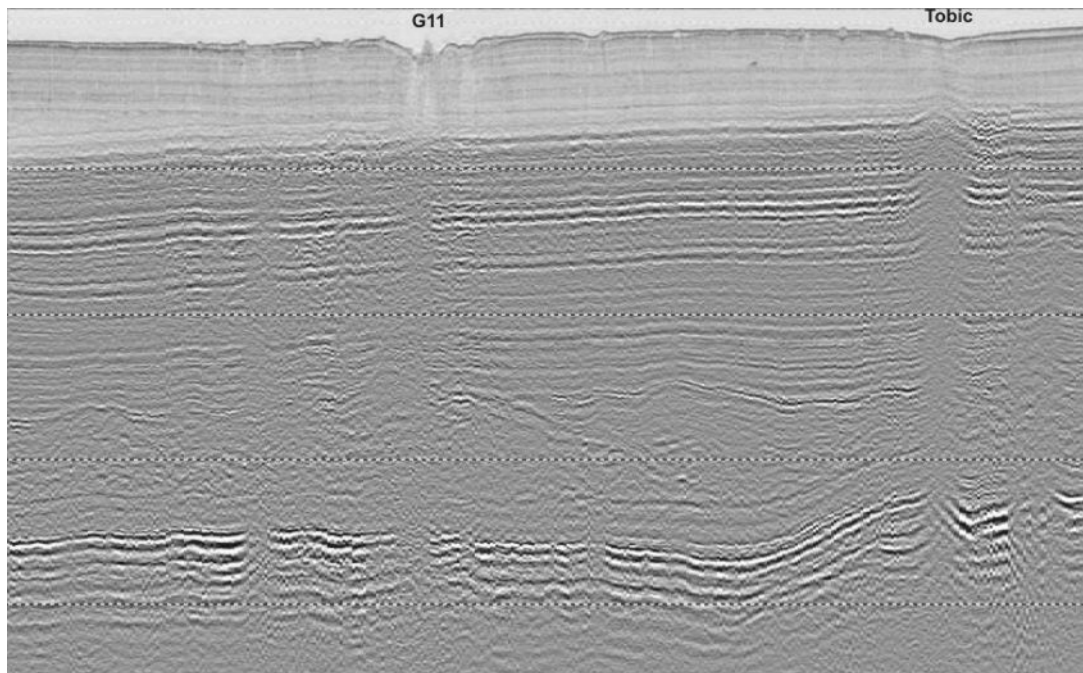


Figure 37. Section of seismic line PSAT387, running SE-NW (left to right), in which part of the top 100 ms has been progressively replaced (faded in) by the 5 kHz profiler record from MAK line 144, which was run along the same track. Horizontal dotted lines are separated vertically by 100 ms. The width of the section shown in the figure is ~5 km.

seabed. One line (146) was run with the 30 kHz sonar, 100 m above the seabed. Several of the lines were run primarily to use the sub-bottom profiler records to define the shallow structure of the pockmarks, and so were closely spaced, giving significant redundancy for the sidescan sonar records (Figs. 35 and 36).

The MAK lines, as well as providing high resolution sidescan images of the seabed, which supplement the multibeam bathymetry in the areas of the two pockmarks, providing valuable information on the nature of the seabed, provided 5 kHz sub-bottom profiler sections. These sections show reflectors to a depth of ~70 m beneath the seabed at a trace spacing of ~1 m. They are very informative about the detail of the shallowest structure and stratigraphy, and they overlap the images from the mini GI gun sections. MAK lines were run along the seismic lines to provide this. This is illustrated for seismic line PSAT-387 (Fig. 37), in which the 5 kHz section is faded into the seismic section over about 70 m sub-seabed. In the lower part of the fade, there is a clear correspondence between the GI gun reflectors

and the 5 kHz reflectors. Near the seabed, the 5 kHz section provides detail, to a resolution of about 0.2 m, that is irresolvable in the source signature of the GI gun. The MAK profiler sections show clear evidence of differential pull-up at the CN03 (Fig. 35b) and CN01 pockmarks, among others.

III.2.4. Sea floor observations and bottom sampling

A. MAZZINI, M. IVANOV, V. BLINOVA AND THE
SEDIMENTOLOGY TEAM OF LEG 3.

During Leg 3 six seepage features were explored with TV remote controlled grab and gravity corer devices (Fig. 38). These structures include CNO3 (Area1 in the northern part of the polygon), and G11 (Hovland et al., 2005; Hovland and Svensen, 2006; Mazzini et al., 2006), Tobic (Kenyon et al., 2001; Mazzini et al., 2005) and three new structures named Dodo, Sharic and Bobic (all five narrowly grouped in Area 2 in the southern part of the polygon). A total of 23 sampling stations were completed (Tables 8 and 9 and Annex I).

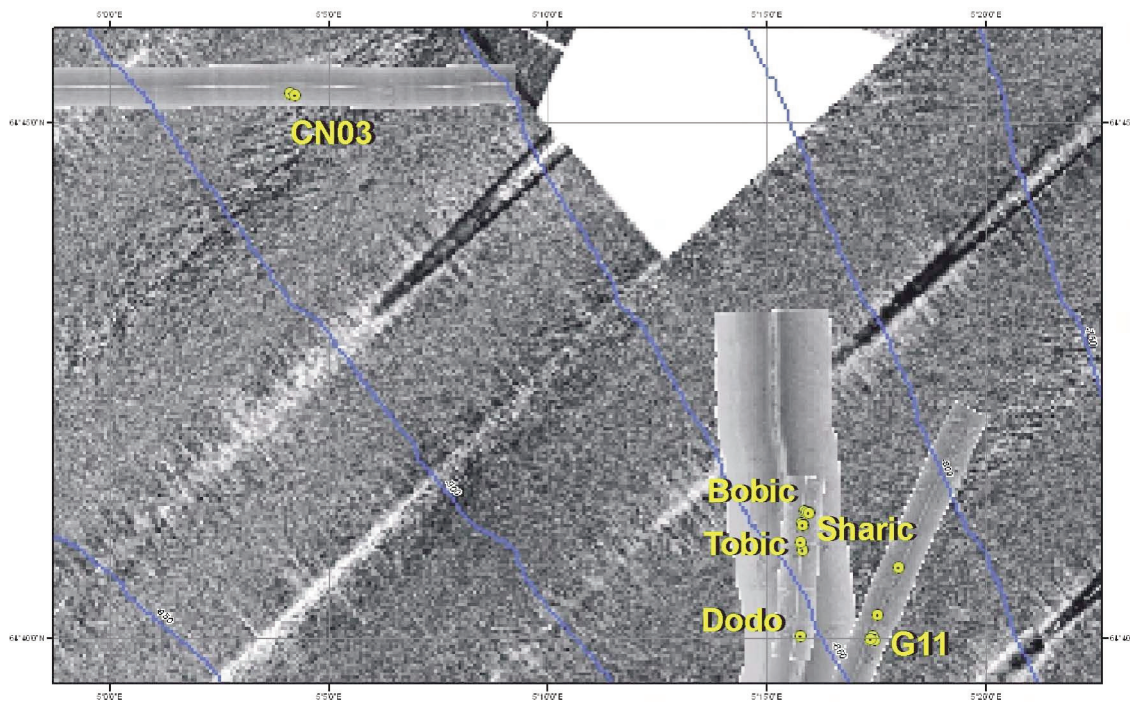


Figure 38. Summary map of principal sample areas and pockmark/mound names, superimposed on low resolution and high resolution sidescan sonar images.

Table 8. General information on the cores from the Voring Plateau, Leg 3.

Core №	Date	Time, UTC	Latitude	Longitude	Depth, m	Recovery, cm
TTR16-AT627GR	17.06.06	13:36	64°40.017N	05°17.411E	735	0.5 t
TTR16-AT628G	19.06.06	20:59	64°45.278N	05°04.107E	726	539 cm
TTR16-AT629GR	21.06.06	04:14	64°41.097N	05°15.832E	725	0.5 t
TTR16-AT630GR	21.06.06	06:36	64°40.864N	05°15.823E	725	0.5 t
TTR16-AT631GR	26.06.06	05:50	64°40.019N	05°15.771E	740	0.5 t
TTR16-AT632G	29.06.06	06:00	64°40.219N	05°17.542E	740	401
TTR16-AT633G	29.06.06	07:04	64°40.678N	05°18.019E	715	456
TTR16-AT634G	30.06.06	02:24	64°45.290N	05°04.120E	727	443
TTR16-AT635G	30.06.06	03:11	64°45.270N	05°04.220E	731	453
TTR16-AT636G	30.06.06	05:19	64°41.214N	05°15.965E	725	285
TTR16-AT637G	30.06.06	06:05	64°41.113N	05°15.797E	720	344
TTR16-AT638G	30.06.06	06:46	64°41.098N	05°15.835E	720	82
TTR16-AT639GR	30.06.06	09:35	64°41.228N	05°15.865E	720	0.5 t
TTR16-AT640G	30.06.06	10:23	64°41.096N	05°15.830E	725	106
TTR16-AT641GR	30.06.06	13:02	64°40.851N	05°15.821E	725	0.5 t
TTR16-AT642G	30.06.06	13:50	64°40.851N	05°15.822E	725	244
TTR16-AT643G	30.06.06	14:29	64°40.930N	05°15.780E	720	132
TTR16-AT644G	30.06.06	15:26	64°39.990N	05°17.370E	736	201
TTR16-AT645G	30.06.06	16:08	64°39.974N	05°17.452E	742	403
TTR16-AT646G	30.06.06	16:58	64°39.988N	05°17.372E	735	529
TTR16-AT647K	30.06.06	18:36	64°41.224N	05°15.914E	720	20 cm
TTR16-AT648K	30.06.06	19:13	64°41.211N	05°15.963E	720	60 cm
TTR16-AT649K	30.06.06	19:54	64°41.094N	05°15.825E	725	CC

Table 9. Sedimentological, acoustic and geological characteristics of sampling stations from the Voring Plateau.

Core №	Geographical setting	Sedimentary summary	Instrumentation	Acoustic characteristics
TTR16-AT627GR	G11 pockmark	Hemipelagic sediments. Carbonate crusts, shell debris cemented by carbonates, dropstones with fauna, worms, two types of Pogonophoras	MAKAT140, hull mounted profiler	High backscattering
TTR16-AT628G	CN03 pockmark	Hemipelagic sediments strongly bioturbated	MAKAT141, hull mounted profiler	High backscattering
TTR16-AT629GR	Sharic pockmark (northern Tobic structure)	Hemipelagic sediments. Carbonate crusts, shell debris cemented by carbonates, worms, Pogonophoras	Previous investigation. ORAT25, (TTR8, 1998), MAKAT142	High backscattering
TTR16-AT630GR	Tobic structure	Hemipelagic sediments, shell debris. Carbonate crusts, dropstones with fauna, worms, Pogonophoras	Previous investigation ORAT25, (TTR8, 1998), MAKAT142	High backscattering
TTR16-AT631GR	Dodo pockmark (southern Tobic structure)	Hemipelagic sediments, carbonate crusts, dropstones	Previous investigation ORAT25, (TTR8, 1998), MAKAT142	High backscattering
TTR16-AT632G	Pimple northern G11	Hemipelagic sediments, hydrotroillite	Previous investigation (TTR8, 1998), MAKAT143	High backscattering, circular shape
TTR16-AT633G	Field northern G11	Hemipelagic sediments, hydrotroillite, sand layer	Previous investigation (TTR8, 1998), MAKAT143	High backscattering, strong reflector 2 m below sea floor
TTR16-AT634G	CN03 pockmark, pingo	Hemipelagic sediments with trace of gas hydrates	MAKAT141, 145, hull mounted profiler	High backscattering
TTR16-AT635G	CN03 pockmark	Hemipelagic sediments, 5-6 cm of pure aragonite at the depth ~200 cm	MAKAT141, 145, hull mounted profiler	High backscattering, strong reflector 2 m below sea floor
TTR16-AT636G	Pirillo (Bobic) structure	Hemipelagic sediments with trace of gas hydrates	MAKAT142, hull mounted profiler	High backscattering
TTR16-AT637G	Pirillo (Bobic) structure	Hemipelagic sediments with trace of gas hydrates	MAKAT142, hull mounted profiler	High backscattering
TTR16-AT638G	Sharic structure	Gas hydrates at the depth ~ 70 cm in a hemipelagic sediments	MAKAT142, hull mounted profiler	High backscattering
TTR16-AT639GR	Pirillo (Bobic) structure	Hemipelagic sediments, carbonate crusts	MAKAT142, hull mounted profiler	High backscattering
TTR16-AT640G	Sharic structure	Big gas hydrates at the depth ~ 70-100 cm in a hemipelagic sediments	MAKAT142, hull mounted profiler	High backscattering
TTR16-AT641GR	Tobic structure	Hemipelagic sediments, shell debris. Carbonate crusts, dropstones with fauna, worms, Pogonophoras	MAKAT142, Previous investigation ORAT25, (TTR8, 1998)	High backscattering
TTR16-AT642G	Tobic structure	Hemipelagic sediments, shell debris.	MAKAT142, Previous investigation ORAT25, (TTR8, 1998)	High backscattering
TTR16-AT643G	Tobic structure	Hemipelagic sediments, shell debris.	MAKAT142, Previous investigation ORAT25, (TTR8, 1998)	High backscattering
TTR16-AT644G	G11 pockmark	Gas saturated hemipelagic sediments with sandy lenses	MAKAT140, hull mounted profiler	High backscattering
TTR16-AT645G	G11 pockmark	Hemipelagic sediments. Carbonate crusts.	MAKAT140, hull mounted profiler	High backscattering
TTR16-AT646G	G11 pockmark	Gas saturated hemipelagic sediments and carbonate crusts.	MAKAT140, hull mounted profiler	High backscattering
TTR16-AT647-8K	Bobic structure	Hemipelagic sediments	MAKAT142, hull mounted profiler	High backscattering
TTR16-AT649K	Sharic structure	Hemipelagic sediments	MAKAT142, hull mounted profiler	High backscattering

Area 1

Structure CN03

AT628G

539 cm of sediments were recovered at this station. The upper 3 cm consist of brown, water-saturated marl, with fine sand-silty admixture. The underlying unit (3-69 cm) consists of brownish structureless, bio-

turbated grey clay, with silty, fine sand admixture. Between 47-69 cm the sediment becomes more greyish and the amount of silty-fine sand admixture decreases. A thin sand rich layer was observed at 61-63 cm. The lower part of the core consists of grey clay, structureless, with black hydrotroillite patches and evidence of bioturbation distributed throughout. No H₂S smell was detected.

AT634G

This station aimed to sample one of the pingo structures observed during previous TV seafloor observations (Vicking cruise, 2006). The recovery revealed the presence of a 10 cm thick silty sandy marl layer containing Pogonophoras capping clayey hemipelagic succession with layers of semilithified carbonate-rich clay where strong bubbling (almost certainly due to gas hydrate dissociation) was observed during splitting operations. The carbonate-rich intervals could be linked with precipitation of carbonate via anaerobic oxidation of methane where gas hydrates were present. Measurements of the sediment temperature in the core catcher gave $-0.4\text{ }^{\circ}\text{C}$. A strong smell of H_2S was detected.

Strong reflector

AT635G

In the vicinity of structure CN03, a strong reflector was seen on the sub-bottom profiler at $\sim 240\text{ cm}$ below the seabed. Sampling revealed the presence of a 6 cm-thick layer of pure aragonite botryoids standing out within the clayey sediment at 240 cm.

Area 2

Structure G11

AT627Gr

A TV- controlled grab profile was conducted at the G11 structure in order to find evidence of active seepage within the pockmark (Fig. 39). TV-profile was planned to cross the pockmark from the southern part running through its centre and finishing in the northern part, which is characterized by high backscatter on the sidescan sonar. The seabed outside of the pockmark is flat, and numerous burrows were observed (Fig. 40a). Inside the pockmark extensive fields of shell debris and tube worms were recognized (Fig. 40b, c and d). In the central part of the structure carbonate slabs and blocks and small

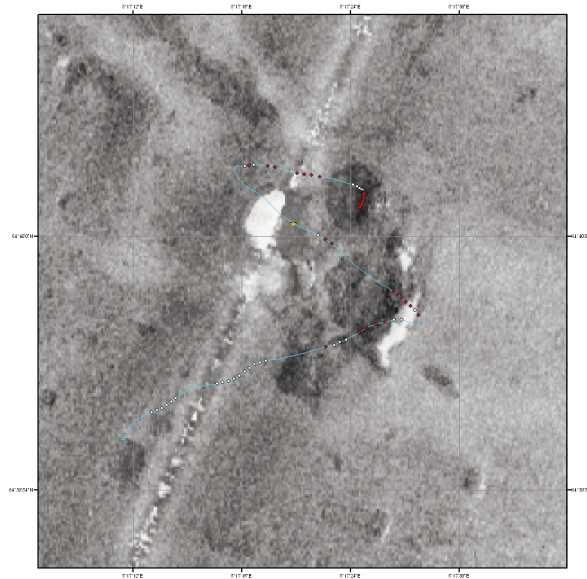


Figure 39. Track of the TV run AT627Gr across G11 structure.

uplifts on the sea bottom (about 1 m in diameter) were observed. Such pingo-structures are characterized by extensive tube worm fields in the central part and grey fresh clay with possible white microbial mats around. A TV-grab was collected from a carbonate crust and shell field. The grab had full recovery consisting of grey clay with a silty admixture and foraminifera and several authigenic carbonates. Numerous worms, shells, sponges, gastropods and pogonophoras were collected from the top surface which was also covered with microbial films in places (Fig. 41) The carbonate crusts recovered were subdivided into two types. The first group consisted of irregular shaped slabs (up to 25 cm in size and up to 5 cm in thickness) with cemented bivalves. The external surfaces are irregular and very porous displaying vesicles throughout. The second group consists of thin irregular shaped plates, greyish in colour, within the hemipelagic sediment. Plates vary in size from 1 cm to 5 cm across and a few mm in thickness. These consist of hemipelagic clay cemented by micritic carbonate showing a concave shape on their bottom surface, almost certainly ascribed to the fluids rising from depth and deforming the clayey sediment. Drop stones of different lithology and size (up to 10 cm in size) were also recovered.

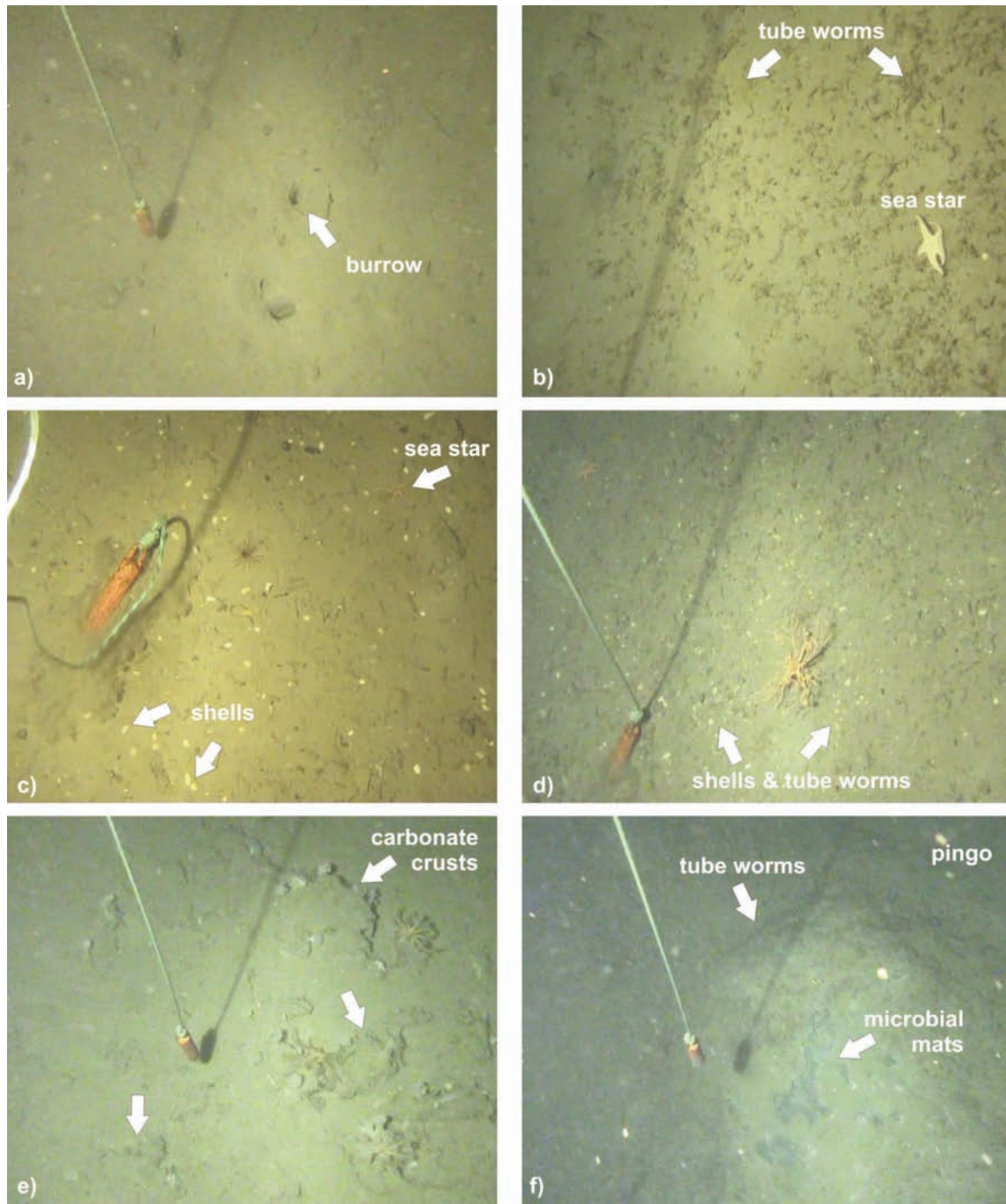


Figure 40. Still images from TV run AT627Gr at G11 structure.

AT644G and AT646G

Two attempts were made to sample a pingo structure. Both cores revealed the presence of a strong smell of H_2S . Gas saturated clay with bubbling through the sediment was seen during the splitting operations of the core. These observations and the presence of water saturated vesicles in the porous

texture of the sediment suggest that gas hydrates were dissociating during the retrieval operations of the core. Sandy lenses and shell debris were also observed in core AT646G below 228 cm.

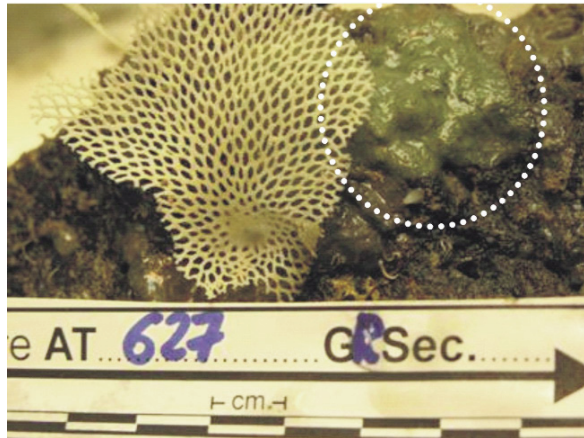


Figure 41. Authigenic carbonate block, with greenish microbial film on the external surface (framed in dotted line), in a grab sample taken from the G11 pock-mark.

AT645G

An inferred seepage site was sampled at this station. It is similarly to stations AT644G and AT646G gas saturated clay, but to a lesser extent, with water saturated vesicles in the porous sediment.

AT633G

One of the intriguing structures present in a field north of G11 was sampled at this site. The recovery was a 456 cm long core showing a hemipelagic succession with bioturbation and hydrotroillite-rich intervals. Carbonate slabs were sampled in the top 5 cm.

Positive features field

AT632G

To the north of G11 a field of closely spaced positive subcircular features (a few metres in diameter) was sampled. The core revealed the presence of normal hemipelagic deposition with occasional layers richer in sandy admixture and hydrotroillite. At 185 cm there was a coral fragment (2x2 cm in size). The content of sandy admixture and small rock fragments increases towards the bottom. The presence of a coral fragment is not sufficient to speculate the all the field of subcircular features consist of small “young”

coral mounds. In fact no coral fragments were observed in the top part of the core and more debris would be expected in the neighbouring area if the field was due to coral mounds.

Structure Sharic

AT629Gr

A TV-run was done on a structure situated to the north of Tobic, later named as Sharic. The TV line crossed two ridges, which are characterized by strong backscatter on the OreTech-sonograph (Fig. 42). Extensive fields of carbonate crusts and blocks were found (Fig. 43) with associated fauna. Fields of shell debris and tube worms have been observed close to pingo structures. About 8 pingos were detected during the observation. Around each pingo very dense fields of tube worms were seen (Fig. 43, b, j-k). At the top of these structures fresh grey clay, buried by hemipelagic material, and microbial communities, whitish or reddish in colour, were observed (Fig. 43, c, j-k). One of these small (< 1 m) positive features was sampled with the TV-Grab. The top surface of the sediment retrieved was heavily colonized by pogonophoras. A strong smell of H₂S was also detected particularly where

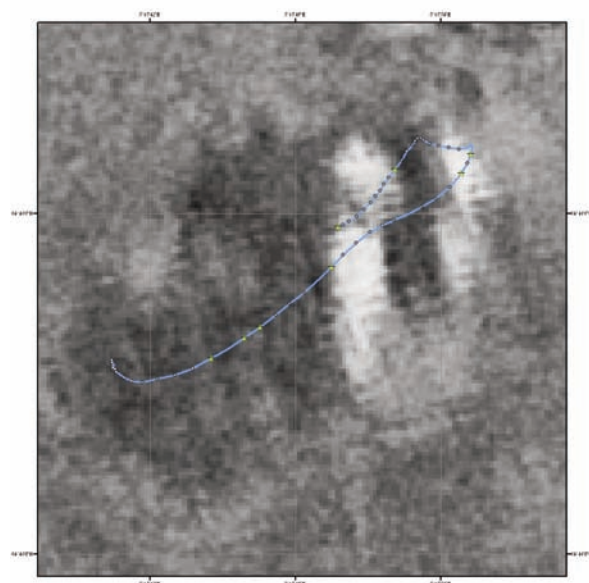


Figure 42. Track of the TV run AT629Gr across Sharic structure.

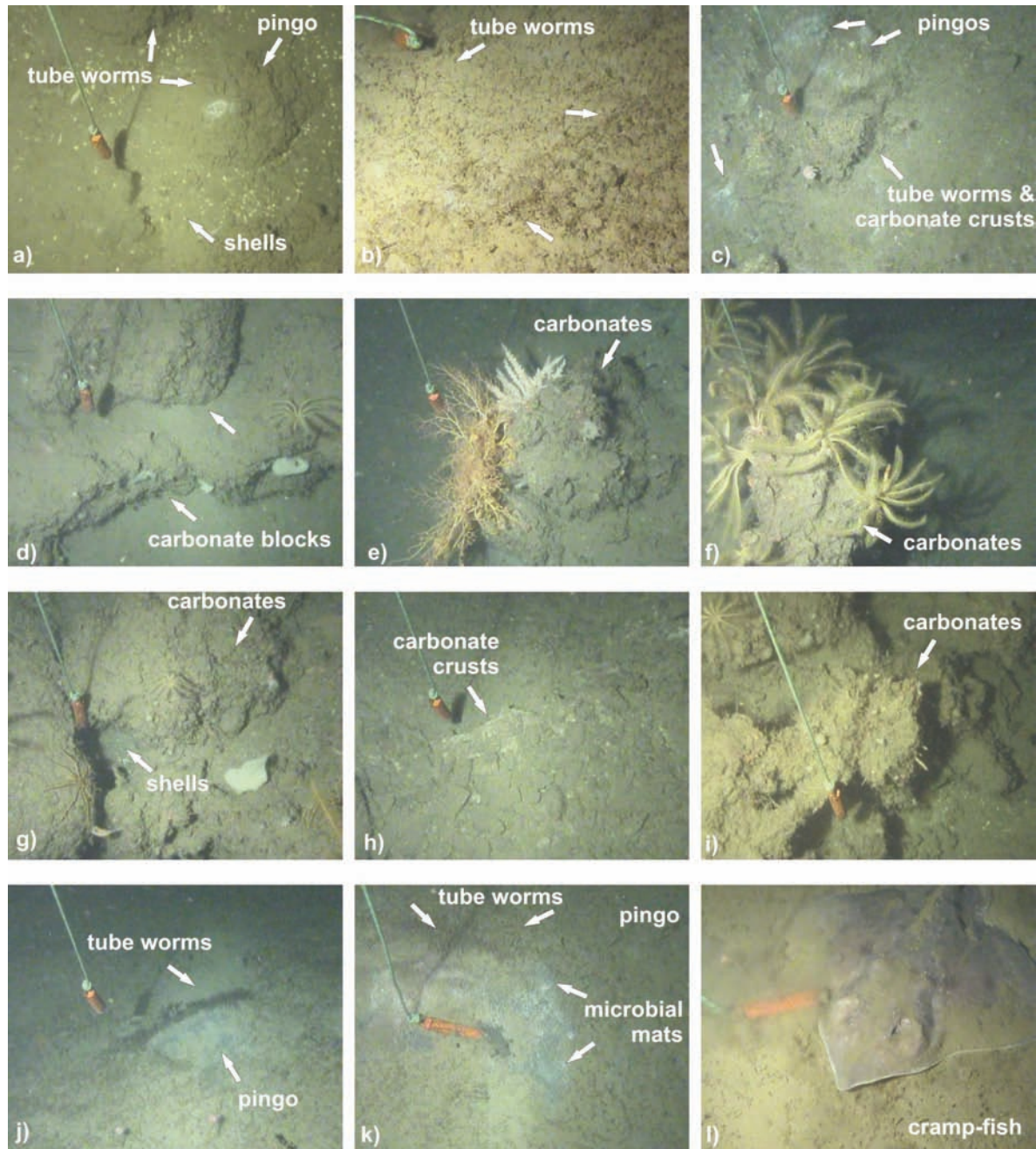


Figure 43. Still images from TV run AT629Gr at Sharic structure.

dark grey (pyrite- and organic-rich) sediment was observed (i.e. from the internal part of the grab). Irregular shaped and porous carbonate concretions up to 35 cm in size were also sampled mainly from the top surface. Most of them consisted of carbonate cemented shells with relatively small amount of hemipelagic sediment present. In the central part a large (~20 cm³) amount of bivalves (up to 2 cm in size) was present in a constrained zone. These bivalves

were not cemented and were covering a large irregularly shaped block (40 cm in size). The block consists of micrite cemented hemipelagic sediment and is split in two parts by a 10 cm wide subvertically oriented unit entirely filled by carbonate cemented bivalves almost devoid of hemipelagic sediment. This shelly deposit presumably represented a fracture that acted as pathway for the fluids. At this site shells and other organisms preferentially thrived and, ultimately,

were cemented by authigenic carbonate. The seepage of hydrocarbon-rich fluids is supported by the presence of whitish filaments (microbial) observed within the semilithified greyish hemipelagic sediment.

AT637G

The highest point of the Sharic structure was sampled at this station. The 344 cm long core had a top 78 cm consisting of sandy sediment, extremely rich in large (up to 1.5 cm in size) shell fragments and small clasts. The remaining part of the core consists of bioturbated clayey silt with locally richer sandy intervals (334-341 cm), hydrotroillite rich layers (78-115, ~200 cm), and shell-rich layers, especially towards the bottom of the core. This shell debris presumably prevented further penetration of the corer.

AT638G and AT640G

One of the pingo structures observed during the TV survey AT629Gr was sampled twice in order to investigate the internal structure of such a feature. In both cases cores were short (up to 106 cm) consisting of a few cm of thick brown marl with a sandy admixture and pogonophoras, capping grey clay containing gas hydrates in the lower part. In both cases the gas hydrates appear to be pore filling or formed into plates (up to 3 mm thick). A burning test on sediment sam-

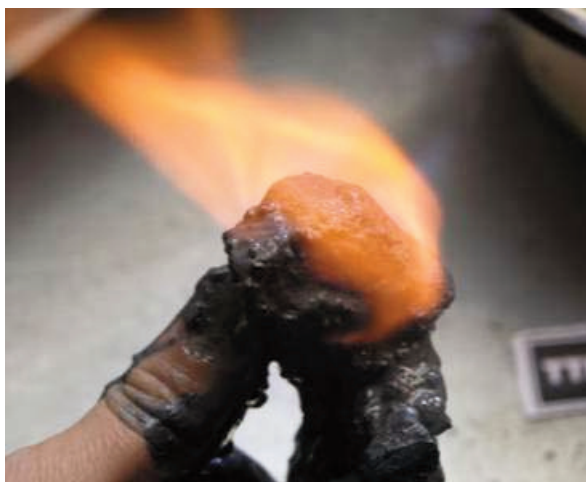


Figure 44. Burning methane from dissociating methane hydrate in a sample taken from gravity core AT640G.

ples containing hydrates revealed that despite the high clay content flames lasted for several minutes although only a small amount of gas hydrate was visible to the naked eye (Fig. 44). This confirms that there was a large amount of pore- or microfracture- filling hydrates. Immediately above the gas hydrate-rich unit (core AT640 G) were subvertical flame shaped burrows containing semilithified clay. These could represent pathways of fluid escape (from gas hydrates?) that induced the precipitation of authigenic carbonate. In core AT638G a small flattish carbonate crust sample was seen at 40 cm.

AT649K

A further attempt to collect a larger amount of gas hydrates for laboratory analyses failed and the Kasten corer was found to be nearly empty.

Structure Tobic

AT630Gr

The Tobic structure, previously sampled during the TTR-10 cruise when a large block of carbonate cemented shells was recovered was revisited after completing an initial TV-line (Figs. 45 and 46). Big fields of carbonate blocks and shells were observed in the central part of the structure (Fig. 47). There were also thin carbonate crusts and massive blocks covered by tube worms and a different sea bottom fauna (including starfish, cnidarians and soft corals). One pingo structure was observed (Fig. 47, i). At the top of this pingo a small white patch of probable microbial communities were recognised. The TV-grab sampled a field of shells and carbonate crusts. The top 3 cm of sediment consists of brownish marl with poorly sorted sand. Pogonophoras, tubular and curly (pink in colour) tube worms, sea spiders, and small shrimps were observed colonizing the surface carbonate slabs. These carbonate crusts (up to 20 cm in size) consist mainly of carbonate cemented shell debris (Fig. 48). A ~5 cm thick layer of shells lies underneath the

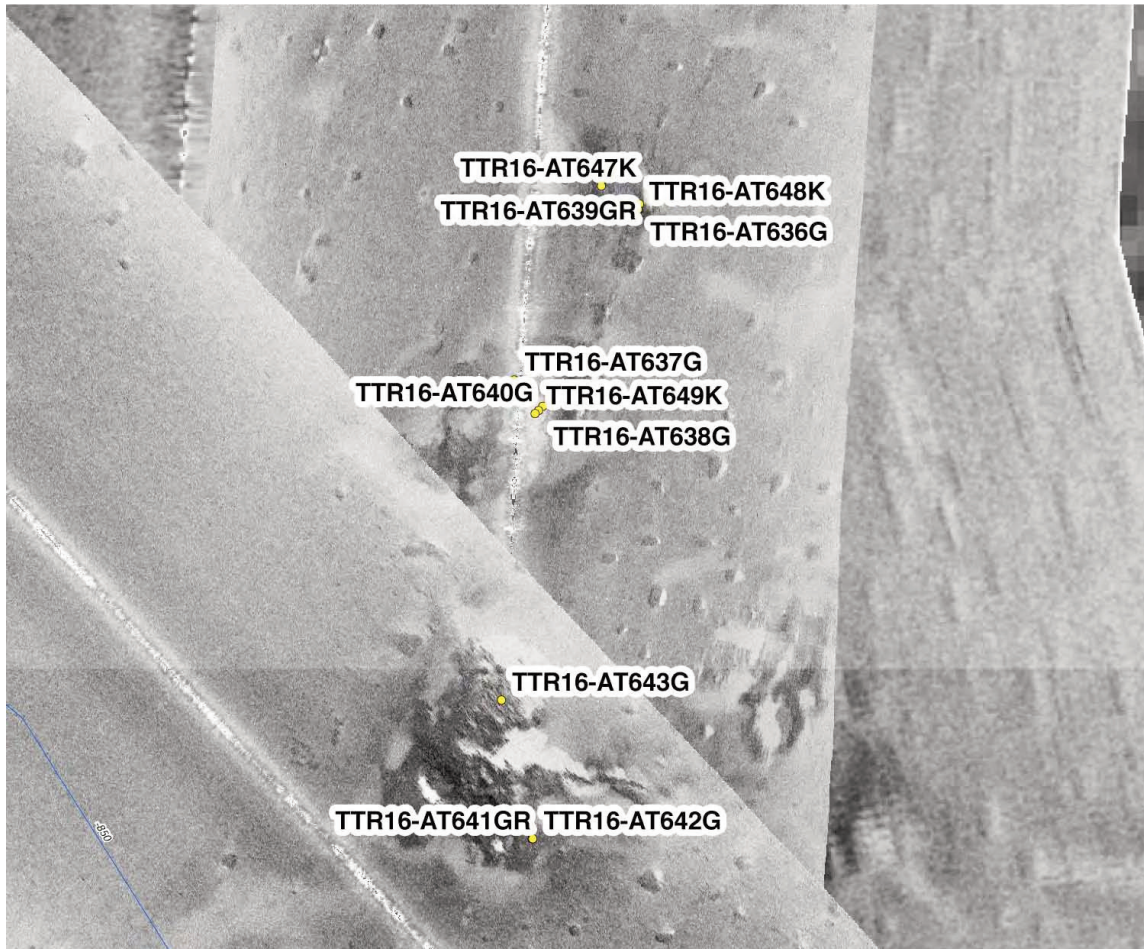


Figure 45. Positions of core and grab samples in the Tobic area and associated structures, superimposed on sidescan sonar images.

marl. Locally this shelly layer is cemented by authigenic carbonate forming irregular shaped blocks. The bottom part of the sediment recovered consists of grey clay. A smell of H₂S was detected.

AT641Gr

A second TV-line was run across the Tobic structure. Nine pingo structures were observed during the run. The TV grab sampled one of these structures and produced a full recovery of sandy clayey marl with numerous pogonophoras and thin carbonate crusts and big blocks within the clayey unit.

AT642G

An attempt was made to core a pingo at this station. The core had a 3 cm thick marly and shell-rich layer, capping a shell

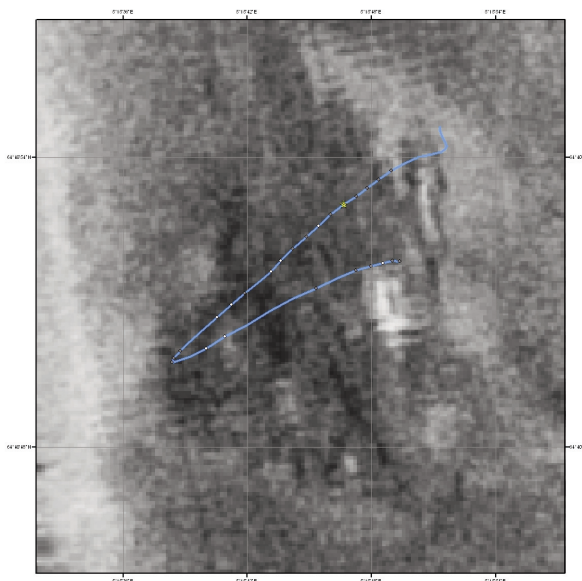


Figure 46. Track of the TV run AT630Gr across the Tobic structure.

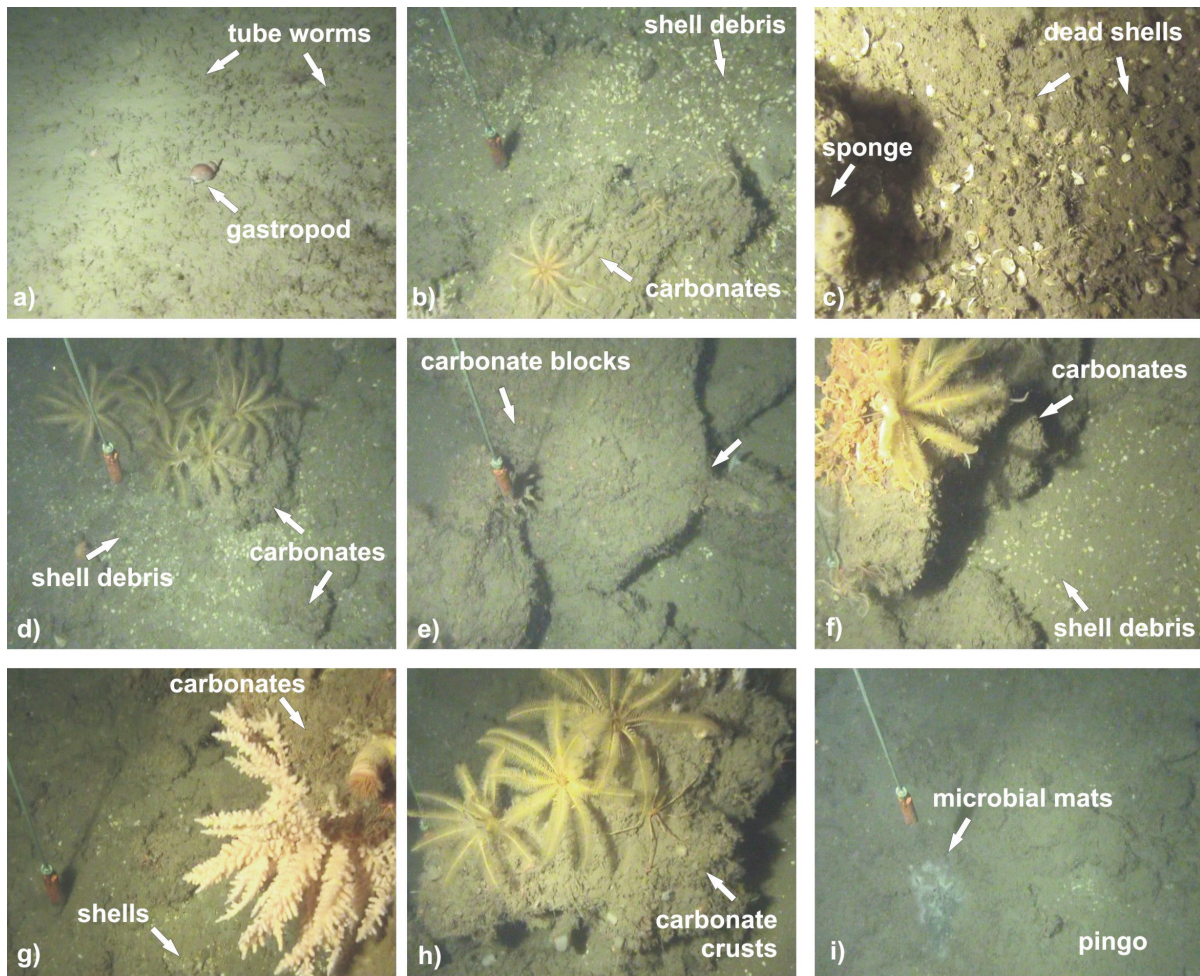


Figure 47. Still images from TV run AT630Gr at the Tobic structure.



Figure 48. Carbonate-cemented chemosynthetic bivalves, which form extensive slabs on the seafloor, from TV grab AT630GR.

debris interval (3-75 cm) containing two types of bivalves averagely 2 cm in size. In the clayey unit below subvertical and flame shaped features of indurated clay could represent fluid pathways where carbonate precipitated. A smell of H₂S was detected.

AT643G

132 cm of sediment was recovered at this station. The core consists mainly of homogeneous clay with some discontinuous sandy lenses. Porous texture and degassing features were observed in the lower part of the core. Bubbling was seen in the core catcher suggesting the presence of gas hydrates dissociating during the extrusion operations. A strong smell of H₂S was detected.

Structure Dodo

AT631Gr

This pockmark was previously investigated during the TTR-8 cruise with sidescan sonar and bottom sampling devices (station AT139G) revealing the presence of high backscatter zones and irregular sea floor morphology. A TV profile was planned based on the OreTech images (ORAT-25) (Fig. 49). The TV-record showed mainly hemipelagic sediment with burrows and rare cnidarians on the drop-stones. Station AT631Gr sampled a flattish area where fragments of crusts appear to be partly covered by recent hemipelagic sediment. The top surface is brownish grey, colonised by sea spiders, star fish, and a few tube worms. The clayey sediment is mixed with poorly sorted sand, gravels and rounded drop stones (up to 16 cm) of different lithology. The majority of the sediment consists of homogeneous grey hemipelagic clay. Three different types of carbonate crusts were observed. Since the recovery was heavily disturbed during the opening of the grab device, in some cases it was difficult to establish the correct stratigraphic order of the samples. The first group is represented by tabular shaped slabs with a thickness up to 0.5 cm revealing parallel layering of white carbonate (aragonite?) alter-

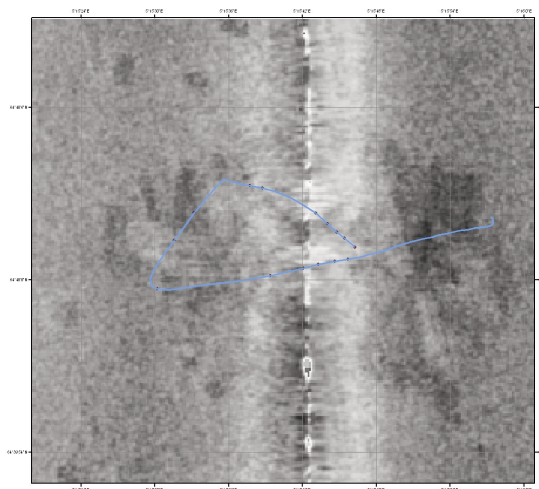


Figure 49. Track of the TV run AT631Gr across the Dodo structure.

nating with more porous darker (organic-rich) layers. This carbonate appears extremely similar to a type described from G11 pockmark (see above). The top and bottom surfaces of these slabs appear smooth and the absence of siliclastic sediment within the carbonate cement suggests that they precipitated very close to the sea floor. The second group consist of brownish grey mainly tabular shaped samples with irregular surfaces and numerous microvesicles that presumably protrude in the internal part of the sample. The flattish shape and the presence of a black (organic?) coating, suggest that these are also some of the carbonate fragments observed on the seafloor during the TV-record. The third group is represented by light grey irregular shaped concretions displaying very porous texture and irregular surfaces. Due to the lighter colour, the irregular shape and the higher amount of carbonate cemented clayey fraction, it is suspected that these crusts were forming in the subsurface within the clayey unit.

Structure Bobic

AT639Gr

A TV-grab survey was completed on the Bobic structure. Escarpments of large blocks and extensive carbonate crusts were seen. Fields of tube worms and shells were seen and also four pingoes. The TV grab was



Figure 50. Large collection of authigenic carbonates with different shapes and textures from TV grab AT639Gr.

full. The top few cm consisted of brown marl with silty-sandy admixture. In the lower part of the grab the sediment becomes greyish. Carbonate crusts were collected mainly from the sediment surface (Fig. 50). They all showed very irregular and porous surfaces. The top surface was generally dark in colour. In several of the carbonates there is a subparallel layering of thick layers separated by more porous layers. Some of the carbonates collected from the internal part of the grab showed a similar irregular shape but had a grayish colour.

AT636G

One of the seepage structures observed was sampled at this site. There was sandy clay in the top 37 cm. The remaining part of the core consisted of clayey sediment with subvertical and flame shaped features of clayey and water saturated sediment that could represent pathways for fluid seepage (10-122 cm). The porous texture and the evident degassing observed in the lower part of the core strongly suggest the presence of gas hydrates that were dissociating during the splitting operations.

AT647K and AT648K

At two more sites Kastan corers were deployed in the attempt to collect gas hydrate samples from the Bobic structure. Both the attempts were unsuccessful and retrieved only the top 50 cm of sediment without gas hydrates. The penetration of the corer may have been prevented by the gas hydrates themselves.

Summary

No obvious evidence of fluid seepage was observed during the TV surveys and no living chemosynthetic bivalves were observed or sampled from the inferred seepage sites. Nevertheless, several elements supporting possible active fluid-seepage at these structures were collected. A strong smell of H_2S was frequently detected, whitish microbial colonies were observed on the seafloor and microbial filaments were seen within the hemipelagic sediment in the subsurface associated with authigenic carbonate, suggesting that AOM is currently ongoing. The presence of large amounts of shell debris in the subsurface forming subvertical narrow deposits,

suggest that chemosynthetic colonies were thriving along fluid pathways when methane-rich fluids were seeping in a different mode to that at present. Subvertical flame-shaped carbonate-rich features resemble to carbonate concretions collected during the TTR-8 cruise and could represent indications of fluid seepage and induced carbonate precipitation.

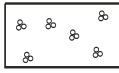


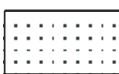
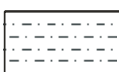
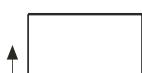






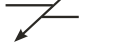
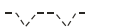















For the first time, gas hydrates were sampled from the Nyegga region, supporting the inference of several authors that hydrate was present, but which had not been verified by tangible evidence. As gas hydrate or strong bubbling were generally observed in the bottom part of several cores from different structures, it is inferred that the presence of gas hydrate prevented further penetration of the gravity corer at these sites. Although the presence of gas hydrates does not necessarily provide evidence of actual or very recent flow of free gas at the locations investigated, a near-constant flux of methane-rich fluid through the features containing hydrate is required to maintain the continued existence of hydrate, so close to the seabed.

REFERENCES

- Auzende, J.M., Olivet, J.L. and Pastouret, L., 1981. Implication structurales et paléogéographiques de la présence de Messinien à l'ouest de Gibraltar. *Marine Geology* 43, 9-18.
- Baraza, J. and Ercilla, G., 1996. Gas-charged sediments and large pockmark like features on the Gulf of Cadiz slope (SW Spain). *Marine and Petroleum Geology*, 13, 253-261.
- Berndt, C., Bunz, S. and Mienert, J., 2003. Polygonal fault systems on the mid-Norwegian margin: a long-term source for fluid flow. In: Van Rensbergen, P., Hillis, R.R., Maltman, A.J. and Morley, C.K. (eds) *Subsurface Sediment Mobilization*. Geological Society, London, Special Publication, 216, 283-290.
- Bonnel, C., Dennielou, B., Droz, L., Mulder, T. and Berne', S., 2005. Architecture and depositional pattern of the Rhone Neofan and recent gravity activity in the Gulf of Lions (western Mediterranean). *Marine and Petroleum Geology*, 22, 827-843.
- Bonnin, J., Olivet, J.L. and Auzende, J.M., 1975. Structure en nappe à l'ouest de Gibraltar. *C.R. Academy of Science* 280 (5), 559-562.
- Borges, J.F., Fitas A.J.S., Bezzeghoud M. and Teves-Costa, P., 2001. Seismotectonics of Portugal and its adjacent Atlantic area. *Tectonophysics* 337, 373-387.
- Bouriak, S., Vanneste, M. and Saoutkine, A., 2000. Inferred gas hydrates and clay diapirs near the Storegga Slide on the southern edge of the Voring Plateau, offshore Norway. *Marine Geology*, 163(1-4), 125-148.
- Bunz, S., Mienert, J. and Berndt, C., 2003. Geological controls on the Storegga gas-hydrate system of the mid-Norwegian continental margin. *Earth and Planetary Science Letters*, 209, 291-307.
- Canals, M., Puig, P., Durrieu de Madron, X., Heussner, S., Palanques, A. and Fabres, J., 2006. Flushing submarine canyons. *Nature*, 444, 354-357.
- Dewey, J.F., Helman, M.L., Turco, E., Hutton, D.H.W. and Knott, 1989. Kinematics of the western Mediterranean. *Tectonics*, 7, 1123-1139.
- Diaz-del-Rio, V., Somoza, L., Martinez-Frias, J., Mata, M., Delgado, A., Hernandez-Molina, F., Lunar, R., Martín-Rubí, J., Maestro, A., Fernández-Puga, M.C., León, R., Llave, E., Medialdea, T. and Vázquez, J.T., 2003. Vast fields of hydrocarbon-derived carbonate chimneys related to the accretionary wedge/olistostrome of the Gulf of Cadiz. *Marine Geology*, 195, 177-200.
- Droz, L. and Bellaiche, G., 1985. Rhone Deep-Sea Fan: morphostructure and growth pattern. *American Association of Petroleum Geologists Bulletin*, 69, 460-479.
- Fukao, Y., 1973. Thrust faulting at a lithospheric plate boundary, the Portugal Earthquake of 1969. *Earth plan. Sci. Lett.* 18, 205-216.
- Gardner, J.M., 1999. Mud volcanoes on the Moroccan Margin. *EOS Transactions*, 80, 483.
- Gardner, J.M., 2001. Mud volcanoes revealed and sampled on the Moroccan continental margin. *Geophysical Research Letters*, 28, 339-342.
- Gutscher, M.-A., Luis, J., Rosas F. and Gente P., 2004. DELILA Project. Cruise report.
- Gutscher, M.-A., Malod, J., Rehault, J.-P., Contrucci, I., Klingelhoefer, F., Mendes-Victor, L. and Spakman, W., 2002. Evidence for active subduction beneath Gibraltar. *Geology*, 30, 1071-1074.
- Kenyon, N.H., Droz, L., Ferentinos, G., Palanques, A., Cronin, B., Hasiotis, T., Millington, J. and Valensela, G., 1993. Sidescan sonar facies. In: A.F. Limonov, J.M. Woodside and M.K. Ivanov (Eds). *Geological and geophysical investigations of Western Mediterranean deep sea fans*. UNESCO reports in marine science, 62, 32-51.
- Kenyon, N.H., Millington, J., Droz, L. and Ivanov, M.K., 1995. Scour holes in a channel-lobe transition zone on the Rhone cone. In: Pickering, K.T., Hiscott, R.N., Kenyon, N.H., Lucchi, F.R., Smith, R.D.A. (eds.), *Atlas of Deep-water Environments: Architectural Styles in Turbidite Systems*. Chapman and Hall, London, 212-215.
- Kenyon, N.H., Ivanov, M. K., Akhmetzanov, A. and Akhmanov, G. G.,

2000. Multidisciplinary study of geological processes on the North East Atlantic and Western Mediterranean margins. IOC Technical Series, 56, UNESCO.
- Kenyon, N.H., Ivanov, M.K., Akhmetzhanov, A.M. and Akhmanov, G.G., 2003. Interdisciplinary geoscience research on the NorthEast Atlantic margin, Mediterranean Sea and Mid-Atlantic Ridge. Preliminary results of investigations during the TTR-12 cruise of RV Professor Logachev June-August, 2002. IOC Technical Series, 67. UNESCO, 112 pp.
- Kenyon, N.H., Ivanov, M.K., Akhmetzhanov, A.M. and Akhmanov, G.G., 2000. Multidisciplinary study of geological processes on the North East Atlantic and Western Mediterranean Sea margins. Preliminary results of geological and geophysical investigations during the TTR-9 cruise of R/V Professor Logachev June-July, 1999. IOC Technical Series, 56. UNESCO, 102 pp.
- Kenyon, N.H., Ivanov, M.K., Akhmetzhanov, A.M. and Akhmanov, G.G., 2001. Interdisciplinary Approaches to Geoscience on the North East Atlantic Margin and Mid-Atlantic Ridge. Preliminary results of investigations during the TTR-10 cruise of RV Professor Logachev. July-August, 2000. IOC Technical Series, 60. UNESCO, 104 pp.
- Lonergan, L. and White, N., 1997. Origin of the Betic-Rif mountain belt. *Tectonics*, 16, 504-522.
- Maldonado, A. and Comas, M. C., 1992. Geology and geophysics of the Alboran Sea: An Introduction. *Geo-Marine Letters*, 12, 61-65.
- Maldonado, A., Somoza, L. and Pallarés, L., 1999. The Betic orogen and the Iberian-African boundary in the Gulf of Cadiz: geological evolution (Central North Atlantic). *Marine Geology*, 155, 9-43.
- Mear, Y., 1984. Sequences et unites sedimentaires du glacis rhodanien (Mediterranee occidentale). Thesis Doct. 3eme cycle, University of Perpignan.
- Pinheiro, L.M., Ivanov, M.K., Sautkin, A., Akhmanov, G., Magalhaes, V.H., Volkonskaya, A., Monteiro, J.H., Somoza, L., Gardner, J., Hamouni, N. and Cunha, M.R., 2003. Mud volcanism in the Gulf of Cadiz: results from the TTR-10 cruise. *Marine Geology*, 195, 131-151.
- Rosenbaum G., Lister G.S. and Duboz C., 2002. Reconstruction of the tectonic evolution of the western Mediterranean since the Oligocene. In: Rosenbaum G. and Lister G.S. (eds). Reconstruction of the evolution of the Alpine-Himalayan Orogen. *Journal of the Virtual Explorer*, 8, 107-126.
- Royden, L.H., 1993. The tectonic expression of slab pull at continental convergent boundaries. *Tectonics*, 12, 303-325.
- Torres, J., Droz, L., Savoye, B., Terentieva, E., Cochonat, P., Kenyon, N.H. and Canals, M., 1997. Deep-sea avulsion and morphosedimentary evolution of the Rhone Fan Valley and Neofan during the Late Quaternary (north-western Mediterranean Sea). *Sedimentology*, 44, 457-477.
- Wilson, R.C.L., Hiscott, M.G. and Gradstein, F.M., 1989. The Lusitanian Basin of West Central Portugal. Mesozoic and Tertiary tectonic, stratigraphy and subsidence history. In: Tankard, A.J. and Balkwill, H.R. (eds.), *Extensional Tectonics and Stratigraphy of the North Atlantic Margins*. AAPG Mem. 46, 341-361.

ANNEX I. CORE LOGS

LEGEND	
	Foraminifera rich sediment
	marl
	mud/clay
	sand
	silt
	turbidite
	debris flow
	slump
	planar lamination
	cross lamination
	gradational boundary
	irregular boundary
	fault
	firm ground
	hard ground
	corals
	echinoderms
	gastropods
	plant debris
	shell fragments
	gas hydrate
	drop stones
	others
	lithoclasts
	oxidized layer
	dark layer
	flow in
	bioturbation
	burrows
	soupy sediment

ANNEX I. CORE LOGS (LEG 1, the Rhone Neofan)

R/V Professor Logachev TTR-16		CORE MS363G	
Location: Distal part of the Rhone Neofan Latitude: 41°33,758 Date: 19.05.2006 Longitude: 04°48,103 Recovery: 114 cm Water Depth: 2552 m			
AGE: LP - Late Pleistocene EP - Early Pleistocene H - Holocene		SUBSAMPLING CODES: 1- Express analysis 3- Geochemistry 5- Other 2- Sedimentology 4- Palaeontology	

Depth, cm	LITHOLOGY		Age	Colour	Section	Samples
	Photo	Grain size Cl Slt FMSMSCSGr Description				
0		SILTY CLAY: 0-31 cm. Brown, oxydized, with small amount of foraminifera. The top of the interval is rich in foraminifera. Intervals with large amount of foraminifera and pteropoda fragments from 6 to 8 cm, 11-13 cm, 17-18 cm are detected. Strongly oxidized interval from 27 to 31 cm.	2.5Y 5/3 LOB		1	
		CLAY: 31-41 cm. Brown, with small amount of foraminifera. The layer is oxydized. The bottom of the layer is iron-rich. At 40 cm a sulfide concretion is observed (1x2 cm).	2.5Y 6/3 LYB			
		SAND: 40-42 cm. Dark grey, fine-grained.	2.5Y 5/3 LOB			
		CLAY: 42-73 cm. Grey, with small amount of foraminifera.	2.5Y 5/2 OG			
		CLAY: 73-79 cm. Dark grey. At 78 cm there is a silty, burrowed interval.				
		SILTY CLAY: 79-109 cm. Grey, with small amount of foraminifera.	5Y 5/1 G			
100		SAND: 109-114 cm. Dark gray, coarse grained. At 112 cm two shell fragments 1 mm in size are visible.			2	



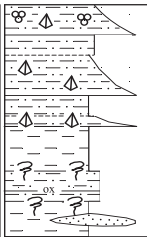
Core log TTR16-MS363G

R/V Professor Logachev TTR-16		CORE MS362G	
Location: Distal part of the Rhone Neofan Latitude: 41°33,763 Date: 19.05.2006 Longitude: 04°48,005 Recovery: 89 cm Water Depth: 2548 m			
AGE: LP - Late Pleistocene EP - Early Pleistocene H - Holocene		SUBSAMPLING CODES: 1- Express analysis 3- Geochemistry 5- Other 2- Sedimentology 4- Palaeontology	


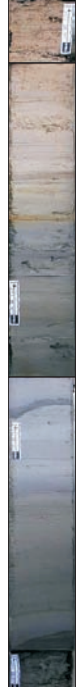
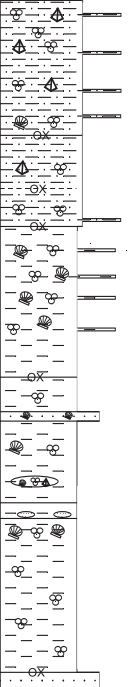
Depth, cm	LITHOLOGY		Age	Colour	Section	Samples
	Photo	Grain size Cl Slt FMSMSCSGr Description				
0		SILTY CLAY: 0-24 cm. Brown, with large amount of foraminifera, shell debris and gastropoda from 8 to 13 cm in size from 4 to 7 mm were detected. The layer is oxidized from 20 to 24 cm. High concentration of iron.	2.5Y 5/4 LOB		1	
		SILTY CLAY: 24-42 cm. Light brown, oxidized throughout the layer, with foraminifera and shell debris.	2.5Y 5/6 LOB			
		SILTY CLAY: 42-53 cm. Grey, with foraminifera and shell debris.	2.5Y 5/0 G			
		CLAY: 53-58 cm. Dark grey, oxidized at the bottom.	2.5Y 4/2 DGB			
		SILTY CLAY: 58-84 cm. Brownish grey, with sandy layer from 66 to 68 cm. Interval from 79 to 84 cm is strongly oxidized.	10YR 4/0 DG			
		CLAY: 84-89 cm. Dark brown, with foraminifera.	2.5Y 5/0 G			
					2	

Core log TTR16-MS362G

ANNEX I. CORE LOGS (LEG 1, the Rhone Neofan)


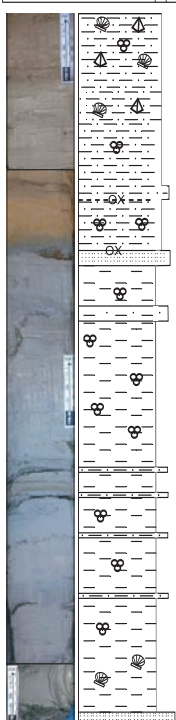


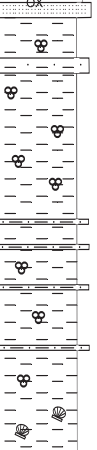

R/V Professor Logachev TTR-16		CORE MS364G					
Location: Distal part of the Rhone Neofan Latitude: 41°31,705 Date: 19.05.2006 Longitude: 04°48,200 Recovery: 46 cm Water Depth: 2558 m							
							
		AGE: LP - Late Pleistocene EP - Early Pleistocene H - Holocene					
		SUBSAMPLING CODES: 1- Express analysis 3- Geochemistry 5- Other 2- Sedimentology 4- Palaeontology					
Depth, cm	LITHOLOGY			Age	Colour	Section	Samples
	Photo	Grain size CI Silt FSMSCSGr	Description				
0			SILTY CLAY: 0-6 cm, Light-brown, with admixture of sand, foraminifera and pteropoda fragments.	2.5Y 7/4 PY	1		
10			SILTY CLAY: 6-10 cm, Brown, Lower boundary is gradual.				
20			SILTY CLAY: 10-18 cm, Brown, with admixture of pteropoda fragments, Lower boundary is sharp.				
30			SILTY CLAY: 18-23 cm, Brown, lower boundary is gradual.				
40			SILTY CLAY: 23-25 cm, With amount of shell debris and pteropoda fragments, Lower boundary is sharp.				
			CLAY: 25-33 cm, Brownish grey, The colour gradually becomes lighter to the bottom, Interval is bioturbated.				
			SILTY CLAY: 33-39 cm, Brown with grey spots, bioturbated, Oxidized interval at 38 cm, A black spot 2 cm in size at 35 cm, Lower boundary is bioturbated.				
		CLAY: 39-46 cm, Light grey, with oxidized brownish grey spots, A lens of dark grey sand from 40 to 43 cm, A lens of clay at 39,5 cm.		2.5Y 6/4 LYB			

Core log TTR16-MS364G


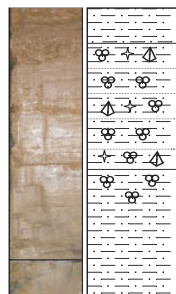

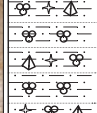
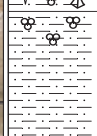
R/V Professor Logachev TTR-16		CORE MS365G					
Location: Distal part of the Rhone Neofan Latitude: 41°49,513 Date: 19.05.2006 Longitude: 04°54,051 Recovery: 220 cm Water Depth: 2444 m							
							
		AGE: LP - Late Pleistocene EP - Early Pleistocene H - Holocene					
		SUBSAMPLING CODES: 1- Express analysis 3- Geochemistry 5- Other 2- Sedimentology 4- Palaeontology					
Depth, cm	LITHOLOGY			Age	Colour	Section	Samples
	Photo	Grain size CI Silt FSMSCSGr	Description				
0			SILTY CLAY: 0-43 cm, Brown, with foraminifera and bioclasts, There are 4 silty-sandy beds (6-8 cm, 15-17 cm, 27-31 cm, 39-43 cm) with high concentration of foraminifera and pteropods (turbidites).	2.5Y 6/4 LYB	1		
50			SILTY CLAY: 43-60 cm, Brown, with small amount of foraminifera, There is one layer from 52-55 cm with high concentration of foraminifera and pteropod, At the bottom of the layer there is interval (57-59 cm) of dark brown silty clay with foraminifera (oxidized, turbidite).				
			SILTY CLAY: 60-72 cm, Grey-brown, with small amount of foraminifera, The layer is strongly oxidized.				
			CLAY: 72-120 cm, Grey, with foraminifera, There are 4 layers (78-80 cm, 85-86 cm, 94-95 cm, 106-109 cm) with large amount of foraminifera and shell fragments, The bottom of the layer is strongly oxidized.				
			CLAY: 120-131 cm, Grey, with small amount of foraminifera.				
			SAND: 131-134 cm, Dark grey, fine grained, with small amount of shell fragments.				
			CLAY: 134-160 cm, Light grey, with foraminifera and shell fragments, At 154 cm there is a small burrow filled with light grey clay, shell fragments and pteropods.				
			CLAY: 160-165 cm, Dark grey clay, At the bottom of the layer small sandy lens.				
			CLAY: 165-214 cm, Light grey clay with foraminifera, At 170 cm thin layer (2 cm) with high concentration of foraminifera and shell fragments is observed, The bottom of the layer is strongly oxidized.				
			SAND: 214-220 cm, Dark grey, fine grained.				
				2.5Y 6/3 LYB 2.5Y 5/3 LOB 2.5Y 5/6 LOB 2.5Y 5/0 G	2		
				5Y 4/1 DG 5Y 5/1 G	3		

Core log TTR16-MS365G

ANNEX I. CORE LOGS (LEG 1, the Rhone Neofan)

R/V Professor Logachev TTR-16		CORE MS366G					
Location: Distal part of the Rhone Neofan							
Latitude: 41°49,517	Date: 19.05.2006						
Longitude: 04°53,532	Recovery: 142 cm						
Water Depth: 2430 m	AGE:						
		SUBSAMPLING CODES:					
<small>LP - Late Pleistocene EP - Early Pleistocene H - Holocene</small>		<small>1- Express analysis 3- Geochemistry 5- Other 2- Sedimentology 4- Palaeontology</small>					
Depth, cm	LITHOLOGY			Age	Colour	Section	Samples
	Photo	Grain size Cl Slt FS MSCS Gr	Description				
0			<p>SILTY CLAY: 0-37 cm, Brown, with small amount of foraminifera at the top. There are three small layers (0-3 cm, 11-15 cm, 20-22 cm) with high concentration of Foraminifera, bioclasts and Pteropoda fragments. From 34 to 37 cm dark brown silty clay is observed. The layer is strongly oxidized.</p>	2.5Y 6/4 LYB	1		
50			<p>SILTY CLAY: 37-47 cm, Light brown, with high concentration of iron and foraminifera. The layer is oxidized.</p>	2.5Y 7/4 PY			
100			<p>CLAY: 47-129 cm, Grey, with silt admixture and foraminifera. At the top of the layer there is a burrow (3x5 cm) filled with oxidized fine-grained sand. Through the layer silty beds (47-50 cm, 58-61 cm, 90-91 cm, 95-96 cm, 103-104 cm, 115-116 cm, 129 cm) are observed. Upper 3 cm of the layer are darker than the rest.</p>	2.5Y 7/4 PY	2		
142			<p>SAND: 138-142 cm, Dark grey, terrigenous, fine-grained.</p>	CC			

Core log TTR16-MS366G

R/V Professor Logachev TTR-16		CORE MS367G					
Location: Distal part of the Rhone Neofan							
Latitude: 41°49,512	Date: 19.05.2006						
Longitude: 04°52,759	Recovery: 62 cm						
Water Depth: 2445 m	AGE:						
		SUBSAMPLING CODES:					
<small>LP - Late Pleistocene EP - Early Pleistocene H - Holocene</small>		<small>1- Express analysis 3- Geochemistry 5- Other 2- Sedimentology 4- Palaeontology</small>					
Depth, cm	LITHOLOGY			Age	Colour	Section	Samples
	Photo	Grain size Cl Slt FS MSCS Gr	Description				
0			<p>SILTY CLAY: 0-7 cm. Light grey, water - saturated in the upper part.</p>	2.5Y 6/4 LOB	1		
50			<p>SILTY CLAY: 7-32 cm. Light brownish, with foraminifera through out the layer. Intervals from 7 to 12, from 17 to 22, from 28 to 32 rich in foraminifera, and pteropods debris.</p>	2.5Y 5/6 LYB			
62			<p>SILTY CLAY: 32 - 62 cm. Light grey, with large amount of foraminifera in the upper part.</p>	2.5Y 7/2 L.G	2		

Core log TTR16-MS367G

R/V Professor Logachev TTR-16		CORE MS368G	
Location:	Distal part of the Rhone Neofan		
Latitude:	41°49,514	Date:	19.05.2006
Longitude:	04°52,237	Recovery:	123 cm
Water Depth:	2435 m	AGE:	
LP - Late Pleistocene EP - Early Pleistocene H - Holocene		1- Express analysis 3- Geochemistry 5- Other 2- Sedimentology 4- Palaeontology	
SUBSAMPLING CODES:			

Depth, cm	LITHOLOGY			Age	Colour	Section	Samples
	Photo	Grain size Cl Slt F SM SC SGr	Description				
0			SILTY CLAY: 0-23 cm. Brownish grey, with foraminifera throughout the layer. The layer is bioturbated from 19 to 23 cm. Between 20 and 21 cm with silty admixture.	2.5Y 5/3 LOB	1		
23			SILTY CLAY: 23-28 cm. Greyish brown, slightly bioturbated. Small amount of foraminifera.	2.5Y 5/2 GB			
28			SILTY CLAY: 28-42 cm. Yellowish grey, with foraminifera. The layer is oxidized. The lower boundary is irregular.	2.5Y 6/3LYB 2.5Y 7/4 PY			
42			SILTY CLAY: 42-67 cm. Grey, bioturbated throughout the layer, with foraminifera. The layer of sandy clay is observed at the bottom. Intervals from 45 to 49 and from 62 to 67 are oxidized.	5Y 5/1 G 2.5Y 6/2 LBG			
67			SILTY CLAY: 67-89 cm. Grey, with foraminifera, except interval from 85 to 87 cm. Silty admixture was observed at the bottom of the layer.	5Y 4/1 DG 2.5Y 6/2 LOG			
89			SILTY CLAY: 89-107 cm. Grey, with two lenses of silt at 91 and 95 cm. Oxidized layer was detected at 103 cm. The lower boundary is sharp.	5Y 4/1 DG 5Y 5/2 OG 5Y 5/1 G			
107	SILTY CLAY: 107-123 cm. Grey, with a lens of fine sand from 112 to 117 cm.	5Y 5/2 OG					

Core log TTR16-MS368G

R/V Professor Logachev TTR-16		CORE MS369G	
Location:	Distal part of the Rhone Neofan		
Latitude:	41°33,764	Date:	20.05.2006
Longitude:	04°47,996	Recovery:	83 cm
Water Depth:	2552 m	AGE:	
LP - Late Pleistocene EP - Early Pleistocene H - Holocene		1- Express analysis 3- Geochemistry 5- Other 2- Sedimentology 4- Palaeontology	
SUBSAMPLING CODES:			

Depth, cm	LITHOLOGY			Age	Colour	Section	Samples
	Photo	Grain size Cl Slt F SM SC SGr	Description				
0			SILTY CLAY: 0-9 cm. Light brownish grey, with abundant foraminifera. The sediment is bioturbated (mostly in lower part of the interval). At 9 cm an oxidized layer is observed.	2.5Y 5/3 LOB	1		
9			SILTY CLAY: 9-26 cm. Yellowish grey, the sediment is lighter in colour and contains less foraminifera than the previous interval. Between 20-26 cm the sediment is bioturbated. Iron oxidation is observed throughout the interval at patches up to 4 cm in diameter.	2.5Y 7/4 PY			
26			SILTY CLAY: 26-32 cm. The interval is similar to previous but contains more foraminifera and is lighter in colour.	2.5Y 6/3 LYB			
32			SILTY CLAY: 32-37 cm. Dark grey, the sediment doesn't contain foraminifera. Upper boundary is gradual.	5Y 5/2 OG			
37			SILTY CLAY: 37-47 cm. Grey, with foraminifera, bioturbated.	5Y 5/2 OB			
47			SAND: 47-48 cm. 1 cm thick layer of fine-grained sand in muddy matrix. Boundaries are irregular and sharp.	5Y 6/2 LOB			
48			SILTY CLAY: 48-63 cm. Grey, with foraminifera, the layer is bioturbated. At 63 cm an oxidized layer is observed.	5Y 5/2 OG			
63	SILTY CLAY: 63-66 cm. Dark grey, slightly water-saturated.	5Y 5/2 OG					
66	SILTY CLAY: 66-83 cm. Grey, bioturbated, with several beds (at 70, 74, 83 cm) of very fine grey sand.						

Core log TTR16-MS369G

ANNEX I. CORE LOGS (LEG 1, the Rhone Neofan)

R/V Professor Logachev TTR-16		CORE MS371G					
Location: Distal part of the Rhone Neofan Latitude: 41°29,178 Date: 20.05.2006 Longitude: 04°46,741 Recovery: 33 cm Water Depth: 2572 m							
AGE: LP - Late Pleistocene EP - Early Pleistocene H - Holocene		SUBSAMPLING CODES: 1- Express analysis 3- Geochemistry 5- Other 2- Sedimentology 4- Palaeontology					
Depth, cm	LITHOLOGY			Age	Colour	Section	Samples
	Photo	Grain size Cl Silt FMSCSGr	Description				
0			CLAY: 0-4 cm, Light brown, pteropoda and foraminifera rich.	10 YR 5/4 YB	1		
			SILTY CLAY: 4-16 cm, Light brown, with small amount of foraminifera. Lower boundary is bioturbated.	2.5Y 5/3 LOB			
			SAND: 16-21 cm, Brown. Intervals from 16 to 17 and from 20 to 21 cm contain coarse sand admixture and a lot of shell debris. Planar lamination can be detected from 17 to 20 cm.	2.5Y 6/4 LYB			
			SILTY CLAY: 21-31 cm, Yellowish brown, foraminifera rich, bioturbated. Dark brown oxidized intervals at 29 and 31 cm. Lower boundary is sharp.				
			CLAY: 31-33 cm, Yellowish brown, with small amount of foraminifera.				

Core log TTR16-MS371B


R/V Professor Logachev TTR-16		CORE MS372G					
Location: Distal part of the Rhone Neofan Latitude: 41°34,006 Date: 23.05.2006 Longitude: 04°48,028 Recovery: 60 cm Water Depth: 2545 m							
AGE: LP - Late Pleistocene EP - Early Pleistocene H - Holocene		SUBSAMPLING CODES: 1- Express analysis 3- Geochemistry 5- Other 2- Sedimentology 4- Palaeontology					
Depth, cm	LITHOLOGY			Age	Colour	Section	Samples
	Photo	Grain size Cl Silt FMSCSGr	Description				
0			CLAY: 0-2 cm: dark olive brown, with large amount of foraminifera, water-saturated.	2.5 Y 5/3 LOB	1		
			SILTY CLAY: 2-4 cm: olive brown. Colour becomes darker towards the bottom.	2.5 Y 6/4 LYB			
			CLAY: 4-36 cm: yellowish brown, with strongly oxidized layers at 5, 10, 21, 24 cm. At 11 cm sandy lens and 21 cm foraminifera-rich layer with silty admixture are observed.	2.5 Y 7/3 PY			
			CLAY: 36-60 cm: dark olive grey, with large amount of foraminifera from 36 to 38 cm, Content of foraminifera decreases towards the bottom, Silty layer black in colour is detected from 42 to 43 cm.	2.5 Y 7/2 LG			
50				2.5Y 5/2 GB			

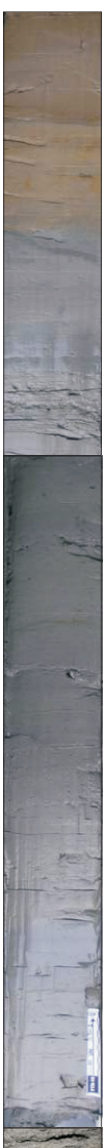
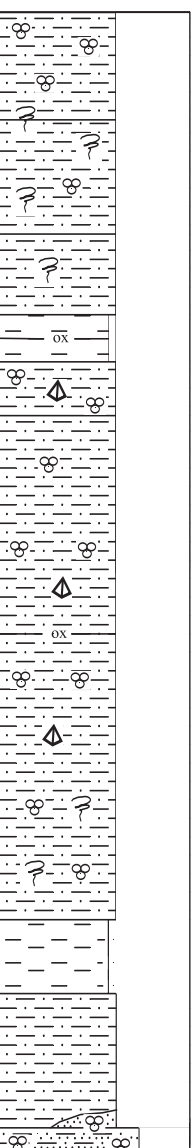
Core log TTR16-MS372G

R/V Professor Logachev TTR-16		CORE MS373G					
Location: Distal part of the Rhone Neofan Latitude: 41°34,016 Date: 23.05.2006 Longitude: 04°47,984 Recovery: 42 cm Water Depth: 2544 m							
AGE: LP - Late Pleistocene EP - Early Pleistocene H - Holocene		SUBSAMPLING CODES: 1- Express analysis 3- Geochemistry 5- Other 2- Sedimentology 4- Palaeontology					
Depth, cm	LITHOLOGY			Age	Colour	Section	Samples
	Photo	Grain size Cl Silt FMSCSGr	Description				
0			CLAY: 0-14 cm: yellowish brown, with silty admixture at the top and foraminifera, towards the bottom clay content increases.	5Y 6/4 P03 5Y 5/6 O	1		
			CLAY: 14-27 cm: olive brown, with large amount of foraminifera, oxidized. Coarse sandy layer from 19 to 22 cm and a lens of medium sand at 15 cm are detected.	5Y 4/3 P0			
			CLAY: 27-42 cm: yellowish grey, with foraminifera, slightly oxidized.	5Y 4/1 G			

Core log TTR16-MS373G

ANNEX I. CORE LOGS (LEG 1, the Rhone Neofan)

R/V Professor Logachev TTR-16		CORE MS374G	
			
Location:	Distal part of the Rhone Neofan		
Latitude:	41°31,109	Date:	23.05.2006
Longitude:	04°48,058	Recovery:	171 cm
Water Depth:	2544 m	AGE:	SUBSAMPLING CODES:
LP - Late Pleistocene EP - Early Pleistocene H - Holocene		1- Express analysis 3- Geochemistry 5- Other 2- Sedimentology 4- Palaeontology	

Depth, cm	LITHOLOGY			Age	Colour	Section	Samples
	Photo	Grain size Cl Slt FSMSCSGr	Description				
0			SILTY CLAY: 0-16 cm. Brown, foraminifera rich, bioturbated from 14 to 16 cm.	2.5Y5/3 LOB	1		
			SILTY CLAY: 16-33 cm. Yellowish grey, with small amount of foraminifera. The interval is strongly bioturbated and oxidized.	2.5Y6/3 LYB			
			SILTY CLAY: 33-45 cm. Light grey, bioturbated. Dark grey burrows are observed throughout the layer.	2.5Y6/3 LBG 5Y6/1 G			
50			CLAY: 45-52 cm. Dark grey with little silty admixture. An oxidized interval is observed at 48 cm. Lower boundary is sharp.	5Y5/1 G 5Y5/2 OG			
			SILTY CLAY: 52-60 cm. Grey, foraminifera and pteropoda rich.				
			SILTY CLAY: 60-135 cm. Grey, with foraminifera and pteropoda fragments. Interval is slightly bioturbated. Foraminifera rich interval from 79 to 81 cm, 98-100 cm. Some burrows filled with foraminifera are observed from 118 to 119 cm, 125-130 cm. An oxidized layer is detected at 92 cm.				
100							2
			CLAY: 135-146 cm. Dark grey, with some silty admixture.	5Y5 MG			
			SILTY CLAY: 146-166 cm. Grey, with foraminifera, bioturbated. A lens of foraminifera rich sand from 165 to 166 cm is observed. Foraminifera rich interval with sand admixture is detected from 166 to 171 cm.	5Y5/2 OG			
150							3

Core log TTR16-MS374G

ANNEX I. CORE LOGS (LEG 1, the Rhone Neofan)

R/V Professor Logachev TTR-16		CORE MS377G					
Location: Distal part of the Rhone Neofan		Date: 23.05.2006					
Latitude: 41°33,925		Recovery: 268 cm					
Longitude: 04°47,959		AGE:					
Water Depth: 2551 m		SUBSAMPLING CODES:					
<small>LP - Late Pleistocene EP - Early Pleistocene H - Holocene</small>		<small>1- Express analysis 3- Geochemistry 5- Other 2- Sedimentology 4- Palaeontology</small>					
LITHOLOGY							
Depth, cm	Grain size		Age	Colour	Section	Samples	
	Photo	Cl Slt F SM SCS Gr					Description
0			PTEROPOD LAYER: 0-37 cm. Pteropods with silty admixture. Intervals of silty clay from 16 to 21 cm, from 23 to 26 cm are observed.				1
50			PTEROPOD LAYER : 37-109 cm. Pteropods with intervals of grey silty mud from 41 to 43 cm, from 58 to 59, from 72 to 73, from 75 to 76, from 91 to 92, from 97 to 99 cm.				2
100			SILTY CLAY: 109-137 cm. Grey, with foraminifera and pteropods throughout the layer. Sandy interval from 123 to 126 cm.				3
150			SILTY CLAY: 137-179 cm. Grey, slight silty, with foraminifera and pteropods. Intervals from 155 to 157 cm, from 163 to 165 cm, from 179 to 181 cm consists of large amount of pteropods and foraminifera. The layer is bioturbated from 166 to 179 cm.				3
200			SILTY CLAY: 181-191 cm. Grey, with foraminifera and pteropods throughout the layer.				3
210			SILTY CLAY: 191-203 cm. Grey, slight silty, with foraminifera and pteropods.				3
220			SILTY CLAY: 203 - 222 cm. Grey, bioturbated, with large amount of foraminifera and pteropods at the top of the layer.				3
230			SILTY CLAY: 222 - 237 cm. Grey, slightly silty, bioturbated, with foraminifera and pteropods.				4
250			SILTY CLAY: 237- 268 cm. Grey, with foraminifera and pteropods.				4

Core log TTR16-MS377G

R/V Professor Logachev TTR-16		CORE MS378G	
Location: Distal part of the Rhone Neofan Latitude: 41°34,020 Date: 23.05.2006 Longitude: 04°47,987 Recovery: 33 cm Water Depth: 2555 m			
AGE: LP - Late Pleistocene EP - Early Pleistocene H - Holocene		SUBSAMPLING CODES: 1- Express analysis 3- Geochemistry 5- Other 2- Sedimentology 4- Palaeontology	

Depth, cm	LITHOLOGY			Age	Colour	Section	Samples
	Photo	Grain size Cl Slt FSMSCSGr	Description				
0			SILTY CLAY: 0-2 cm. Foraminifera rich, lower boundary is bioturbated.			1	2.5Y7/3 PY
			SILTY CLAY: 2-14 cm. Pale yellow, with small amount of foraminifera. Oxidized levels are observed at 6, 7, 9 and 12 cm.			2	2.5Y6/4 LYB 7.5YR 5/6 SB
			SAND: 14-15 cm. Rusty, lithified, strongly oxidized.				
			SILTY CLAY: 15-33 cm. Yellowish brown, foraminifera rich. Oxidized levels at 16, 18, 24, 27 cm.				10YR 5/4 YB

Core log TTR16-MS378G

R/V Professor Logachev TTR-16		CORE MS379G	
Location: Distal part of the Rhone Neofan Latitude: 41°34,120 Date: 23.05.2006 Longitude: 04°48,032 Recovery: 48 cm Water Depth: 2550 m			
AGE: LP - Late Pleistocene EP - Early Pleistocene H - Holocene		SUBSAMPLING CODES: 1- Express analysis 3- Geochemistry 5- Other 2- Sedimentology 4- Palaeontology	

Depth, cm	LITHOLOGY			Age	Colour	Section	Samples
	Photo	Grain size Cl Slt FSMSCSGr	Description				
0			SILTY CLAY: 0-9 cm. Dark brown, with small amount of foraminifera. The layer is oxidized.			1	2.5Y 5/4 LOB 2.5Y 6/2 LYB
			CLAY: 9-41 cm. Brown, with small admixture of silt and small amount of foraminifera. The layer is oxidized, the interval from 28 to 30 cm is strongly oxidized. An interval from 30 to 41 cm is darker than the rest of the layer.				2.5Y 6/5 LYB 2.5Y 5/3 LOB
			CLAY: 41-48 cm. Brown, structureless.				CC

Core log TTR16-MS379G

R/V Professor Logachev TTR-16		CORE MS380G	
Location: Distal part of the Rhone Neofan Latitude: 41°33,847 Date: 23.05.2006 Longitude: 04°47,995 Recovery: 22 cm Water Depth: 2552 m			
AGE: LP - Late Pleistocene EP - Early Pleistocene H - Holocene		SUBSAMPLING CODES: 1- Express analysis 3- Geochemistry 5- Other 2- Sedimentology 4- Palaeontology	

Depth, cm	LITHOLOGY			Age	Colour	Section	Samples
	Photo	Grain size Cl Slt FSMSCSGr	Description				
0			SAND: 0-2cm: grey, medium-coarse, water-saturated.			1	5Y 5/2 OG 5Y 6/4 PO 2.5Y 5/2 GR
			CLAY: 2-19 cm: light yellowish brown, with large amount of foraminifera, with silty admixture in the upper part. At 6 cm small lens of fine sand, dark grey in colour.				
			CLAY: 19-22 cm: grey, with foraminifera and silty admixture.				



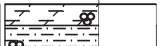

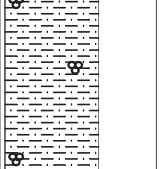

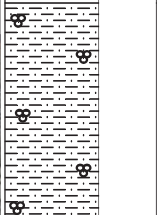

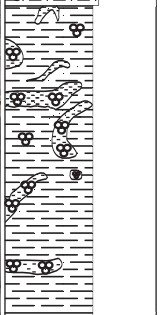

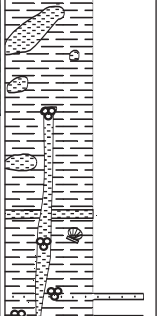

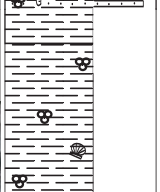
Core log TTR16-MS380G

R/V Professor Logachev TTR-16		CORE MS381G	
Location: Distal part of the Rhone Neofan Latitude: 41°33,764 Date: 23.05.2006 Longitude: 04°47,996 Recovery: 42 cm Water Depth: 2552 m			
AGE: LP - Late Pleistocene EP - Early Pleistocene H - Holocene		SUBSAMPLING CODES: 1- Express analysis 3- Geochemistry 5- Other 2- Sedimentology 4- Palaeontology	

Depth, cm	LITHOLOGY			Age	Colour	Section	Samples
	Photo	Grain size Cl Slt FSMSCSGr	Description				
0			SILTY CLAY: 0-11 cm. Brown, with foraminifera throughout the layer. Interval with large amount of pteropods from 0 to 7 cm was detected.			1	2.5Y 5/3 LOB 2.5Y 7/4 PY 2.5Y 6/3 LYB 5Y 5/2 OG
			SILTY CLAY: 11-20 cm. Brown, rich in foraminifera. Pteropods layers from 15 to 17 cm, from 21 to 22 cm were detected.				
			SILTY CLAY: 22-24 cm. Brown, with foraminifera and pteropods debris.				
			PTEROPOD LAYER: 24-29 cm. Some admixture of silty clay.				
			SILTY CLAY: 28-38 cm. Brown, with foraminifera and large amount of pteropods.				
			PTEROPOD LAYER: 38-42 cm. Some admixture of sand, with foraminifera.				




Core log TTR16-MS381B

ANNEX I. CORE LOGS (LEG 2, the Gulf of Cadiz)




R/V Professor Logachev TTR-16		CORE AT601G					
Location: Pen Duick escarpment Latitude: 35°18,764 Date: 28.05.2006 Longitude: 06°48,458 Recovery: 236 cm Water Depth: 642 m							
							
		AGE: LP - Late Pleistocene 3- Geochemistry 5- Other Express analysis 1- EP - Early Pleistocene 2- Sedimentology 4- Palaeontology H - Holocene					
		SUBSAMPLING CODES:					
Depth, cm	LITHOLOGY			Age	Colour	Section	Samples
	Photo	Grain size Cl Slt FMSMCSGr	Description				
0			MARL: 0-4 cm. Brown, with foraminifera and		2.5V 4/3 OB		
			SILTY CLAY: 4-40 cm. Brownish grey with foraminifera and coral debris. Lower boundary is defined by colour change.		2.5V 6/2 LBG		
50			SILTY CLAY: 40-81 cm. Grey, rich in foraminifera, with large amount of coral debris.	5V 5/1 G			
			CLAY: 81-139 cm. Grey, with intervals rich in foraminifera: 81-84 cm, 88-92 cm, 91-94 cm, 95-99 cm, 99-109 cm, 111-121 cm. Burrows at 112 cm and from 129 to 130 cm are observed. An interval from 111-121 cm filled with water-saturated clay, lower boundary is irregular.	5V 6/1 G			
100			CLAY: 139-207 cm. Grey, with abundant foraminifera and rare shell debris. At 149 cm white spot filled with water-saturated clay is observed. Big burrow occurs from 140 to 148 cm. At 170 cm and 181 cm burrows are detected. At 161 cm light grey spot of clay without foraminifera, water-saturated occurs. There are 4 bioclastic sand intervals: 194 cm, 199 cm, 204 cm and 207 cm. At 186 cm shell debris is detected. H ₂ S smell in the lower part of the interval.	5V 5/1 G			
150			CLAY: 207-236 cm. Grey, with foraminifera and rare shell and coral debris. Burrow at 222. H ₂ S smell in the lower part of the interval.	5V 5/1 G			
200							

Core log TTR16-AT601G

ANNEX I. CORE LOGS (LEG 2, the Gulf of Cadiz)

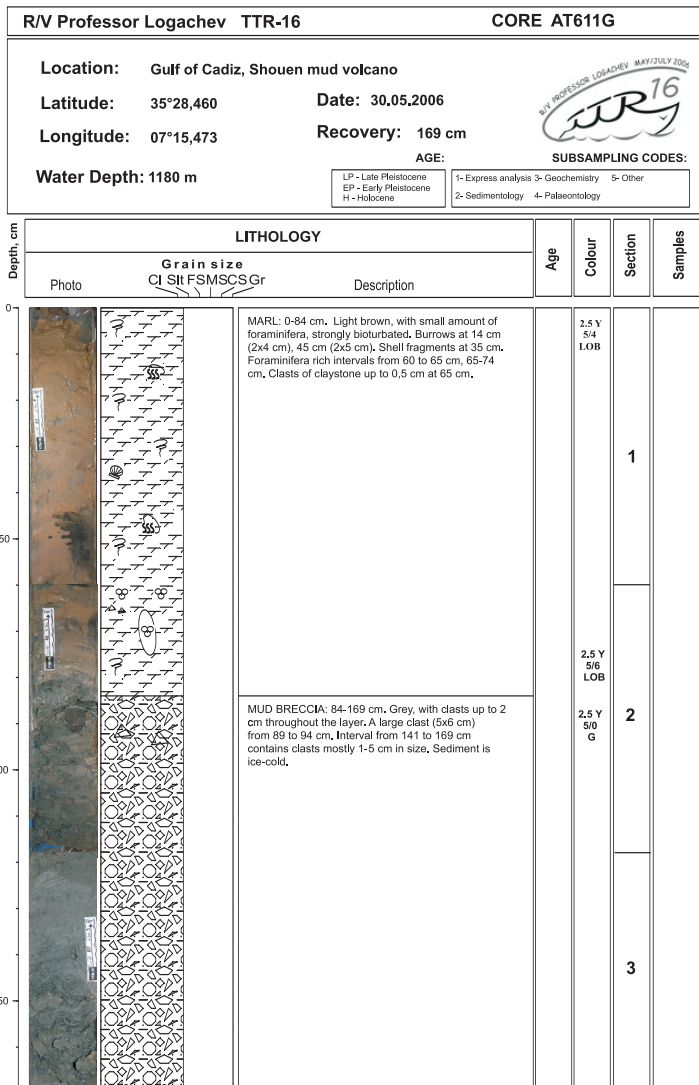
R/V Professor Logachev TTR-16		CORE AT603G					
Location: Yuma mud volcano, Dark patch on the northern slope							
Latitude: 35°18,764	Date: 29.05.2006						
Longitude: 06°48,458	Recovery: 137 cm						
Water Depth: 642 m	AGE:						
		SUBSAMPLING CODES: LP - Late Pleistocene 1- Express analysis 3- Geochemistry 5- Other EP - Early Pleistocene 2- Sedimentology 4- Palaeontology H - Holocene					
Depth, cm	LITHOLOGY			Age	Colour	Section	Samples
	Photo	Grain size Cl Silt FS MSCS Gr	Description				
0			MARL: 0-42 cm, Grey, with large amount of foraminifera, rare shell fragments, oxidised and water-saturated at the upper part. Carbonate crust at 34 cm (6x4cm)	2.5Y 6/3 LYB	1		
50			MUD BRECCIA: 42-118 cm, Grey, with foraminifera and rare shell fragments from 42 to 56 cm. There are dark grey clasts from 48 to 52 cm (4x5 cm), from 66 to 88 (1.5x1.5 cm). Dark grey patches, filled with sand are seen at 87cm, 94 cm, 106 cm (3x3 cm). There are light grey clasts of marlstone (1x1.5 cm) at 105 cm. Bioturbation is seen throughout the layer. Strong smell of H ₂ S.	2.5Y 6/0 G			
100					2.5Y 8/0 W	2	
				2.5Y 5/0 G	3		

Core log TTR16-AT603G

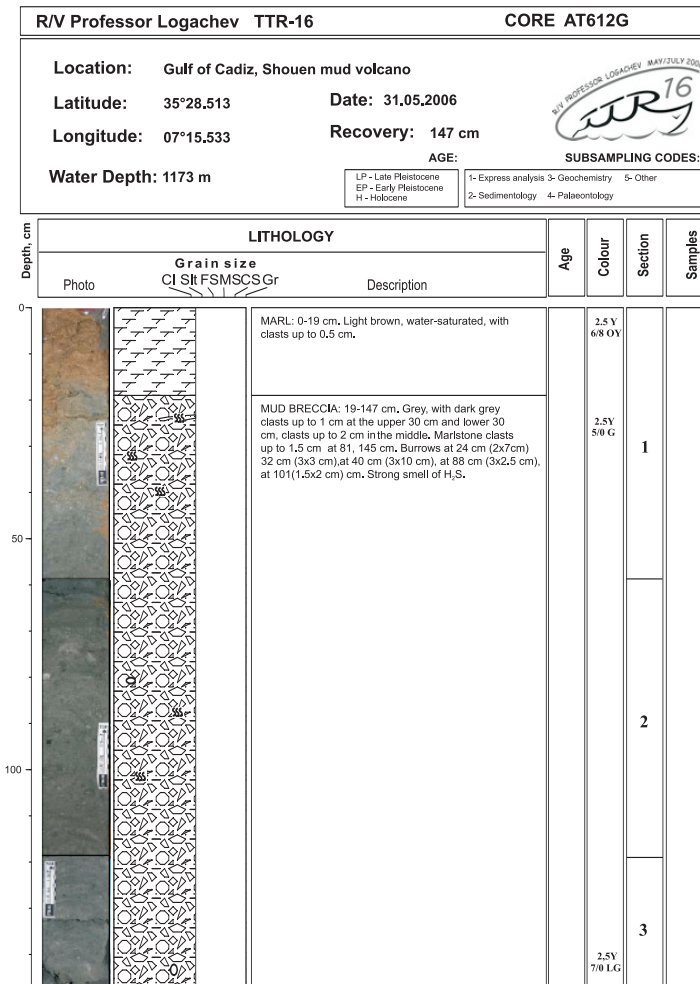
R/V Professor Logachev TTR-16		CORE AT606G					
Location: Ginsburg mud volcano							
Latitude: 35°22.390	Date: 29.05.2006						
Longitude: 07°05.320	Recovery: 60 cm						
Water Depth: 923 m	AGE:						
		SUBSAMPLING CODES: LP - Late Pleistocene 1- Express analysis 3- Geochemistry 5- Other EP - Early Pleistocene 2- Sedimentology 4- Palaeontology H - Holocene					
Depth, cm	LITHOLOGY			Age	Colour	Section	Samples
	Photo	Grain size Cl Silt FS MSCS Gr	Description				
0			MARL: 0-12 cm, Brown, water-saturated, foraminifera rich.	2.5Y 6/3 LYB			
50			MUD BRECCIA: 12-60 cm, Grey, with small amount of foraminifera. Burrows at 33 (1x1 cm), 36 (1x3 cm), 46 (2x3 cm), 51 (1x1 cm) cm. Strong smell of H ₂ S. Dark grey clasts of sandstones and marlstones up to 0.5 cm throughout the interval. Sediment is ice-cold in the lower part. Strong smell of H ₂ S.	2.5Y 5/0 G			

Core log TTR16-AT606G

ANNEX I. CORE LOGS (LEG 2, the Gulf of Cadiz)



Core log TTR16-AT611G



Core log TTR16-AT612G

ANNEX I. CORE LOGS (LEG 2, the Gulf of Cadiz)

R/V Professor Logachev TTR-16		CORE AT613G							
Location: Carlos Ribeiro mud volcano, central part of the crater Latitude: 35°47,260 Date: 31.05.2006 Longitude: 08°25,241 Recovery: 251 cm Water Depth: 2204 m									
AGE: <small>LP - Late Pleistocene EP - Early Pleistocene H - Holocene</small>		SUBSAMPLING CODES: <small>1 - Express analysis 3 - Geochemistry 5 - Other 2 - Sedimentology 4 - Palaeontology</small>							
Depth, cm	LITHOLOGY			Age	Colour	Section	Samples		
	Photo	Grain size Cl Sll FS M SCS Gr	Description						
0			MARL: 0-12 cm, Light brown, water-saturated, with foraminifera, with large coral fragments from 5 to 8 cm.	2.SY 4.3 L1.B	1				
50			MUD BRECCIA: 15-174 cm, Grey, with small amount of foraminifera. Burrow at 24 cm (3x4cm). Strong smell of H ₂ S. Dark grey clasts and marlstone clasts up to 1 cm throughout the interval. Large clast at 246 cm (4x2cm).						
100								2.SY 5.H G	2
150								3	
200								4	
250			5						

Core log TTR16-AT613G

R/V Professor Logachev TTR-16		CORE AT614G					
Location: Carlos Ribeiro mud volcano, central part of the crater Latitude: 35°47,246 Date: 31.05.2006 Longitude: 08°25,298 Recovery: 85 cm Water Depth: 2210 m							
AGE: <small>LP - Late Pleistocene EP - Early Pleistocene H - Holocene</small>		SUBSAMPLING CODES: <small>1 - Express analysis 3 - Geochemistry 5 - Other 2 - Sedimentology 4 - Palaeontology</small>					
Depth, cm	LITHOLOGY			Age	Colour	Section	Samples
	Photo	Grain size Cl Sll FS M SCS Gr	Description				
0			MARL: 0-12 cm, Brown, water-saturated, with small amount of foraminifera, with small clasts up to 0.1cm.	5Y 5/3 G	1		
50			MUD BRECCIA: 5-85 cm, Grey, with grey clasts upto 1 cm, large clast at 35 cm (1.5x3 cm). Sediment is cold and porous at the lower part. Strong smell of H ₂ S.				

Core log TTR16-AT614G

R/V Professor Logachev TTR-16		CORE AT616G	
Location: Carlos Ribeiro MV			
Latitude: 35°47,246N	Date: 31.05.2006		
Longitude: 08°25,300W	Recovery: 167 cm		
Water Depth: 2572 m	AGE:	SUBSAMPLING CODES:	
	LP - Late Pleistocene EP - Early Pleistocene H - Holocene	1- Express analysis 3- Geochemistry 2- Sedimentology 4- Palaeontology	5- Other

Depth, cm	LITHOLOGY			Age	Colour	Section	Samples
	Photo	Grain size Cl Silt FSMSCSGr	Description				
0		<p>MARL: 0-13 cm. Brownish-grey, with clasts up to 0.2 cm, water-saturated, with small amount of foraminifera.</p> <p>MUD BRECCIA: 13-167 cm. Grey, with dark-grey clasts mostly 0,1-0,5 cm in size, the biggest ones up to 5 cm in size, the pore size increases toward the bottom in interval from 106 to 167 cm.</p>	5 Y 5/3 O	1			
50			2.5 Y 5/0 G				
100			2				
150			3				

Core log TTR16-AT616G

R/V Professor Logachev TTR-16		CORE AT619G	
Location: Solovjev MV			
Latitude: 35°12,785	Date: 02.06.2006		
Longitude: 09°06,450	Recovery: 117 cm		
Water Depth: 3295 m	AGE:	SUBSAMPLING CODES:	
	LP - Late Pleistocene EP - Early Pleistocene H - Holocene	1- Express analysis 3- Geochemistry 2- Sedimentology 4- Palaeontology	5- Other

Depth, cm	LITHOLOGY			Age	Colour	Section	Samples
	Photo	Grain size Cl Silt FSMSCSGr	Description				
0		<p>MARL: 0-15 cm. Brown, water-saturated, with small amount of foraminifera.</p> <p>MUD BRECCIA: 13-117 cm. Grey, with clasts of marlstone up to 0.5 cm, with dark grey clasts up to 0.5 cm. Large clast at 30 cm (5x8 cm). Bioturbation from 13 to 20 cm. Strong smell of H₂S. Very porous in the lower 10 cm. Bubbling was observed in core catcher possibly due to dissociation of small gas hydrates.</p>	2.5Y 5/6 LOB	1			
50			2.5Y 6/0 G				
100			2.5Y 7/0 LG				
150			2.5Y 4/0 DG	2			
			2.5Y 5/0 G				

Core log TTR16-AT619G

ANNEX I. CORE LOGS (LEG 2, the Gulf of Cadiz)

R/V Professor Logachev TTR-16		CORE AT621G	
Location: Gulf of Cadiz, Porto mud volcano Latitude: 35°33,778 Date: 02.06.2006 Longitude: 09°30,396 Recovery: 135 cm Water Depth: 3921 m			
AGE: LP - Late Pleistocene EP - Early Pleistocene H - Holocene		SUBSAMPLING CODES: 1- Express analysis 3- Geochemistry 5- Other 2- Sedimentology 4- Palaeontology	



Depth, cm	LITHOLOGY		Age	Colour	Section	Samples
	Photo	Grain size Cl Silt FS MSCS Gr Description				
0		MARL: 0-16 cm: brown, water-saturated.	5Y 6/3 PO			
		CLAY: 16-32 cm: grey, with water-saturated spot at 30 cm (5x2 cm).	5Y 6/0 G			
		MUD BRECCIA: 32-99 cm: grey, with clasts up to 0,5 cm in size and patches of carbonate stiff clay at 66, 69, 90 cm.	5Y 6/1 G			
		MUD BRECCIA: 99-105 cm: dark grey, with clasts up to 1 mm.	5Y 5/1 G			
		MUD BRECCIA: 105-116 cm: light grey, with a lot of clasts. Lower boundary is irregular.	2.5Y 7/0 LG			
		MUD BRECCIA: 116-135 cm: dark grey, with patches of light grey stiff clay up to 0,4 cm. A clast of marlstone at 135 cm (2x1cm).	2.5Y 5/0 G			

Core log TTR16-AT621G

R/V Professor Logachev TTR-16		CORE AT623G	
Location: Porto MV Latitude: 35°33,761N Date: 03.06.2006 Longitude: 09°30,459W Recovery: 162 cm Water Depth: 3875 m			
AGE: LP - Late Pleistocene EP - Early Pleistocene H - Holocene		SUBSAMPLING CODES: 1- Express analysis 3- Geochemistry 5- Other 2- Sedimentology 4- Palaeontology	

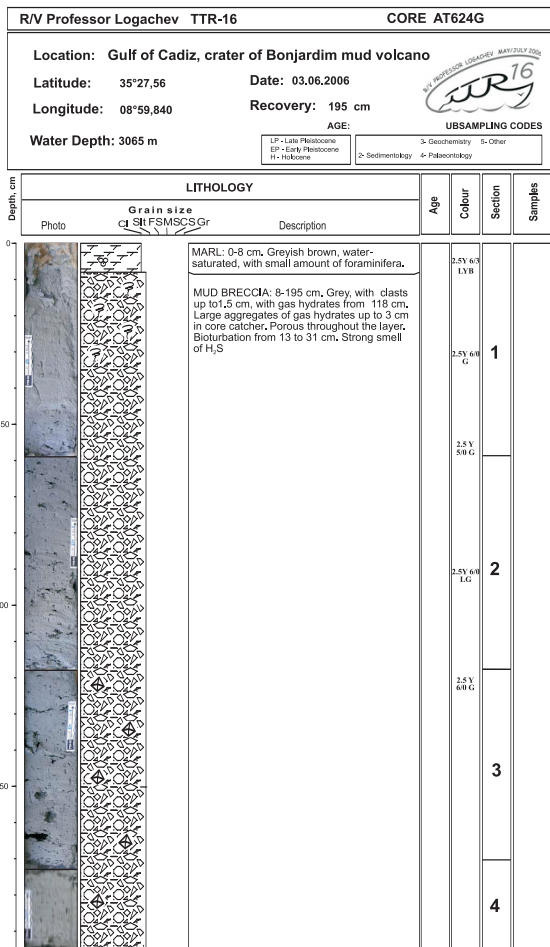


Depth, cm	LITHOLOGY		Age	Colour	Section	Samples
	Photo	Grain size Cl Silt FS MSCS Gr Description				
0		MARL: 0-34 cm. Brown, with small amount of foraminifera, water-saturated in the upper part.	5Y 5/3 O		1	
		MUD BRECCIA: 34-82 cm. Grey, with small amount of foraminifera at the top of the layer, with black spot of bioturbation from 34-38 cm. Abundant pogonofora are observed throughout the layer. Semilitified clasts up to 0,2 cm are visible.	5Y 5/1 G		2	
		MUD BRECCIA: 82-102 cm. Dark grey, with clasts up to 0,5 cm throughout the layer, sediment is darker in the upper 2 cm of the interval.	2.5Y 5/0 5Y 5/1 G		3	
		MUD BRECCIA: 102-133 cm. Grey, the most common size of clasts is about 1 mm. Lower boundary is bioturbated. The layer is slightly porous. At the bottom of the layer small amount of gas bubbles is detected.	5Y 6/1 G			
		MUD BRECCIA: 133-162 cm. Grey, the most common size of clasts is about 1mm.	5Y 5/1 G			

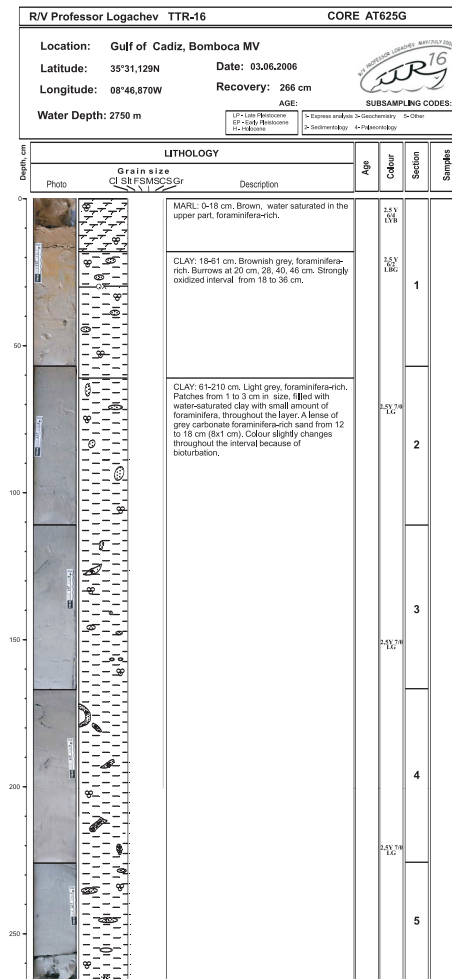
Core log TTR16-AT623G

ANNEX I. CORE LOGS (LEG 2, the Gulf of Cadiz)

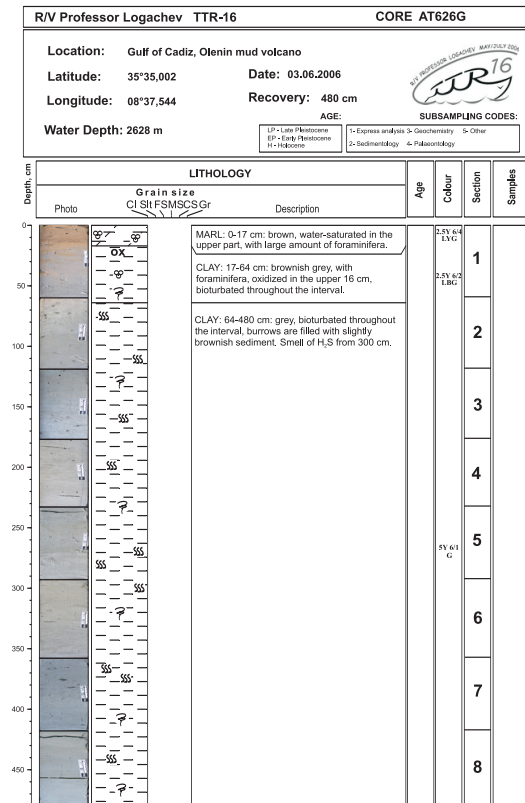
ANNEX I. CORE LOGS (LEG 2, the Gulf of Cadiz)



Core log TTR16-AT624G




Core log TTR16-AT625G





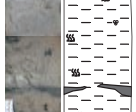







Core log TTR16-AT626G

R/V Professor Logachev TTR-16 CORE AT628G

Location: CN03 structure, Norwegian margin
 Latitude: 64°45,278 Date: 19.06.2006
 Longitude: 05°04,107 Recovery: 539 cm
 Water Depth: 726 m



 SUBSAMPLING CODES:
 1- Express analysis 3- Geochemistry 5- Other
 2- Sedimentology 4- Palaeontology



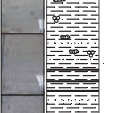








Depth, cm	LITHOLOGY			Colour	Section	Samples
	Photo	Grain size Cl Slt FMSMCSGr	Description			
0-37			MARL: 0-3 cm. Brown, water-saturated, with fine sand-silty admixture.	SY 49 U 3 OG	1	3
37-69			CLAY: 3-69 cm. Brownish grey, with silty, fine sand admixture. Structureless, bioturbation burrows are observed at 37 cm. Between 47-69 cm the sediment becomes more greyish and the amount of silty - fine sand admixture decreases. Between 61-63 cm brownish sand-rich layer was observed.	SY 51 G	1	3
69-539			CLAY: 69-539 cm. Grey, structureless, with black hydrotroilite patches distributed throughout the section particularly between 69-75, 123-131, 209-213, 307-312, 375-383, 450-459, 521-524, 524-539 cm. Bioturbation distributed through the section with larger water saturated burrows between 123-132, 197-201, 261-265, 306-320, 340-345, 361-367, 469-481 cm. The silty admixture gradually increases towards the bottom of the core.	SY 52 OG SY 30 VDL 2.5 Y 4.9 G	2	3
539-500				SY 51 G	3	3
500-460				SY 31 VDG	3	3
460-420					4	3
420-380					5	3
380-340					6	3
340-300					7	3
300-260					8	3
260-220					9	3
220-180					10	3

Core log TTR16-AT628G

R/V Professor Logachev TTR-16 CORE AT632G

Location: Small positive feature north of G11, Norwegian margin
 Latitude: 64°40,219N Date: 29.06.2006
 Longitude: 05°17,542E Recovery: 401 cm
 Water Depth: 740 m



 SUBSAMPLING CODES:
 1- Express analysis 3- Geochemistry 5- Other
 2- Sedimentology 4- Palaeontology



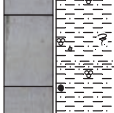
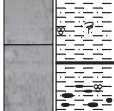






Depth, cm	LITHOLOGY			Age	Colour	Section	Samples
	Photo	Grain size Cl Slt FMSMCSGr	Description				
0-5			MARL: 0-5 cm. Brown, water-saturated with large amount of foraminifera and fine sand admixture. Lower boundary is gradual.	SY 53 U 3 OG	1		
5-401			CLAY: 5-401 cm. Brownish grey clay with some silt admixture and foraminifera. There are two intervals (8-15 cm, 18-19 cm) rich in fine grained sand. Dark brown spots of water-saturated sediment are detected between 5-104 cm. Intervals between 104-171 cm and 325-401 cm contain high concentration of hydrotroilite patches. At 185 cm - 2 cm wide coral fragment is observed. At 191 cm patch of brownish grey clay with a halo of more greyish clay rich in silt admixture is detected. Below 229 cm admixture of fine sand appears. The interval between 229-263 cm contains some rock fragments (up to coarse sand in size) and some patches filled with grey clay with silty admixture. At 283 cm, 273 cm, 263 cm hydrotroilite-rich layers are observed. Two dashes (1x1 cm) are visible at 356 cm and 363 cm. Shell fragments appear towards the bottom of the core.	SY 54 U 3 OG SY 52 OG SY 51 G SY 53 U 3 OG SY 51 G SY 52 OG SY 52 OG	2		
401-360							
360-320							
320-280							
280-240							
240-200							
200-160							
160-120							
120-80							
80-40							

Core log TTR16-AT632G

R/V Professor Logachev TTR-16 CORE AT633G

Location: North of G11 structure, Norwegian margin
 Latitude: 64°40,678N Date: 29.06.2006
 Longitude: 05°18,019E Recovery: 456 cm
 Water Depth: 715 m

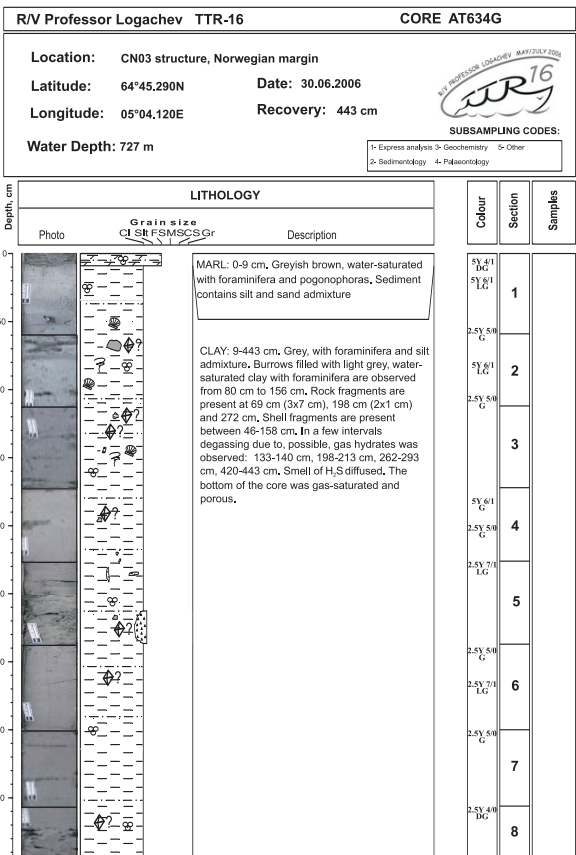

 SUBSAMPLING CODES:
 1- Express analysis 3- Geochemistry 5- Other
 2- Sedimentology 4- Palaeontology

Depth, cm	LITHOLOGY			Colour	Section	Samples
	Photo	Grain size Cl Slt FMSMCSGr	Description			
0-11			MARL: 0-0 cm. Brown, water saturated in the upper part, with fine sand admixture, with large black clast (4x4cm), foraminifera-rich. Carbonate crust (1x1cm) in the top part.	SY 43 U 3 OG	1	
11-104			CLAY: 5-115 cm. Olive grey, strongly bioturbated, with silty admixture and foraminifera throughout. Greenish spot with foraminifera is observed at 11 cm. Hydrotroilite patches are distributed throughout the interval. Extremely high concentration of hydrotroilite is observed between 318-396 cm. Hydrotroilite layer with sharp boundaries can be seen between 306-307 cm. A clast of marlstone 0.5 cm in diameter at 203 cm. A rock fragment is observed at 249 cm (1x1cm). Shell fragments are observed at 249 cm, 45 cm, 93 cm, 414 cm.	SY 41 OG SY 41 OG SY 41 OG	2	
104-93						
93-81						
81-69						
69-57						
57-45						
45-33						
33-21						
21-9						

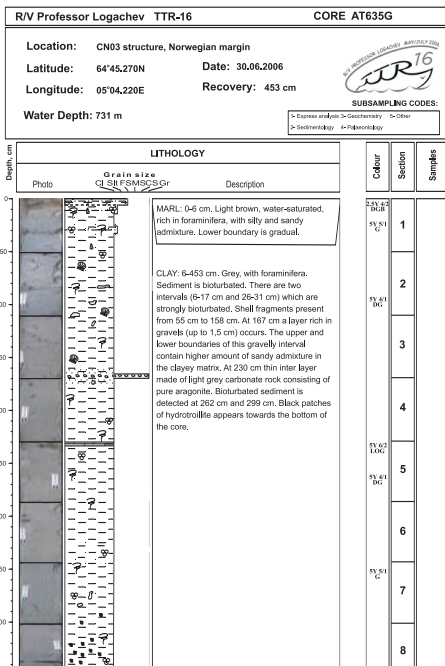
Core log TTR16-AT633G

ANNEX I. CORE LOGS (LEG 3, the Norwegian Margin)

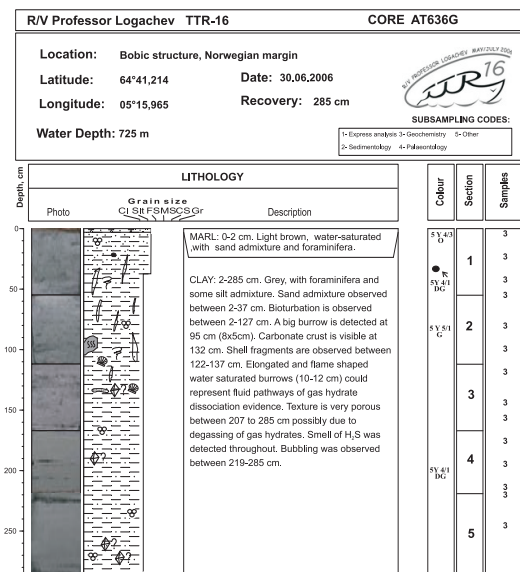
ANNEX I. CORE LOGS (LEG 3, the Norwegian Margin)



Core log TTR16-AT634G

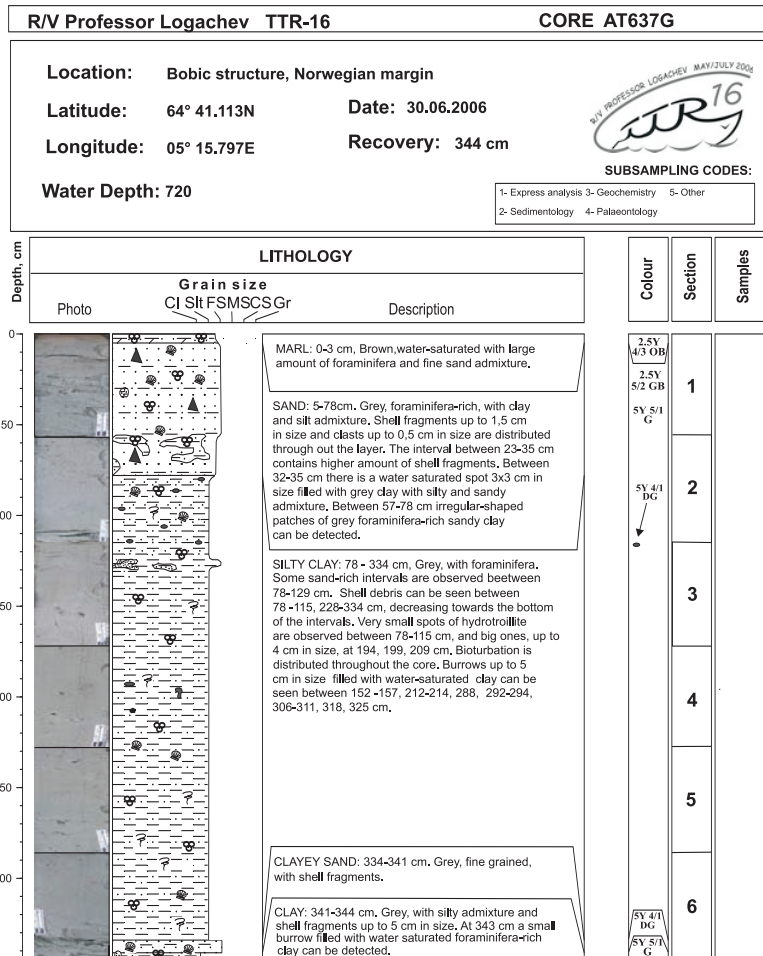


Core log TTR16-AT635G

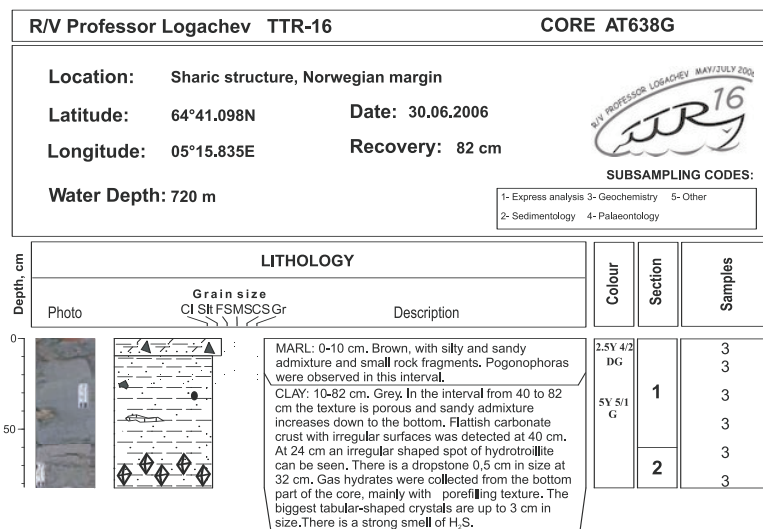


Core log TTR16-AT636G

ANNEX I. CORE LOGS (LEG 3, the Norwegian Margin)

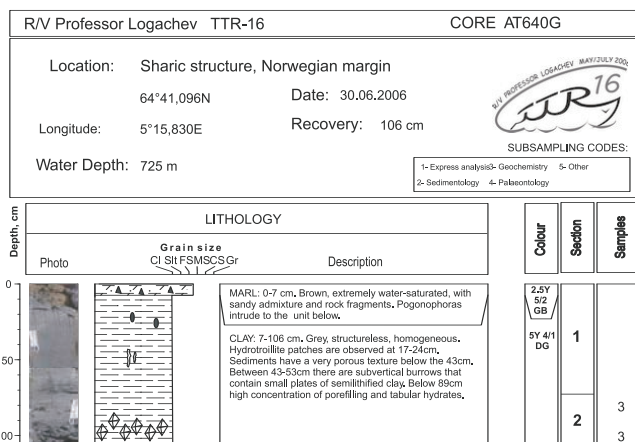


Core log TTR16-AT637G

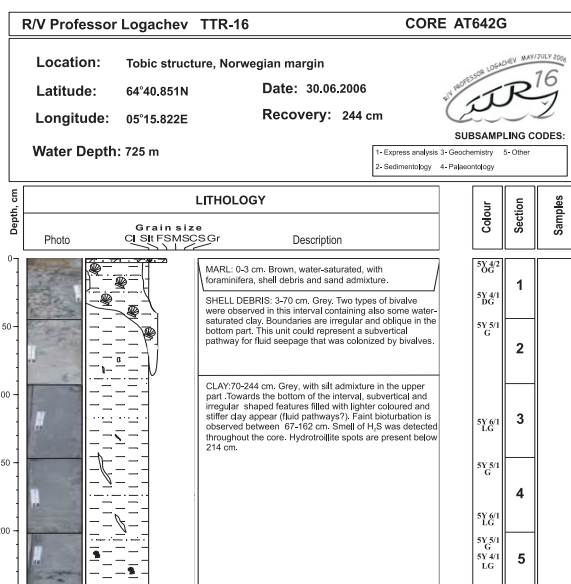


Core log TTR16-AT638G

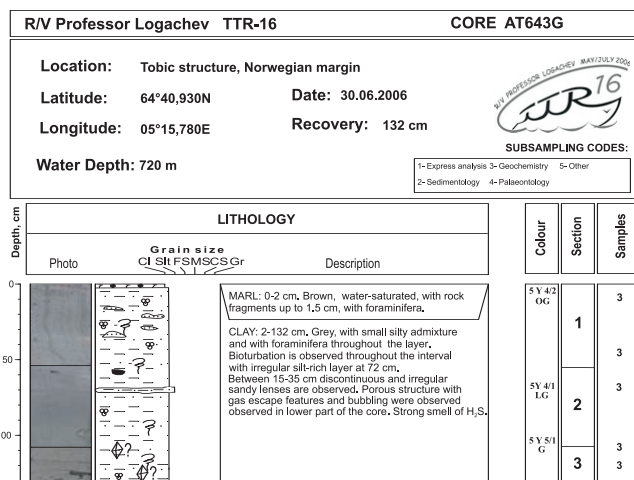
ANNEX I. CORE LOGS (LEG 3, the Norwegian Margin)



Core log TTR16-AT640G

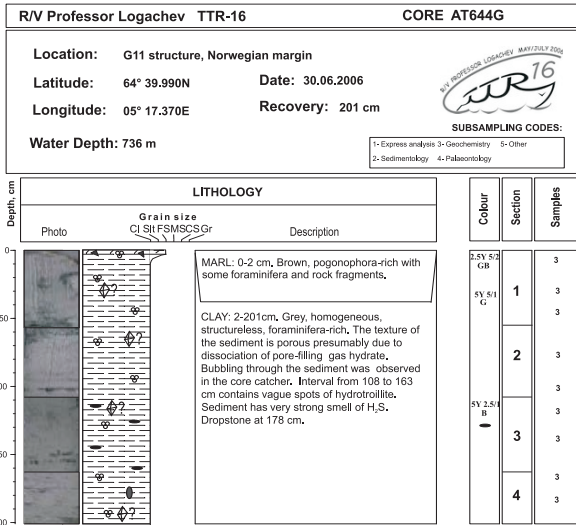


Core log TTR16-AT642G

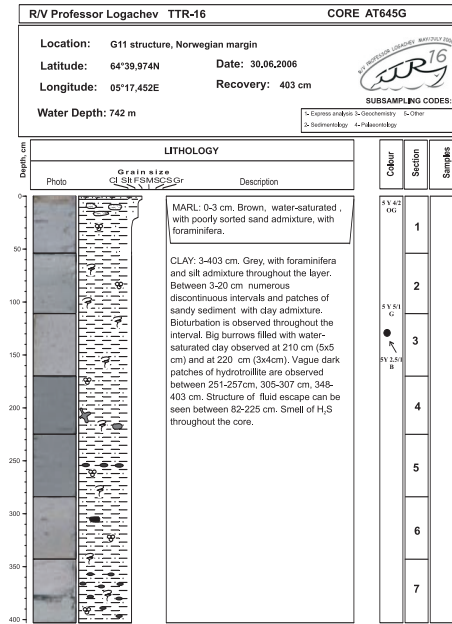


Core log TTR16-AT643G

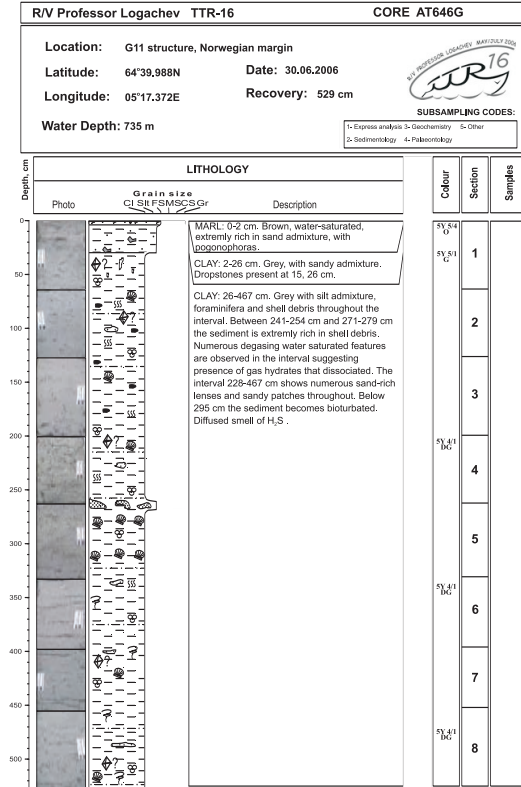
ANNEX I. CORE LOGS (LEG 3, the Norwegian Margin)



Core log TTR16-AT644G



Core log TTR16-AT645G



Core log TTR16-AT646G

ANNEX II. LIST OF TTR-RELATED REPORTS

- Limonov, A.F., Woodside, J.M. and Ivanov, M.K. (eds.), 1992. Geological and geophysical investigations in the Mediterranean and Black Seas. Initial results of the "Training through Research" Cruise of R/V *Gelendzhik* in the Eastern Mediterranean and the Black Sea (June-July 1991). UNESCO Reports in Marine Science, 56, 208 pp.
- Limonov, A.F., Woodside, J.M. and Ivanov, M.K. (eds.), 1993. Geological and geophysical investigations of the deep-sea fans of the Western Mediterranean Sea. Preliminary report of the 2nd cruise of the R/V *Gelendzhik* in the Western Mediterranean Sea, June-July, 1992. UNESCO Reports in Marine Science, 62, 148 pp.
- "Training-Through-Research" Opportunities Through the UNESCO/TREDMAR Programme. Report of the first post-cruise meeting of TREDMAR students. Moscow State University, 22-30 January, 1993. MARINF, 91, UNESCO, 1993.
- Limonov, A.F., Woodside, J.M. and Ivanov, M.K. (eds.), 1994. Mud volcanism in the Mediterranean and Black Seas and Shallow Structure of the Eratosthenes Seamount. Initial results of the geological and geophysical investigations during the Third UNESCO-ESF "Training-through-Research" Cruise of R/V *Gelendzhik* (June-July 1993). UNESCO Reports in Marine Science, 64, 173 pp.
- Recent Marine Geological Research in the Mediterranean and Black Seas through the UNESCO/TREDMAR programme and its "Floating University" project, Free University, Amsterdam, 31 January-4 February 1994. Abstracts. MARINF, 94, UNESCO, 1994.
- Limonov, A.F., Kenyon, N.H., Ivanov, M.K. and Woodside J.M. (eds.), 1995. Deep sea depositional systems of the Western Mediterranean and mud volcanism on the Mediterranean Ridge. Initial results of geological and geophysical investigations during the Fourth UNESCO-ESF "Training through Research" Cruise of R/V *Gelendzhik* (June-July 1994). UNESCO Reports in Marine Science, 67, 171 pp.
- Deep-sea depositional systems and mud volcanism in the Mediterranean and Black Seas. 3rd post-cruise meeting, Cardiff, 30 January - 3 February 1995. Abstracts. MARINF, 99, UNESCO, 1995.
- Ivanov, M.K., Limonov, A.F. and Cronin, B.T. (eds.), 1996. Mud volcanism and fluid venting in the eastern part of the Mediterranean Ridge. Initial results of geological, geophysical and geochemical investigations during the 5th Training-through-Research Cruise of R/V *Professor Logachev* (July-September 1995). UNESCO Reports in Marine Science, 68, 127pp.
- Sedimentary basins of the Mediterranean and Black Seas. 4th Post-Cruise Meeting, Training-through-research Programme. Moscow and Zvenigorod, Russia, 29 January-3 February. Abstracts. MARINF, 100, UNESCO, 1996.
- Woodside, J.M., Ivanov, M.K. and Limonov, A.F. (eds.), 1997. Neotectonics and Fluid Flow through Seafloor Sediments in the Eastern Mediterranean and Black Seas. Preliminary results of geological and geophysical investigations during the ANAXIPROBE/TTR-6 cruise of R/V *Gelendzhik*, July-August 1996. Vols. 1, 2. IOC Technical Series, 48, UNESCO, 226 pp.
- Gas and Fluids in Marine Sediments: Gas Hydrates, Mud Volcanoes, Tectonics, Sedimentology and Geochemistry in Mediterranean and Black Seas. Fifth Post-cruise Meeting of the Training-through-research Programme and International Congress, Amsterdam, The Netherlands, 27-29 January 1997. IOC Workshop Reports, 129, UNESCO, 1997.
- Geosphere-biosphere coupling: Carbonate Mud Mounds and Cold Water Reefs. International Conference and Sixth Post-Cruise Meeting of the Training-through-Research Programme, Gent, Belgium, 7-11 February 1998. IOC Workshop Reports, 143, UNESCO, 1998.
- Kenyon, N.H., Ivanov, M.K. and Akhmetzhanov, A.M. (eds.), 1998. Cold water carbonate mounds and sediment transport on the Northeast Atlantic Margin. IOC Technical Series, 52, UNESCO, 178 pp.
- Kenyon, N.H., Ivanov, M.K. and Akhmetzhanov, A.M. (eds.), 1999. Geological Processes on the Northeast Atlantic Margin. IOC Technical Series, 54, UNESCO, 141 pp.
- Geological Processes on European Continental Margins. International Conference and Eighth Post-cruise Meeting of the Training-Through-Research Programme, University of Granada, Spain, 31 January - 3 February 2000. IOC Workshop Reports, 168, UNESCO, 2000.

Kenyon, N.H., Ivanov, M.K., Akhmetzhanov, A.M. and Akhmanov, G.G., (eds.), 2000. Multidisciplinary study of geological processes on the Northeast Atlantic and Western Mediterranean margins. IOC Technical Series, 56, UNESCO, 119 pp.

Geological processes on deep-sea European margins. International Conference and Ninth Post-Cruise Meeting of the Training-through-Research Programme. Moscow/Mozhenka, Russia, 28 January - 3 February 2001. IOC Workshop Reports, 175. UNESCO, 2001, 76 pp.

Kenyon, N.H., Ivanov, M. K., Akhmetzhanov, A. and Akhmanov, G. G. (eds.), 2001. Interdisciplinary Approaches to Geoscience on the North East Atlantic Margin and Mid-Atlantic Ridge. IOC Technical Series, 60, UNESCO, 134 pp.

Geosphere/Biosphere/Hydrosphere Coupling Processes, Fluid Escape Structures and Tectonics at Continental Margins and Ocean Ridges. International Conference and Tenth Post-Cruise Meeting of the Training-through-Research Programme. Aveiro, Portugal, 30 January - 2 February 2002. IOC Workshop Reports, 183. UNESCO, 2002, 50 pp.

Kenyon, N.H., Ivanov, M. K., Akhmetzhanov, A. and Akhmanov, G. G. (eds.), 2002. Interdisciplinary studies of geological processes in the Mediterranean and Black Seas and North East Atlantic. IOC Technical Series, 62, UNESCO, 134 pp.

Geological and biological processes at deep-sea European margins and oceanic basins. International Conference and Eleventh Post-Cruise Meeting of the Training-through-Research Programme. Bologna, Italy, February 2-6, 2003. IOC Workshop Reports, 187. UNESCO, 2003, 32 pp.

Kenyon, N.H., Ivanov, M. K., Akhmetzhanov, A. and Akhmanov, G. G. (eds.), 2003. Interdisciplinary geoscience research on the North East Atlantic margin, Mediterranean Sea and Mid-Atlantic Ridge. IOC Technical Series, 67, UNESCO, 152 pp.

North Atlantic and Labrador Sea Margin architecture and sedimentary processes. International Conference and Twelfth Post-Cruise Meeting of the Training-through-Research Programme. Copenhagen, Denmark, January 29-31, 2004. IOC Workshop Reports, 191. UNESCO, 2004, 47 pp.

Kenyon, N.H., Ivanov, M.K., Akhmetzhanov, A.M., Kozlova, E.V. and Mazzini, A. (eds.), 2004. Interdisciplinary studies of North Atlantic and Labrador Sea Margin Architecture and Sedimentary Processes. Preliminary results of investigations during the TTR-13 cruise of RV Professor Logachev, July-September, 2003, IOC Technical Series, 68 , 92 pp & annexes.

Geosphere-Biosphere coupling processes: the TTR interdisciplinary approach towards studies of the European and North African margins. International Conference and Post-Cruise Meeting of the Training-Through-Research Programme, Marrakech, Morocco, 2 - 5 February 2005. IOC Workshop Reports, 197, UNESCO, 2005, 71 pp.

Kenyon, N.H., Ivanov, M.K., Akhmetzhanov, A.M. and Kozlova, E.V., (eds.), 2006. Interdisciplinary geoscience studies of the Gulf of Cadiz and Western Mediterranean basins. IOC Technical Series, 70, UNESCO, 115 pp & annexes.

Geological processes on deep-water European margins. International Conference and 15th Anniversary Post-Cruise Meeting of the Training-Through-Research Programme, Moscow/Zvenigorod, Russia, 29 January-4 February 2006. IOC Workshop Reports, 201, UNESCO, 2007, 73 pp.

Akhmetzhanov, A.M., Ivanov, M.K., Kenyon, N.H. and Mazzini, A. (eds.), 2007. Deep-water cold seeps, sedimentary environments and ecosystems of the Black and Tyrrhenian Seas and Gulf of Cadiz. IOC Technical Series, 72, UNESCO, 99 pp & annexes.

Geo-marine research along European Continental Margins. International Conference and Post-Cruise Meeting of the Training-through-Research Programme. Bremen, Germany, 29 January - 1 February 2007. IOC Workshop Reports, 204, UNESCO, 2007, 48 pp & annexes.

IOC Technical Series

No.	Title	Languages
1	Manual on International Oceanographic Data Exchange. 1965	(out of stock)
2	Intergovernmental Oceanographic Commission (Five years of work). 1966	(out of stock)
3	Radio Communication Requirements of Oceanography. 1967	(out of stock)
4	Manual on International Oceanographic Data Exchange - Second revised edition. 1967	(out of stock)
5	Legal Problems Associated with Ocean Data Acquisition Systems (ODAS). 1969	(out of stock)
6	Perspectives in Oceanography, 1968	(out of stock)
7	Comprehensive Outline of the Scope of the Long-term and Expanded Programme of Oceanic Exploration and Research. 1970	(out of stock)
8	IGOSS (Integrated Global Ocean Station System) - General Plan Implementation Programme for Phase I. 1971	(out of stock)
9	Manual on International Oceanographic Data Exchange - Third Revised Edition. 1973	(out of stock)
10	Bruun Memorial Lectures, 1971	E, F, S, R
11	Bruun Memorial Lectures, 1973	(out of stock)
12	Oceanographic Products and Methods of Analysis and Prediction. 1977	E only
13	International Decade of Ocean Exploration (IDOE), 1971-1980. 1974	(out of stock)
14	A Comprehensive Plan for the Global Investigation of Pollution in the Marine Environment and Baseline Study Guidelines. 1976	E, F, S, R
15	Bruun Memorial Lectures, 1975 - Co-operative Study of the Kuroshio and Adjacent Regions. 1976	(out of stock)
16	Integrated Ocean Global Station System (IGOSS) General Plan and Implementation Programme 1977-1982. 1977	E, F, S, R
17	Oceanographic Components of the Global Atmospheric Research Programme (GARP) . 1977	(out of stock)
18	Global Ocean Pollution: An Overview. 1977	(out of stock)
19	Bruun Memorial Lectures - The Importance and Application of Satellite and Remotely Sensed Data to Oceanography. 1977	(out of stock)
20	A Focus for Ocean Research: The Intergovernmental Oceanographic Commission - History, Functions, Achievements. 1979	(out of stock)
21	Bruun Memorial Lectures, 1979: Marine Environment and Ocean Resources. 1986	E, F, S, R
22	Scientific Report of the Interecalibration Exercise of the IOC-WMO-UNEP Pilot Project on Monitoring Background Levels of Selected Pollutants in Open Ocean Waters. 1982	(out of stock)
23	Operational Sea-Level Stations. 1983	E, F, S, R
24	Time-Series of Ocean Measurements. Vol.1. 1983	E, F, S, R
25	A Framework for the Implementation of the Comprehensive Plan for the Global Investigation of Pollution in the Marine Environment. 1984	(out of stock)
26	The Determination of Polychlorinated Biphenyls in Open-ocean Waters. 1984	E only
27	Ocean Observing System Development Programme. 1984	E, F, S, R
28	Bruun Memorial Lectures, 1982: Ocean Science for the Year 2000. 1984	E, F, S, R
29	Catalogue of Tide Gauges in the Pacific. 1985	E only
30	Time-Series of Ocean Measurements. Vol. 2. 1984	E only
31	Time-Series of Ocean Measurements. Vol. 3. 1986	E only
32	Summary of Radiometric Ages from the Pacific. 1987	E only
33	Time-Series of Ocean Measurements. Vol. 4. 1988	E only
34	Bruun Memorial Lectures, 1987: Recent Advances in Selected Areas of Ocean Sciences in the Regions of the Caribbean, Indian Ocean and the Western Pacific. 1988	Composite E, F, S

(continued)

No.	Title	Languages
35	Global Sea-Level Observing System (GLOSS) Implementation Plan. 1990	E only
36	Bruun Memorial Lectures 1989: Impact of New Technology on Marine Scientific Research. 1991	Composite E, F, S
37	Tsunami Glossary - A Glossary of Terms and Acronyms Used in the Tsunami Literature. 1991	E only
38	The Oceans and Climate: A Guide to Present Needs. 1991	E only
39	Bruun Memorial Lectures, 1991: Modelling and Prediction in Marine Science. 1992	E only
40	Oceanic Interdecadal Climate Variability. 1992	E only
41	Marine Debris: Solid Waste Management Action for the Wider Caribbean. 1994	E only
42	Calculation of New Depth Equations for Expendable Bathymetographs Using a Temperature-Error-Free Method (Application to Sippican/TSK T-7, T-6 and T-4 XBTS. 1994	E only
43	IGOSS Plan and Implementation Programme 1996-2003. 1996	E, F, S, R
44	Design and Implementation of some Harmful Algal Monitoring Systems. 1996	E only
45	Use of Standards and Reference Materials in the Measurement of Chlorinated Hydrocarbon Residues. 1996	E only
46	Equatorial Segment of the Mid-Atlantic Ridge. 1996	E only
47	Peace in the Oceans: Ocean Governance and the Agenda for Peace; the Proceedings of <i>Pacem in Maribus XXIII</i> , Costa Rica, 1995. 1997	E only
48	Neotectonics and fluid flow through seafloor sediments in the Eastern Mediterranean and Black Seas - Parts I and II. 1997	E only
49	Global Temperature Salinity Profile Programme: Overview and Future. 1998	E only
50	Global Sea-Level Observing System (GLOSS) Implementation Plan-1997. 1997	E only
51	L'état actuel de l'exploitation des pêcheries maritimes au Cameroun et leur gestion intégrée dans la sous-région du Golfe de Guinée (<i>cancelled</i>)	F only
52	Cold water carbonate mounds and sediment transport on the Northeast Atlantic Margin. 1998	E only
53	The Baltic Floating University: Training Through Research in the Baltic, Barents and White Seas - 1997. 1998	E only
54	Geological Processes on the Northeast Atlantic Margin (8 th training-through-research cruise, June-August 1998). 1999	E only
55	Bruun Memorial Lectures, 1999: Ocean Predictability. 2000	E only
56	Multidisciplinary Study of Geological Processes on the North East Atlantic and Western Mediterranean Margins (9 th training-through-research cruise, June-July 1999). 2000	E only
57	Ad hoc Benthic Indicator Group - Results of Initial Planning Meeting, Paris, France, 6-9 December 1999. 2000	E only
58	Bruun Memorial Lectures, 2001: Operational Oceanography – a perspective from the private sector. 2001	E only
59	Monitoring and Management Strategies for Harmful Algal Blooms in Coastal Waters. 2001	E only
60	Interdisciplinary Approaches to Geoscience on the North East Atlantic Margin and Mid-Atlantic Ridge (10 th training-through-research cruise, July-August 2000). 2001	E only
61	Forecasting Ocean Science? Pros and Cons, Potsdam Lecture, 1999. 2002	E only
62	Geological Processes in the Mediterranean and Black Seas and North East Atlantic (11 th training-through-research cruise, July- September 2001). 2002	E only
63	Improved Global Bathymetry – Final Report of SCOR Working Group 107. 2002	E only
64	R. Revelle Memorial Lecture, 2006: Global Sea Levels, Past, Present and Future. 2007	E only

(continued)

No.	Title	Languages
65	Bruun Memorial Lectures, 2003: Gas Hydrates – a potential source of energy from the oceans. 2003	E only
66	Bruun Memorial Lectures, 2003: Energy from the Sea: the potential and realities of Ocean Thermal Energy Conversion (OTEC). 2003	E only
67	Interdisciplinary Geoscience Research on the North East Atlantic Margin, Mediterranean Sea and Mid-Atlantic Ridge (12 th training-through-research cruise, June-August 2002). 2003	E only
68	Interdisciplinary Studies of North Atlantic and Labrador Sea Margin Architecture and Sedimentary Processes (13 th training-through-research cruise, July-September 2003). 2004	E only
69	Biodiversity and Distribution of the Megafauna / Biodiversité et distribution de la mégafaune. 2006 Vol.1 The polymetallic nodule ecosystem of the Eastern Equatorial Pacific Ocean / Ecosystème de nodules polymétalliques de l’océan Pacifique Est équatorial Vol.2 Annotated photographic Atlas of the echinoderms of the Clarion-Clipperton fracture zone / Atlas photographique annoté des échinodermes de la zone de fractures de Clarion et de Clipperton	E F
70	Interdisciplinary geoscience studies of the Gulf of Cadiz and Western Mediterranean Basin (14 th training-through-research cruise, July-September 2004). 2006	E only
71	Indian Ocean Tsunami Warning and Mitigation System, IOTWS. Implementation Plan, July-August 2006. 2006	E only
72	Deep-water Cold Seeps, Sedimentary Environments and Ecosystems of the Black and Tyrrhenian Seas and the Gulf of Cadiz (15 th training-through-research cruise, June–August 2005). 2007	E only
73	Implementation Plan for the Tsunami Early Warning and Mitigation System in the North-Eastern Atlantic, the Mediterranean and Connected Seas (NEAMTWS), 2007–2011. 2007 (<i>electronic only</i>)	E only
74	Bruun Memorial Lectures, 2005: The Ecology and Oceanography of Harmful Algal Blooms – Multidisciplinary approaches to research and management. 2007	E only
75	National Ocean Policy. The Basic Texts from: Australia, Brazil, Canada, China, Colombia, Japan, Norway, Portugal, Russian Federation, United States of America. (Also Law of Sea Dossier 1). 2008	E only
76	Deep-water Depositional Systems and Cold Seeps of the Western Mediterranean, Gulf of Cadiz and Norwegian Continental margins (16 th training-through-research cruise, May–July 2006). 2008	E only

